

**EVALUATION OF AUTOGENOUS HEALING ABILITY OF
CEMENTITIOUS COMPOSITES**

BY

Choonghyun KANG

A Dissertation Submitted to Nagoya University
In Partial Fulfillment of the Requirements for
The Degree of Doctor of Engineering

Department of Civil Engineering
Graduate School of Engineering, Nagoya University
Nagoya, JAPAN

September, 2012

ACKNOWLEDGEMENTS

First of all, I would like to express my deepest appreciation and gratitude to my supervisor Prof. Minoru KUNIEDA for his invaluable guidance, continuous support and encouragement through my doctoral study in Nagoya University. He has also given me an inspiration in the science research, especially in the field of the concrete structure. Surely, without his supports and patient, the dissertation has never been completed. I would like to thank Prof. Hikaru NAKAMURA for his invaluable comments and advices during my research in concrete structure laboratory. I also wish to express my sincere thanks to Prof. Kazuo TATEISHI and Prof. Shinichi IGARASHI for their valuable comments and advices. I would like to thank to assist. Prof. Naoshi UEDA for his continuous helps during my study in the laboratory. I also express my thanks to the former and the current students of the concrete structure laboratory, especially Mr. Takuya MORIMOTO, for their helps and supports not only my study but also my daily life in Japan.

I would like to express my appreciation to my master course supervisor Prof. Yongmyung PARK. His advice and teaching was based on my achievement. I also appreciate to Prof. Intae KIM, who recommended me this doctoral course.

The author of this dissertation gratefully acknowledges that, the Ministry of Education, Culture, Sports, Science and Technology (Monbukagakusho) provided me scholarships to pursue a degree of Doctor Engineering in the field of Civil Engineering in Nagoya University.

I want to thank to my whole friends in Korea. The nick name "Dr. KANG", which they gave to me when I was freshman, makes me get to here, I think. I also express my thanks to many Korean in Japan for their helps and advices. And I want to express my appreciation to Miss. Bohwa SEO. Her cheer was biggest encouragement for me during writing this dissertation.

Last but not least, behind the accomplishment, I would like to express my deep thanks to my parents, Mr. Hagu KANG and Mrs. Jungsoon PARK, and my sister Miss. Yeji KANG for their love, trust and hope on me.

ABSTRACT

Autogenous healing or Self healing of cementitious composite was well known phenomenon as recovery of cracks automatically. The word "Autogenous" emphasizes that cementitious composite material heals a crack without any artificial repair works. Recovery of strength, stiffness, or durability can be expected by autogenous healing.

Maintenance of concrete structures involves the increase of cost for inspection and repair of those. The performance of concrete structures decreased due to initial defects of deterioration, and repair or strengthening increases the performance again, in addition to the increase of cost. If the inside cracks, which is one of the major defects of concrete structures, can recover automatically without any inspection or repair works, it should be useful to decrease the maintenance cost, and it is effective for maintenance framework life cycle cost (LCC) basis.

The purpose of this study is to investigate the evaluation methods and appropriate indices for autogenous healing ability in various kinds of cementitious material. In particular, recovery on not only mechanical properties but also permeability related to durability issue should be discussed. It seems that the investigated indices can also be connected to the usage of autogenous healing ability in existing structures.

In this study, four kinds points of view was investigated of autogenous healing ability, such as index, technique, performance, and crack type. Firstly, the proposed recovery indices were used for more sensitive evaluation of

autogenous healing ability, and its credibility was confirmed by investigation of several effect on autogenous healing. The material type, effect of specimen size, effect of content of fiber type, and recuring condition on autogenous healing were investigated. Secondly, Acoustic Emission (AE) technique, which is a non-destructive method to detect the deterioration of concrete, was applied to evaluate autogenous healing ability. AE sources location and the averaged frequency was measured for comparison between before and after the recuring. Thirdly, Autogenous healing ability of Ultra High Performance Strain Hardening Cementitious Composites (UHP-SHCC), which combines excellent protective performance with a significantly higher tensile strength and strain hardening at tensile strength, was evaluated in protective performance point of view by using air and water permeability tests. Lastly, to detect the recovery of resistance against substance by autogenous healing ability, air permeability test on concrete surface was applied to evaluate the bond cracks along rebar, which is difficult to be detected from surface of concrete. And, visual the change of crack patterns before and after the healing was observed visually by ink injection.

Table of Contents

ACKNOWLEDGEMENTS	i
ABSTRACT	iii
Tables of Contents	v
List of Tables	x
List of Figures	xi
1. Introduction	1
1.1 Background	1
1.2 Autogenous Healing	3
1.2.1 Definition of Autogenous Healing	3
1.2.2 Selected Autogenous Healing	5
1.2.3 Mechanism of Autogenous Healing	6
1.2.4 Literature review	8
1.3 Objective and Contents of the Study	12

2. Evaluation of Autogenous Healing of Concrete	15
2.1 Introduction	15
2.2 Index of Autogenous Healing Ability Using Three-point Bending Test ...	17
2.2.1 Test Method for Evaluation	17
2.2.2 Target Damage (Crack) for Evaluation	19
2.2.3 Testing Procedures	19
2.2.4 Measurement of Gradient in Load-CMOD Curve	20
2.3 Applicability of Index for Various Kinds of Concrete	23
2.3.1 Experimental Program	23
2.3.2 Experimental Results	25
2.4 Modification of Recovery Index for Autogenous Healing Ability	30
2.4.1 Motivation and Objective	30
2.4.2 Modified Index Using The 2nd and The 3rd loading	30
2.4.3 Experimental Setup	31
2.4.4 Experimental Results	33
2.5 Experimental Cause Analysis of Recovery of Initial Gradient	41
2.5.1 Specimen	41
2.5.2 Ink Injection	41
2.5.3 Location of Crack Tip and Its Movement Due to Autogenous Healing	43
2.6 Summary	48

3. Evaluation of Autogenous Healing of Concrete through Modified

Recovery Index	49
3.1 Introduction	49
3.2 Effect of Specimen Size on Autogenous Healing Ability	50
3.2.1 Experimental Program	50
3.2.2 Experimental Results	52
3.3 Effect of Short Fiber Type on Autogenous Healing	56
3.3.1 Experimental Program	56
3.3.2 Experimental Results	58
3.4 Effect of Curing temperature on Autogenous Healing Ability	63
3.4.1 Experimental Program	63
3.4.2 Experimental Results	66
3.5 Summary	69

4. Evaluation of Autogenous Healing through Acoustic Emission

4.1 Introduction	70
4.2 Acoustic Emission	71
4.3 Investigation by Means of Three-point Bending Test	76
4.3.1 Experimental Setup	76
4.3.2 Experimental Results	78
4.4 Investigation by Means of Flexural Test for RC Beam	83
4.4.1 Experimental Setup	83
4.4.2 Experimental Results	87
4.5 Summary	93

5. Evaluation of Autogenous Healing Ability on UHP-SHCC	94
5.1 Introduction	94
5.2 Protective Performance	95
5.2.1 Ultra High Performance - Strain Harding Cementitious Composite	95
5.3 Recovery of Protective Performance due to Autogenous Healing	97
5.3.1 Specimens	97
5.3.2 Air Permeability Test	99
5.3.3 Water Permeability Test	102
5.3.4 Experimental Program	103
5.3.5 Experimental Results	105
5.4 Repeatability of Autogenous Healing of UHP-SHCC	112
5.4.1 Experimental Program	112
5.4.2 Experimental Results	114
5.5 Summary	120
 6. Evaluation of Autogenous Healing Ability on Bond Cracks along Rebar	 121
6.1 Introduction	121
6.2 Bond Cracks along Rebar	122
6.3 Autogenous Healing Ability on Bond Cracks	124
6.3.1 Experimental Program	124
6.3.2 Experimental Results	127
6.4 Summary	133

7. Conclusions	134
7.1 Conclusions	134
7.2 For Future Research	138
References	140

List of Tables

Table 2.1 Mix Proportions of Concrete	23
Table 2.2 Experimental Program Considering Recuring Period and Pre-cracking Age	24
Table 2.3 Mix Proportion of Normal Concrete for Modified Index	32
Table 2.4 Experimental Program for Modified Index	32
Table 3.1 Mix Proportion of Fly Ash Concrete	50
Table 3.2 Mix Proportions of Fly Ash Concrete with Different Short Fiber	56
Table 3.3 Properties of Fibers	57
Table 3.4 Test Program Considering Fiber Difference	57
Table 3.5 Mix Proportions of Normal and Fly Ash Concrete	64
Table 3.6 Experimental Program for Thermal Effect	65
Table 4.1 Mix Proportions of Normal and Fly Ash Concrete	76
Table 5.1 Mix Proportion of UHP-SHCC for Uniaxial Test	97
Table 5.2 Induced Residual Strains and Averaged Crack Widths	106
Table 5.3 Residual Strains and Averaged Crack Widths	115
Table 6.1 Mix Proportions for Tensile Test	124
Table 6.2 Cracks Deformation by Ink Injection	132

List of Figures

Figure 1.1	Crack Close Automatically with Recuring	2
Figure 1.2	Performance and Cost with Elapsed Time	2
Figure 1.3	Definition of Self Healing / Recuring (JCI-075B 2009)	4
Figure 1.4	Ideal and Selected Autogenous Healing	5
Figure 1.5	Framework of the Study	13
Figure 2.1	Shape of Specimen	17
Figure 2.2	Experimental Setup	18
Figure 2.3	Crack Depth with CMOD of 0.05mm (Age 28 days)	19
Figure 2.4	Example of Load-CMOD Curve	20
Figure 2.5	Example of Initial Gradient Using Regression of Selected Data	21
Figure 2.6	Comparison of Recuring Series and Control Series	22
Figure 2.7	Examples of Load-CMOD Curve of 7-49 Case and Control Series of Fly Ash Concrete	26
Figure 2.8	Effect of Recuring Period on Autogenous Healing Ability	27
Figure 2.9	Effect of Pre-cracking Age on Autogenous Healing Ability	27
Figure 2.10	Comparison of Before and After Recuring	31
Figure 2.11	Example of Load-CMOD Curve of Different Recuring Period with Water Recuring Condition	34
Figure 2.12	Example of Load-CMOD Curve of Different Recuring Period with Air Recuring Condition	35

Figure 2.13	Effect of Recuring Period Evaluated Modified Index	36
Figure 2.14	Example of Load-CMOD Curve of Different Pre-cracking Age with Water Recuring Condition	38
Figure 2.15	Example of Load-CMOD Curve of Different Pre-cracking Age with Air Recuring Condition	39
Figure 2.16	Effect of Pre-cracking Age Evaluated Modified Index	40
Figure 2.17	Example of Dyed Crack Area	42
Figure 2.18	Averaged Crack Depth of Each Case	43
Figure 2.19	Four Strain Gauges for Estimation of Crack Tip	44
Figure 2.20	Relation with Load and Estimated Crack Depth with Water Recuring Condition	46
Figure 2.21	Relation with Load and Estimated Crack Depth with Air Recuring Condition	47
Figure 3.1	Shapes of Each Specimen Size	51
Figure 3.2	Different Load-CMOD Curves of	51
Figure 3.3	Example of Load-CMOD Curves of Each Specimen Size with Water Recuring Condition	53
Figure 3.4	Example of Load-CMOD Curves of Each Specimen Size with Air Recuring Condition	54
Figure 3.5	Gradient Ratios of Each Specimen Size	55
Figure 3.6	Sample of PE and PVA fiber	56
Figure 3.7	Example of Load-CMOD Curves of PE Fiber	59
Figure 3.8	Example of Load-CMOD Curves of PVA Fiber	60
Figure 3.9	The Gradient Ratios of PE and PVA Fiber	62
Figure 3.10	Fly Ash Reaction Rate of 20°C and 40°C	63

Figure 3.11 Compressive Strength of Each Recuring Condition	66
Figure 3.12 Example of Load-CMOD Curves of Fly Ash Concrete	67
Figure 3.13 Example of Load-CMOD Curves of Normal Concrete	67
Figure 3.14 Gradient Ratios of Each Recuring Conditions	68
Figure 4.1 Fundamental Basic of Acoustic Emission (AE) Method	72
Figure 4.2 Shape of Specimen and AE Sensor Location	77
Figure 4.3 Example of Load-CMOD Curves of Each Concrete	78
Figure 4.4 Gradient Ratio of Each Concrete	78
Figure 4.5 AE Sources Location of Normal Concrete	80
Figure 4.6 AE Sources Location of Fly Ash Concrete	81
Figure 4.7 Averaged Frequencies of Normal Concrete	82
Figure 4.8 Averaged Frequencies of Fly Ash Concrete	82
Figure 4.9 Shape of Specimen for RC Beam	83
Figure 4.10 Experimental Setup of RC Beam Test	84
Figure 4.11 Example of Load-Displacement Curve of Each Load Case	85
Figure 4.12 AE Sensor Location of RC Beam Test	85
Figure 4.13 Different Load-CMOD Behavior of Each Crack	86
Figure 4.14 AE Sources Location (Upside) and Gradient Ratio and Residual Crack Width (Downside) of NC20 Case	88
Figure 4.15 AE Sources Location (Upside) and Gradient Ratio and Residual Crack Width (Downside) of FC20 Case	89
Figure 4.16 AE Sources Location (Upside) and Gradient Ratio and Residual Crack Width (Downside) of NC40 Case	90
Figure 4.17 AE Sources Location (Upside) and Gradient Ratio and Residual Crack Width (Downside) of FC40 Case	91

Figure 4.18 Averaged Frequencies of Each Case	92
Figure 5.1 Example of Tensile Stress-Strain Response with Difference Fiber Contest (Kamal 2008)	95
Figure 5.2 Multiple Fine Crack of UHP-SHCC	96
Figure 5.3 Shape of Uniaxial Tensile Specimen	98
Figure 5.4 Uniaxial Tensile Test Setup	99
Figure 5.5 Torrent Permeability Tester	100
Figure 5.6 Conceptual Diagram of the Chamber	101
Figure 5.7 Water Permeability Test Setup	102
Figure 5.8 Experimental Procedures of Permeability Test	103
Figure 5.9 Schematic Image of Load-Strain Curves	104
Figure 5.10 Example of Induced Cracks	104
Figure 5.11 Results of Air Permeability Tests	107
Figure 5.12 Results of Water Permeability Tests	109
Figure 5.13 Details of Cracks Before and After Recuring Observed by Using Microscope (Water Recuring Condition)	110
Figure 5.14 Image of Cracked Part by SEM (Water Recuring Condition)	111
Figure 5.15 Image of Cracked Part by EDX Spectrometry (Water Recuring Condition)	111
Figure 5.16 Back Scattered Electron Image of UHP-SHCC (407 day after casting, Hydration ratio: 51.4%)	111
Figure 5.17 Experimental Procedures of Permeability Test under Repeated Loading-Recuring Cycle	113
Figure 5.18 Example of Load-Strain Curves of Each Case under Repeated Loading-Recuring Cycle	113

Figure 5.19 Results of Air Permeability Tests (*Some of 0.2% strain case, air permeability coef. couldn't be measured)	116
Figure 5.20 Results of Water Permeability Tests	118
Figure 6.1 Simple Reaction of Bond Strength	122
Figure 6.2 Bond Cracks along rebar (Goto Cracks, 1971)	123
Figure 6.3 Shape of Specimen for Bond Cracks	125
Figure 6.4 Experimental Setup	125
Figure 6.5 Slits for Ink Injection	126
Figure 6.6 Load-Crack Opening Curves of Tensile Test	127
Figure 6.7 Surface Crack Deformation by Ink Injection	128
Figure 6.8 Results of Air Permeability Test of Normal Concrete	129
Figure 6.9 Results of Air Permeability Test of Fly Ash Concrete	130

1. Introduction

1.1 Background

Autogenous healing or Self healing of cementitious composite was well known phenomenon as recovery of cracks automatically, as shown in **Figure 1.1**. The word "Autogenous" emphasizes that cementitious composite material heals a crack without any artificial repair works. Recovery of strength, stiffness, or durability can be expected by autogenous healing.

Maintenance of concrete structures involves the increase of cost for inspection and repair of those. **Figure 1.2** shows the relation between performance and cost during elapsed time. The performance of concrete structures decreased due to initial defects or deterioration, and repair or strengthening increases the performance again, in addition to the increase of cost. If the inside crack, which is one of the major defects of concrete structures, can recover automatically without any inspection or repair works, it should be useful to decrease the maintenance cost, and it is effective for maintenance framework life cycle cost (LCC) basis.

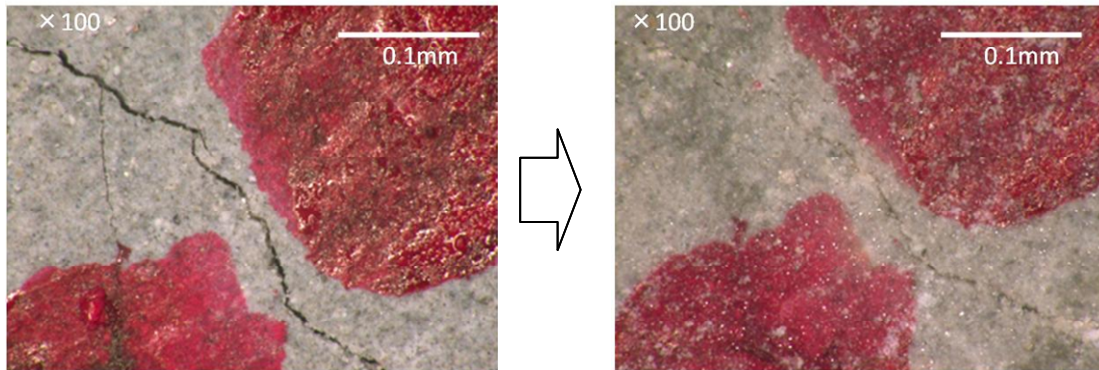


Figure 1.1 Crack Close Automatically with Recuring

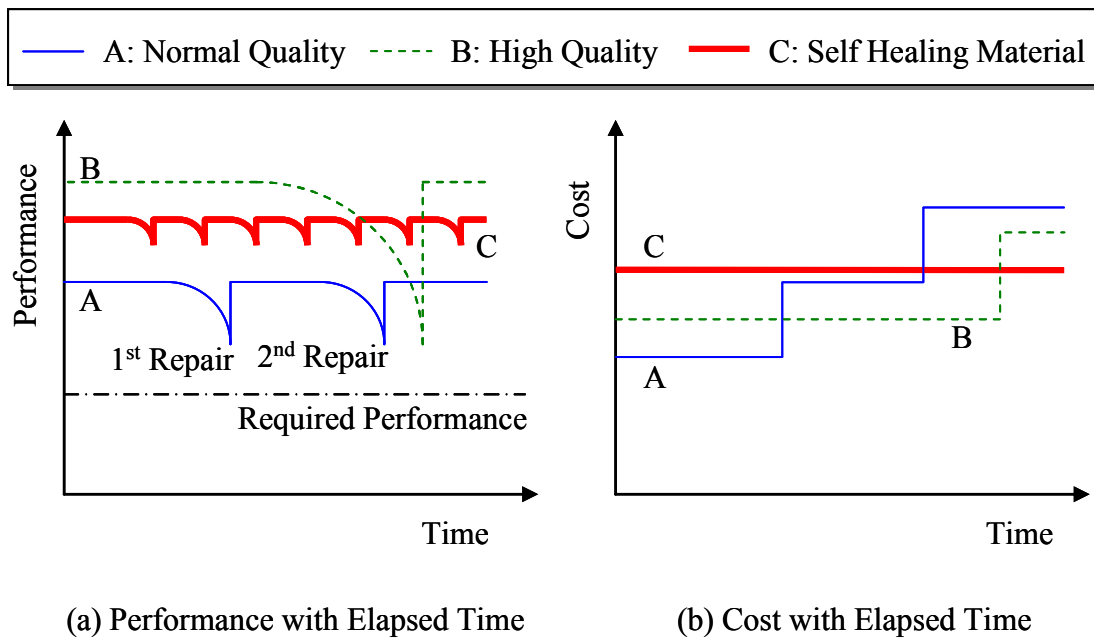


Figure 1.2 Performance and Cost with Elapsed Time

1.2 Autogenous Healing

1.2.1 Definition of Autogenous Healing

Many researchers try to classify the phenomena of autogenous healing. Japan Concrete Institute (Research activity of JCI technical committee TC-075B, Chairman: Prof. Igarashi, S. 2009) categorized the autogenous healing based on its mechanism, as shown in **Figure 1.3**. Autogenous healing is a part of Self Healing/Repairing, which includes Natural Healing, Autonomic Healing, and Activated Repairing. Natural Healing means that crack of concrete is sealed by innate characteristics of concrete, such as, re-hydration of un-hydrated cement and extraction of calcium hydroxide. Autonomic Healing means sealing of crack of concrete with proper additive or admixture to expect high potential of healing effect. An additive or admixture, such as, expansion agent, fly ash, and fresh epoxy, are used to accelerate or increase potential of these innate characteristics. And short fiber are used to control crack width. On the other hand, Activated Repairing means repair of crack using special devices for the recovery, which is not normally used in normal concrete structure, such as micro capsule with adhesive, glass pipe for adhesive injection, and thermal wire. These special devices are set up initially with concrete casting, and act automatically with crack occurrence.

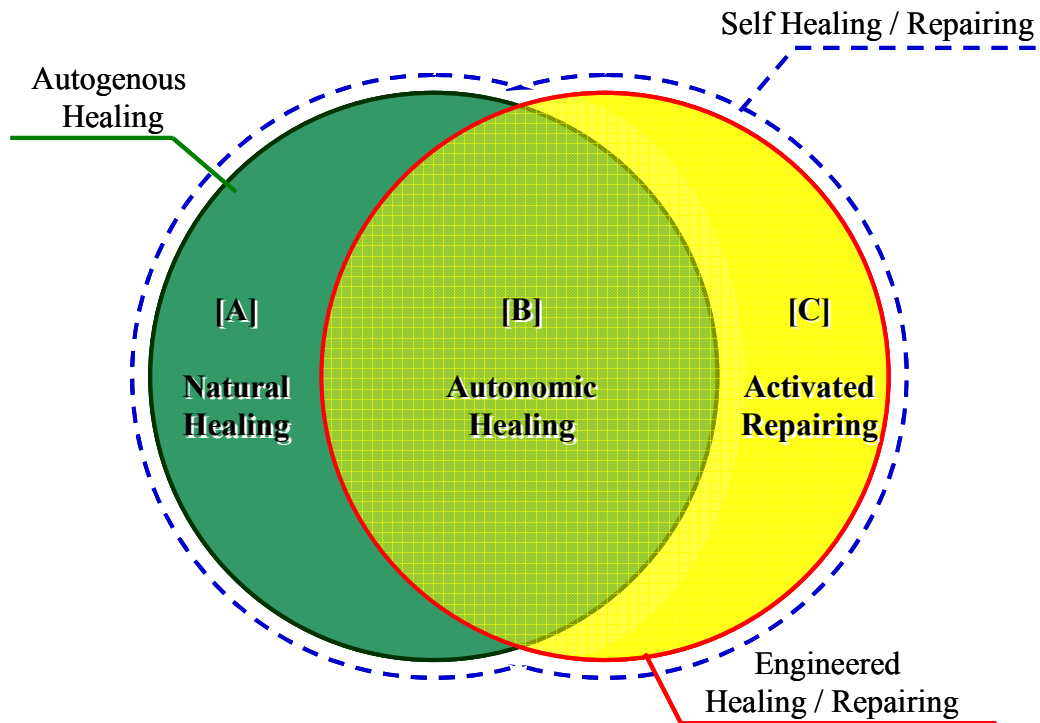


Figure 1.3 Definition of Self Healing / Recuring
(JCI-075B 2009)

Natural Healing and Autonomic Healing for the crack sealing in concrete, and are defined as Autogenous Healing. And, Autonomic Healing and Activated Repairing with some artificial efforts are classified to Engineered Healing/Repairing.

This study focused on Autogenous Healing, thus only Natural Healing and Autonomic Healing were considered.

1.2.2 Selected Autogenous Healing

In general, most people imagine that all physical properties can recover the damaged concrete to an original level by autogenous healing, as shown in **Figure 1.4-(a)**. It should be noted that it is difficult to recover all up to the original level. However, the specific performance such as water tightness is also sufficient based on performance based design concept, as shown in **Figure 1.4-(b)**. For example, there is a concrete structure with water leakage due to cracking. Only water tightness should be recovered urgently, thus strength or stiffness is not concerned.

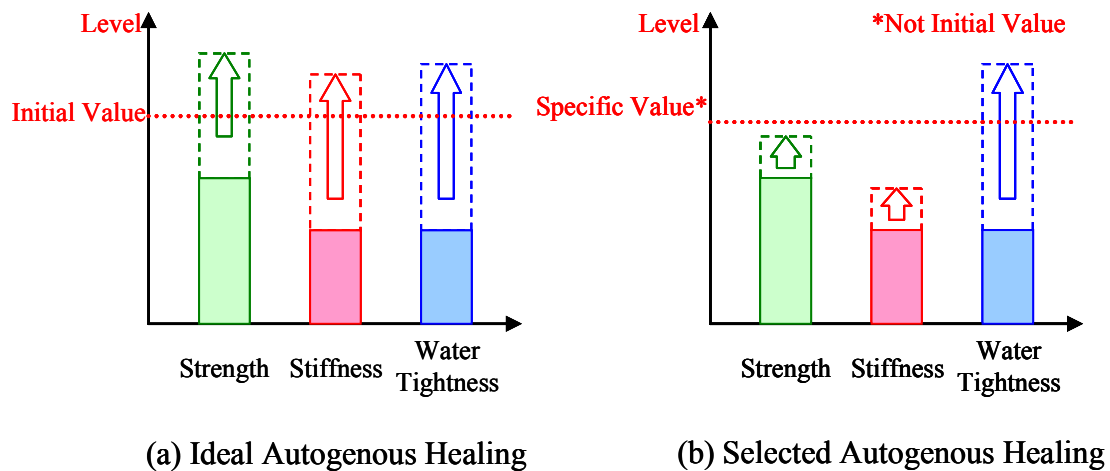


Figure 1.4 Ideal and Selected Autogenous Healing

1.2.3 Mechanism of Autogenous Healing

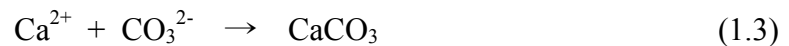
Several possible causes of autogenous healing are reported. Firstly, supposable mechanism is re-hydration of un-hydrated cements. Relatively larger cement particles of concrete could not be possible to hydrate perfectly, and it still remains despite longer age. If a crack crosses the un-hydrated cement particle, it reproduces a chance to react with water that penetrated into the crack, and it produces C-S-H or Ca(OH)_2 . Secondly, the formation of calcium hydroxide can be considered. Calcium hydroxide, which is a reaction product of the hydration of cement, can dissolve in water, and be separated to calcium and hydroxide or precipitate to calcium hydroxide as equation (1.1).



Carbon ion was supplied from CO_2 -containing water as equation (1.2)



Chemical reaction between calcium and carbon ion generates calcium carbonate as equation (1.3)



These reactions occurred inside of crack surfaces, and help to seal the crack. Generated products by these two main mechanisms make crack more smaller,

and eventually the crack surfaces swell. Crack will be eventually healed with this swelling of the cement matrix.

Re-hydration of un-hydrated cements depends on existence rate of un-hydrated cement, thus it can be more expected in concrete structure with early age. On the other hand, forming calcium hydroxide can occur at any time regardless of age. In addition, forming non-water-soluble calcium silicate hydrates due to pozzolanic reaction by included admixture (fly ash or silica fume) is reported to help or accelerate autogenous healing (Termkhajornkit et al. 2009)

1.2.4 Literature review

For evaluating autogenous healing ability and limit, various experimental studies were proposed and investigated. There is a lot of discussion about two main mechanisms of autogenous healing, such as re-hydration of un-hydrated cement and formation of calcium carbonate (Edvardson et al. 1996, Neville 1995, 2002). Edvardson reported that re-hydration of un-hydrated cement and swelling of the cement matrix can be neglected compared to formation of calcium carbonate. Neville, however, concluded that re-hydration of un-hydrated cement is primarily in autogenous healing only for young concrete. Several required circumstance for autogenous healing have been mentioned, such as, presence of water, crack width, water pressure, and stability of the crack, etc. (Lauer 1956, Van Breugel 2003, Edvarsen 1996). Lauer emphasized the importance of relative humidity for autogenous healing. Van Breugel mentioned that the recoverable limit of crack width is under 0.2mm with stability condition, but it also depends on other condition, mainly the water pressure.

Regarding the indices for evaluation of autogenous healing ability, many researchers tried to find appropriate indices, such as Strength, stiffness, and water tightness. Evaluating the recovery of strength is easiest way to for investigation. Jawad and Hadded use compressive strength (Jawad et al 2005, Hadded and Bsoul 1999). Jawad investigates the recovery potential of early age of concrete with different W/C ratio by evaluation of compressive strength, and Hadded investigates the recovery of compressive strength of the fiber reinforced concrete. Both of them use Ultra sonic velocity to prove the recovery reaction. Jacobsen compares the change of resonance frequency and compressive strength before and

after deterioration by free and thaw (Jacobsen et al. 1995). A loss of resonance frequency due to deterioration by rapid freeze and thaw was almost fully recovered, but the compressive strength recovered only 4-5% during healing. Although the compressive strength is general standard for expression of performance of concrete, it is not easy to inspect the damage under compressive force. An additional method, such as resonant frequency measurement, is applied to explain and prove the healing effect. Tensile strength is normally not easy to apply to concrete, but recently it is used for evaluation of autogenous healing of strain hardening material, such as ECC. Yang uses the tensile strength and resonant frequency for evaluation of the self-healing of ECC (Yang et al. 2009).

Bending strength was also used for the index because of ease of crack control of three- or four- point bending test. Granger investigates the recovery of bending strength of UHPC with the different curing aging and different curing condition (Granger et al. 2005). The mechanical reloading behavior was different with different ageing times and recuring condition, and reloading peak load increased with ageing time. He also uses Acoustic Emission system, and micro-cracking maps indicated that crystal have precipitated in the crack during storage in only water recuring condition. Schlanger uses the mechanical behavior of three-point bending test for investigation of crack healing of early age cracks, and he investigates the influence of compression force to close the crack (Schlanger et al. 2005, 2006). Matusita also uses the bending strength to investigate the recovery by autogenous healing of different cement property (Matusita et al. 2003). Previous studies perceive that the ageing effect of un-cracked part is needed to consider for evaluation healing effect, and more

sensitive index or method are needed.

In many research, water tightness was used for evaluation of healing effect. Jacobsen also chloride permeability (Jacobsen et al. 1996). By three months in water, the chloride permeation was recovered to 28-35% of damaged condition, and permeation time also increased. Homma investigates the self-healing capability of fiber reinforced cementitious composites (FRCC and HFRCC) using water permeability test (Homma et al. 2009). Coefficient of water permeability was decreased with recuring time, and he shows that the self-healing products are calcium carbonate crystals by means of raman spectroscopy analysis. Hosoda and Yamada also use the accumulation of water flow to investigate self healing property with expansive additive, and they mention that the water flow was decreased due to sealing of crack (Hosoda et al. 2007, Yamada et al. 2007). You investigates the promoted material blended with carboxylic acid on self healing, and the water permeability and observation using SEM are used (You et al. 2007). Wang performs the water absorption test and the chloride permeability test to investigate self healing effect on reinforced corrosion of concrete, and he also uses SEM observation to confirm generated products during healing (Wang et al. 2007). As previous studies, a permeability test is normally applied to strain hardening material, and not only water or chloride permeability test but also air permeability test can be applied to other strain hardening materials such as, UHP-SHCC.

Recently, a visual inspection was applied with development of Optical observation equipment. As described previously, many research uses microscopic, SEM, or XRD to provide the healing effect. Nijland confirms that self healing

may be effected by the formation of either new Ca-carbonate, CaCO_3 , and Ca(OH)_2 by observation of microscopic (Nijland et al 2007). Kishi investigates the incorporating expansive agent on self healing by using microscopic and XRD observation (Kishi et al. 2007). In addition, non-destructive method was also applied to evaluate or investigate healing effect, such as Ultra sonic method or Acoustic Emission technique, etc.

For the improvement of potential of material itself, not only normal concrete but also high strength concrete, fly ash concrete and fiber reinforced concrete were a target. In particular, crack width control is one of the main factors to obtain the effective autogenous healing, and the use of fiber reinforced cementitious composites with multiple fine cracks was proposed.

Other healing mechanisms are also reported in engineered healing or repairing point of view. It was experimentally investigated that bacteria mixed with concrete helps to close a crack in concrete (Bang et al. 2001, Rodriguez-Navarro et al. 2003, Schlangen et al. 2007). Li used the grass fiber containing a chemical, which is broken with the cracking and close the crack with chemical reaction (Li et al. 1998). Nishiwaki used the heating device and organic film pipe with repair agent. The heating device senses crack occurring by increase of its electric resistance, and heats the organic film to release repair agent out (Nishiwaki et al. 2006). In addition, several other methods used capillary tube and grass capsule are also proposed and investigated.

Only a few analytical study on autogenous healing focusing on re-hydration of cementitious composite (Ye, G. and Van Breugel 2007, Gue Z.Q et al. 2007) was proposed, and further studies are needed.

1.3 Objective and Contents of the Study

The purpose of this study is to investigate the evaluation methods and appropriate indices for autogenous healing ability in various kinds of cementitious material. In particular, recovery not only mechanical properties but also permeability related to durability issue are discussed. It seems that the investigated indices can also be connected to the usage of autogenous healing ability the existing structures. **Figure 1.5** shows a frame of this study.

In Chapter 1, the introduction of the dissertation including background of the study, a definition of autogenous healing, literature review, and study objective is described.

In Chapter 2, recovery indices for autogenous healing were proposed. The initial gradient of the Load-CMOD curve obtained from a three-point bending test was used for a recovery index to represent autogenous healing ability. It was confirmed that recovery evaluated by the proposed index has good agreement with the observation experimentally.

In Chapter 3, the applicability of the proposed index was investigated by using various kinds of cementitious composites. In particular, the effect of specimens size, contents of short fiber and recuring temperature on autogenous healing ability were evaluated by the proposed index.

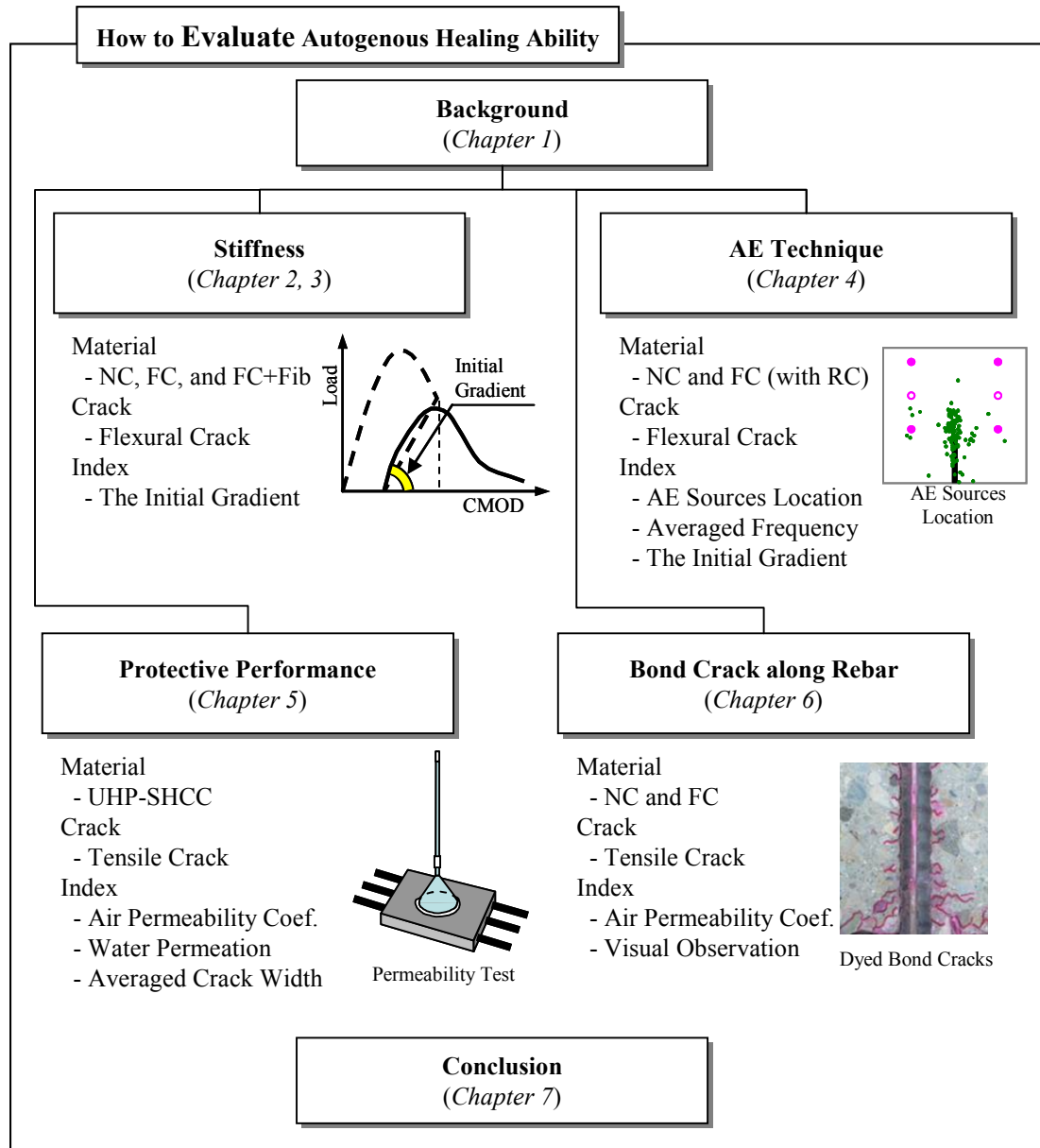


Figure 1.5 Framework of the Study

In Chapter 4, Acoustic Emission (AE) technique was used for investigation of autogenous healing ability. Autogenous healing phenomena in flexural test of plain concrete and reinforced concrete (RC) beam were clarified by means of AE technique.

In Chapter 5, autogenous healing ability of UHP-SHCC was investigated in protective performance point of view. The change of air permeability coefficients and water permeation of UHP-SHCC was observed by autogenous healing ability.

In Chapter 6, autogenous healing ability of bond crack along the rebar was investigated. It should be an effective usage to close the crack automatically. Air permeability test was applied to detect the damage due to micro crack and recovery by autogenous healing ability. And also, the change of crack patterns before and after the healing was observed visually by ink injection.

In Chapter 7, the concluding remarks and proposal for the future works on this study were given.

2. Evaluation of Autogenous Healing of Concrete

2.1 Introduction

Because it is potentially difficult to expect the recovery of all material characteristics by autogenous healing phenomenon, recovery of the specific characteristic, such as strength, stiffness, or durability, should be accepted as a minimum requirement. Normally the recovery of strength and stiffness in bending test was used to evaluate autogenous healing ability. Garanger showed the recovery in strength and stiffness by autogenous healing (Garanger et al. 2005). However, it is difficult to evaluate autogenous healing ability from recovery in strength of concrete, since strength depends on not only a material property but also mechanical reaction in composite element of concrete, and this non-homogeneous characteristic of concrete makes strength result scatter larger. Another index stiffness can be calculated using load and Crack Mouth Opening Displacement (CMOD) data in three-point bending test. Two parameter model (Jenq and Shah, 1985) showed that the compliance between load and CMOD in

three-point bending test directly related to stiffness of material. Stiffness has higher sensitivity to evaluate autogenous healing ability than strength, and increased stiffness due to autogenous healing can be used structurally.

In this chapter, two recovery indices for autogenous healing will be proposed. The initial gradient of the Load-CMOD curve obtained from a three-point bending test for measuring the fracture energy of concrete was used for recovery index due to autogenous healing ability. Effects of concrete type (Normal concrete, Fly ash concrete, Fly ash concrete with short fiber), the recuring period and the pre-cracking age on autogenous healing were investigated using the proposed index.

2.2 Index of Autogenous Healing Ability Using Three-point Bending Test

2.2.1 Test Method for Evaluation

Figure 2.1 shows the shape of specimens and Figure 2.2 shows the experimental setup. Three-point bending test in accordance with JCI (JCI-S-001-2003), which was specified for the measurement of fracture energy of concrete, was used in this chapter. Rectangular specimens with the size of $400 \times 100 \times 100$ mm were prepared. A loading span was 300 mm, and the mechanical jack with a load cell was used for the loading. A capacity and a sensitivity of the load cell were 50 kN and 0.025 kN, respectively. A notch having a depth of 33 mm (one third of specimen depth) and a thickness of 3 mm was induced at the midpoint in all specimens. Each notch was produced by a concrete cutter before a pre-cracking. A clip gauge, with a capacity of 5 mm and a sensitivity of $1/1000$ mm, was used to measure the CMOD.

The initial gradient calculated from the Load-CMOD curve was used as an index of autogenous healing. Actually, an uniaxial tensile stress induced by

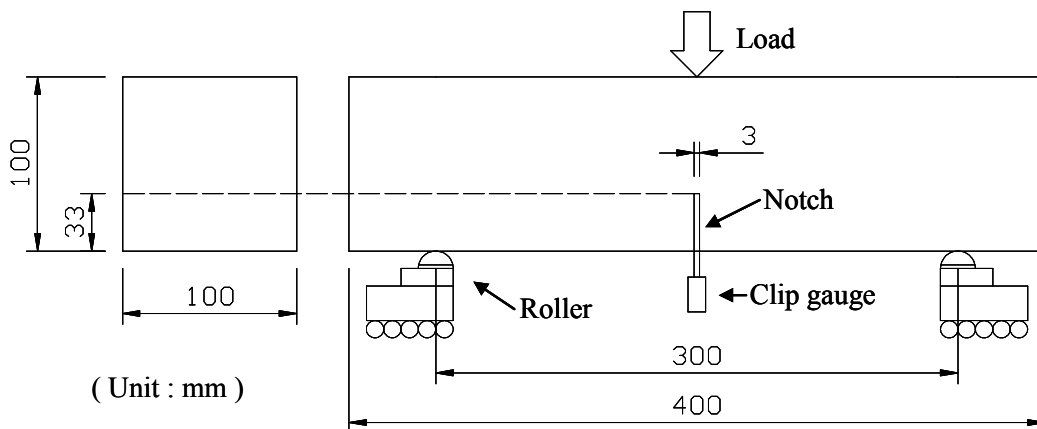


Figure 2.1 Shape of Specimen

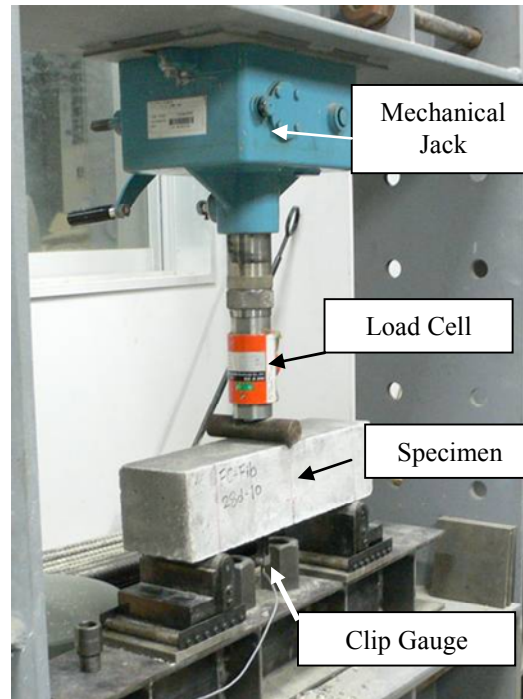


Figure 2.2 Experimental Setup

uniaxial tensile test is more suitable for investigation of the autogenous healing ability. Since nature of concrete is heterogeneous characteristic, it is difficult to conduct ideal uniaxial tensile test, and to control crack width. On the other hand, crack width in the flexural test could be controlled by measuring CMOD using a clip gauge. Tensile stress of three-point bending test is dominant and induces mode I fracture mainly. This is the reason why three-point bending test was adopted in this chapter. Another reason is a micro crack in fracture process zone might be effective target for autogenous healing. It seems that the test method has a higher sensitivity of the micro crack including the recovery due to autogenous healing.

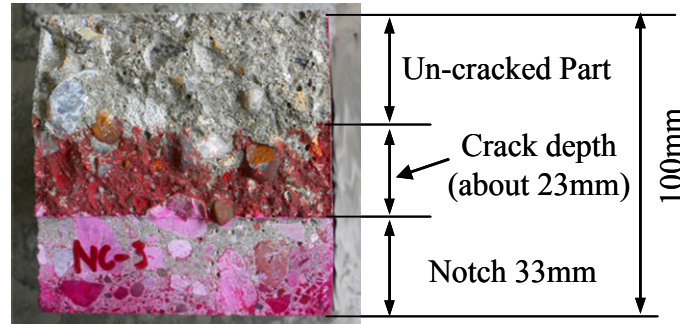


Figure 2.3 Crack Depth with CMOD of 0.05mm (Age 28 days)

2.2.2 Target Damage (Crack) for Evaluation

Damage level is important factor in investigation of autogenous healing ability. Autogenous healing effect will be smaller than age effect with an insufficient damage, and an over damage will makes out of range of healing limit. Unloading point of CMOD of 0.05mm was used for damage level in this study referred previous study (Granger et al. 2005, Schlangen et al. 2005, Matsusita et al. 2003) It seems to be a proper damage level because mechanical behavior due to heterogenous characteristics of concrete influences behavior after a peak load, although Granger used approximately 60% of peak load for unloading point in UHPC. And damage level with CMOD of 0.05mm was confirmed as 20~25mm of crack depth from edge of notch by observation using ink injection, as shown in **Figure 2.3**.

2.2.3 Testing Procedures

The pre-cracking test was performed at a scheduled age, and an unloading point was at CMOD of 0.05mm. After the pre-cracking test, specimens were recured in water or air condition. Water recuring condition is the same condition as the initial curing, in water of 20°C, and air recuring condition is performed in the recuring room in relative humidity of 70~80% and temperature of 20°C.

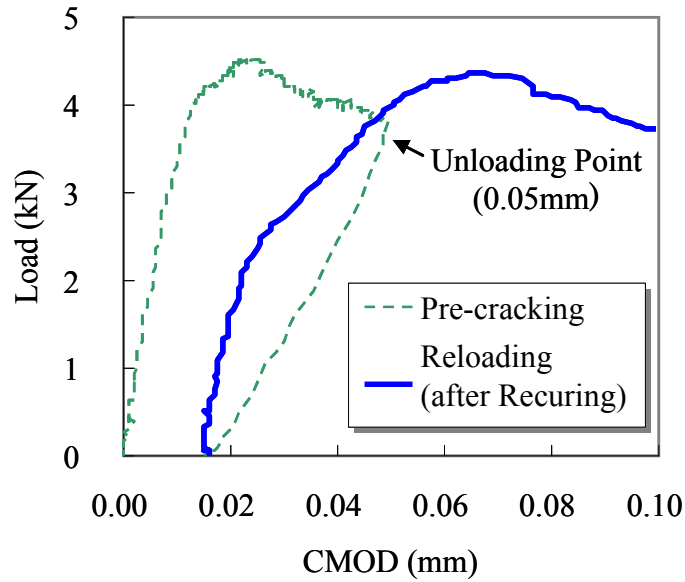


Figure 2.4 Example of Load-CMOD Curve

The reloading test was performed after a scheduled recuring period. **Figure 2.4** shows the example of the Load-CMOD curve of all sequences. The Load and CMOD were measured at every sequence, and residual CMOD was also checked after the unloading.

2.2.4 Measurement of Gradient in Load-CMOD Curve

In this chapter, the initial gradient of the Load-CMOD curve was adopted to evaluate autogenous healing ability. This "gradient" is an inverse value to compliance in two parameter model (Jenq and Shah 1985), which is a rate of CMOD to load. The gradient was used to evaluate autogenous healing ability for the sake of clarity, although compliance is inversely proportion to stiffness. A material stiffness is usually determined by measuring a definite gradient, which is decided by two points in stress-strain curve. In this chapter, the gradient was determined by measuring a secant stiffness of the reloading after the recuring. A secant stiffness used data which ranged between origin and CMOD of

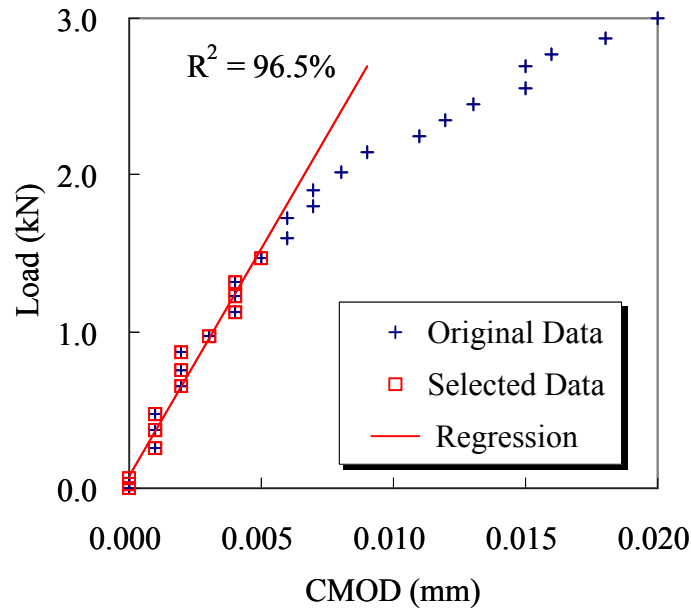


Figure 2.5 Example of Initial Gradient Using
Regression of Selected Data

0.004~0.006mm of the Load-CMOD curve. Some scatter from sensitivity limit of sensor and gauge were converted by using the regression with of more than 95% coefficient of determination. **Figure 2.5** shows an example of the initial gradient, which is determine by the regression of the selected data of the reloading test. The initial gradient obtained from this process was used for the evaluation.

The difference of each the initial gradient was used for the index of autogenous healing ability. Schematic image of the evaluation is shown in **Figure 2.6**. The pre-cracking test of the recuring series was performed at m days after casting, which means the age of m days. All specimens of the recuring series had recuring for r days after the pre-cracking test. The reloading test was performed at n days ($n = m + r$) after the recuring. The initial gradient G_R was calculated from the reloading test after the recuring. On the other hand, both the

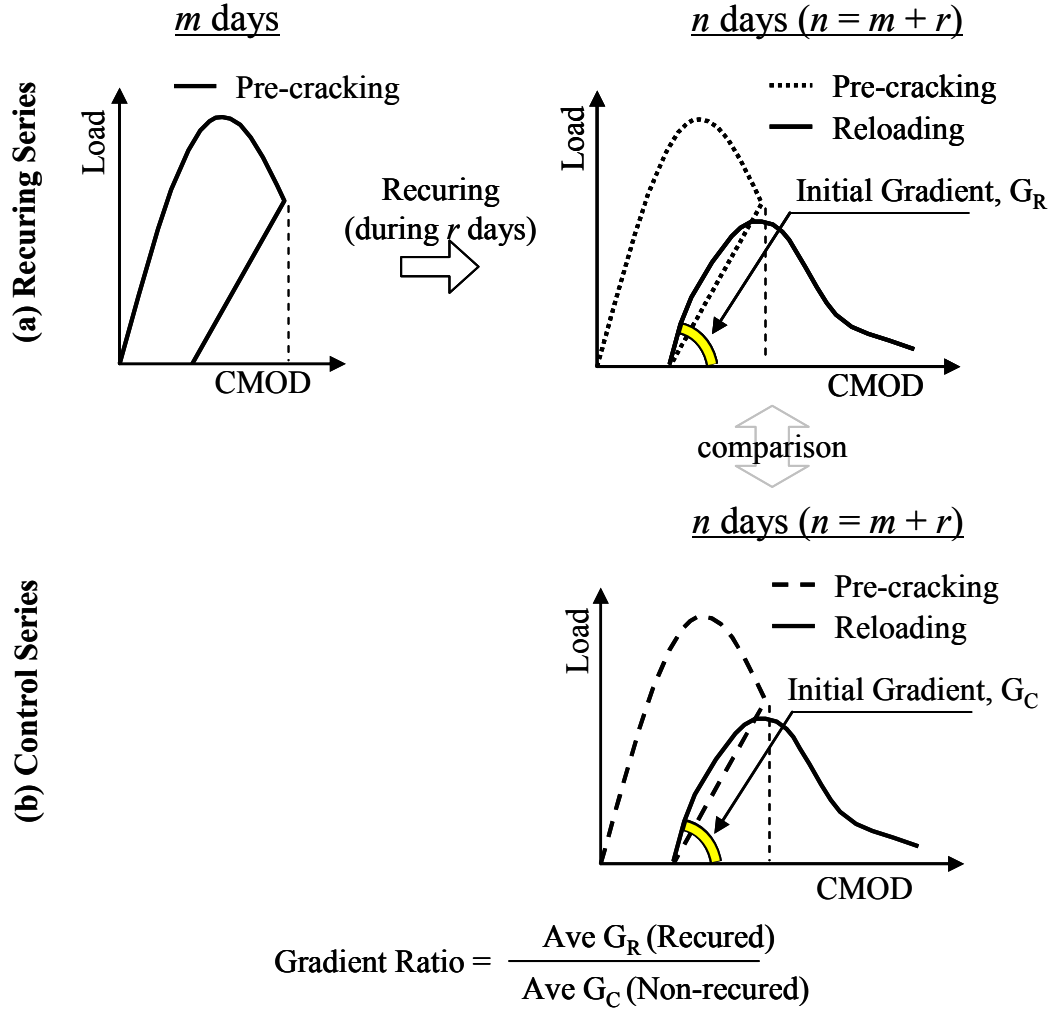


Figure 2.6 Comparison of Recuring Series and Control Series

pre-cracking test and the reloading test of the control series were performed at n days. The initial gradient G_C was also calculated from the reloading test without any recuring process. If the initial gradient G_R of the recuring series is larger than the initial gradient G_C of the control series, it means the pre-crack recovered during recuring process by autogenous healing.

2.3 Applicability of Index for Various Kinds of Concrete

2.3.1 Experimental Program

Three kinds of concrete, which were a normal concrete (NC), a fly ash concrete (FC) and a fly ash concrete with short Fiber (FC+Fib) were used to investigate effect of the pre-cracking age and the recuring period on autogenous healing ability. It has been reported that a fly ash mixed in concrete is effective for improving various properties of concrete, and C-S-H gel produced by the pozzolanic reaction of fly ash may seal micro cracks (Termkhajornkit, 2006 and 2009). And, fly ash helps to increase autogenous healing ability more than a normal concrete, because pozzolanic reaction is also major mechanism of autogenous healing. It was reported that short fiber help autogenous healing (Homma et al, 2009). Fibers bridging across a crack help fixation of calcium carbonate during recuring process, which is another major mechanism of autogenous healing. So, fly ash with short fiber was prepared. Mix proportions of each concrete are shows in **Table 2.1**.

The water to cement ratio (W/C) was 45% in all mixes. An ordinary Portland cement with a density of 3.15g/cm^3 , sand with surface-dry density of 2.51g/cm^3 , a coarse aggregate with surface-dry density of 2.58g/cm^3 and the

Table 2.1 Mix Proportions of Concrete

Case	W/C (%)	Unit Content (kg/m^3)								
		Water	Cement	Sand	Gravel	Fly ash	AE	Fiber	AWR [†]	AEA [‡]
NC	45	175	389	780	879	-	-	-	1.22	0.0156
FC	45	175	389	624	879	137	0.97	-	-	-
FC+Fib	45	175	389	618	879	137	0.97	2.43	-	-

AWR[†] : Water Reducing Agent

AEA[‡] : Air Entraining Agent

maximum size of 20mm were used. A fly ash (the Type II specified in JIS A 6210), which has a density of 2.38g/cm^3 , was used for the fly ash concrete and the fly ash concrete with short fiber, and the replacement ratio of fly-ash to sand was 20%. A polyethylene fiber (PE Fiber) (length of 3mm, diameter of 0.012mm, elastic modulus of 88GPa, tensile strength of 2700MPa and density of 0.97g/cm^3) was used for fly ash concrete with short fiber. A volume fraction of the fiber was 0.2%. In order to obtain better workability, AE water reducing agent (AWR) and an air entraining agent (AEA) were used.

Table 2.2 shows the test program having different recuring period and the pre-cracking age. The case name was defined using the pre-cracking test days (m days) and the reloading test days (n days), respectively. At the pre-cracking test day, a crack was induced in the specimen. An arrow between the pre-cracking

Table 2.2 Experimental Program Considering Recuring Period and Pre-cracking Age

Type	Case	Days after Casting									
		7		28		49		70	91		112
Recuring Period	7-28	Pre	Water → Air	Re							
	7-49	Pre	Water → Air			Re					
Pre- cracking Age	7-28	Pre	Water → Air	Re							
	28-49			Pre	Water → Air	Re					
	49-70					Pre	Water → Air	Re			
	91-112								Pre	Water → Air	Re
Control				C		C		C			C

Pre : Pre-cracking test (m days)

Re : Reloading test (n days)

C : Pre-cracking test and Reloading test without recuring (n days)

Water
→
Air : Recuring in water or air condition during r days

test days and the reloading test days means the recuring period (r days). For example, there was 21 days for the recuring period in the 7-28 case.

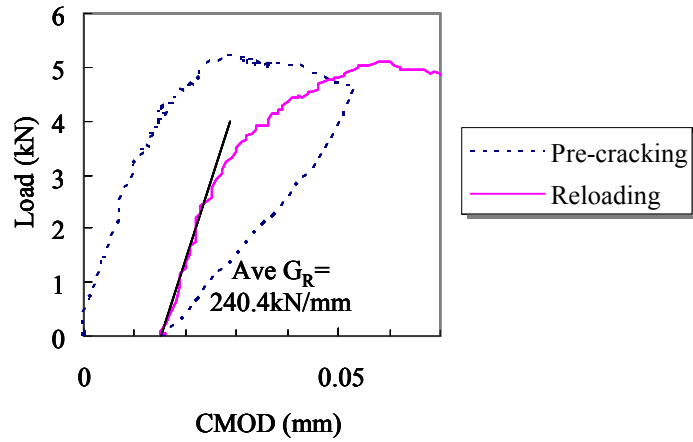
The recuring was performed in either air recuring condition or water recuring condition. Specimens of the control series had no recuring process, because the pre-cracking test and the reloading test were performed at the same days (n days). Five specimens were tested in each case.

Two factors were mainly considered for the test program; the recuring period and the pre-cracking age. The 7-28 case and the 7-49 case were prepared to investigate the effect of the recuring period on autogenous healing ability. The pre-cracking tests of both cases were performed at 7 days of age, but the recuring periods were 21 days and 42 days, respectively. On the other hand, the 7-28, 28-49, 49-70, and 91-112 cases were prepared for assessing the effect of the pre-cracking age on autogenous healing ability. All specimens were recured for 21 days, but the pre-cracking was performed at 7 days, 28 days, 49 days, and 91 days after casting.

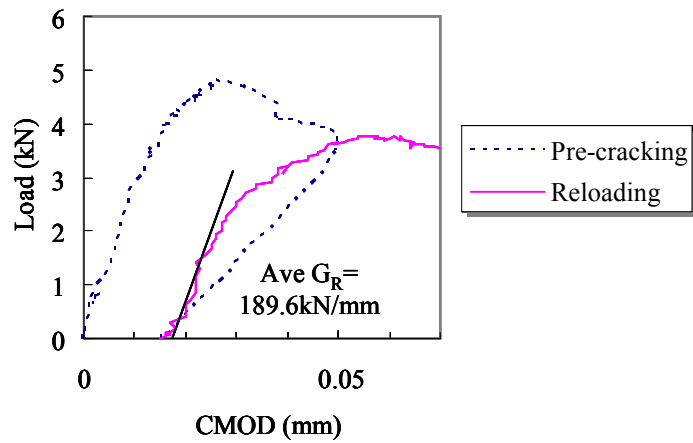
2.3.2 Experimental Results

(a) Effect of Recuring Period

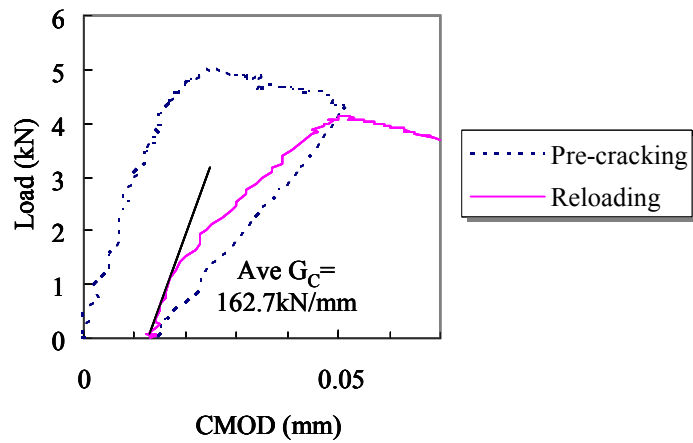
Figure 2.7 shows the examples of the Load-CMOD curves of the fly ash concrete. **Figures 2.7-(a)** and **-(b)** illustrate the results of the 7-49 case with water and air recuring condition, respectively, and **Figure 2.7-(c)** gives the results of the control series to compare with the recuring series. The averaged G_R and G_C are the averaged value of five specimens. The initial gradient ratio of the 7-49 case of fly ash concrete were calculated as the averaged G_R of the water or air recuring series divided by the averaged G_C of the control series.



(a) Example of Water Recuring Series (FC7-49-W2)



(b) Example of Air Recuring Series (FC7-49-A2)



(c) Example of Control Series (FC49-C1)

Figure 2.7 Examples of Load-CMOD Curve of 7-49 Case and Control Series of Fly Ash Concrete

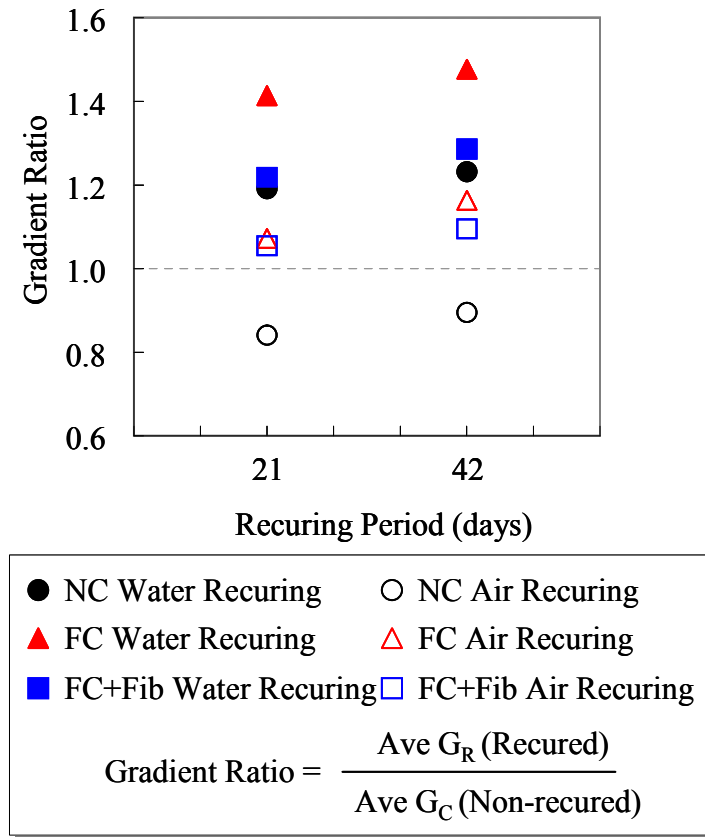


Figure 2.8 Effect of Recuring Period on Autogenous Healing Ability

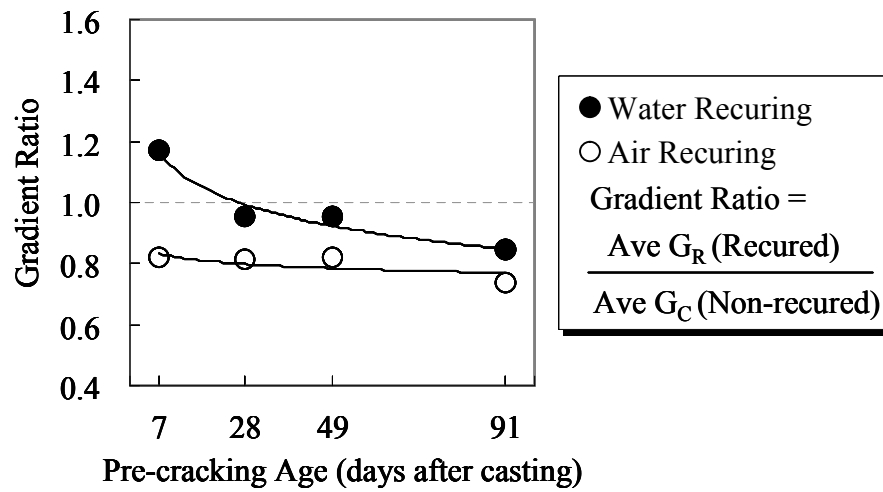
Figure 2.8 shows the gradient ratios depending on the recuring period, which were the ratio of the 7-28 case and the 7-49 case to control case. The initial gradients G_R of the 7-28 case and the 7-49 case were obtained from recured specimens in water and air condition, but the initial gradient G_C of the control series had no recuring process. If the gradient ratio of G_R to G_C is over 1.0, it can be considered that pre-crack was recovered by autogenous healing.

The averaged gradient ratios of the 7-49 case, which had the recuring period for 42 days, were higher than those of the 7-28 case, which had 21 days recuring period. This results were same regardless of material difference and recuring condition, and it means that the gradient ratio increased with increasing of the recuring period. And the gradient ratios with water recuring condition

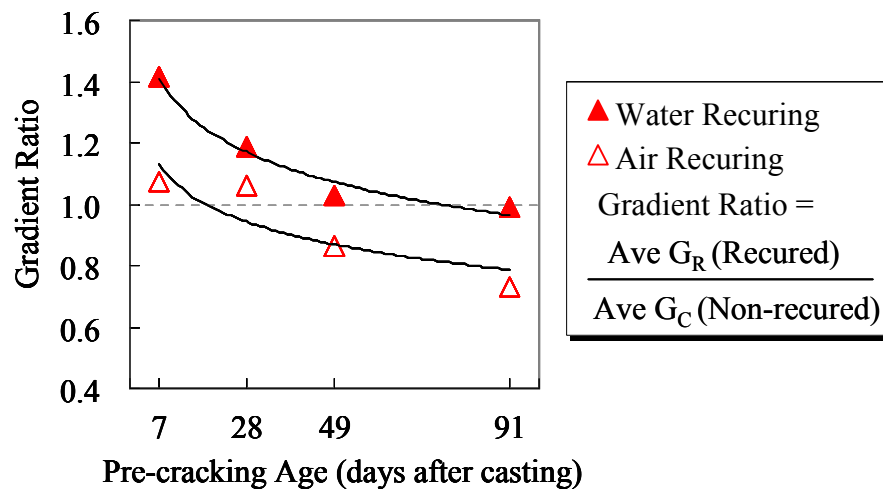
were higher than those with air recuring condition, and it indicates that the state of the water recuring conditions is more efficient to autogenous healing. In addition, the gradient ratios with fly ash concrete and fly ash concrete with short fiber were over 1.0 regardless recuring condition, and higher than those of normal concrete. It seems that pozzolanic reaction by fly ash affects the autogenous healing during the recuring period.

(b) Effect of the Pre-cracking Age

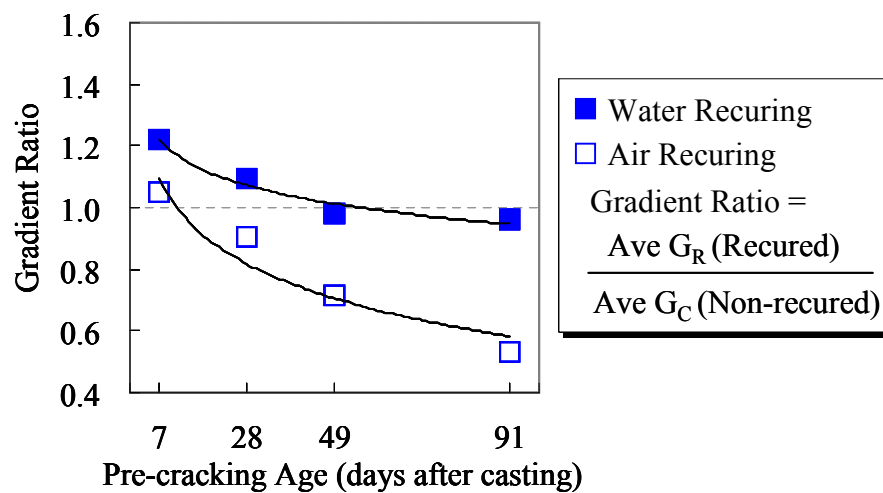
Figure 2.9 shows the gradient ratios of each material depend on the pre-cracking age. The gradient ratios decreased with increasing of the pre-cracking age regardless of material difference and recuring conditions, and these values showed trend of converge with increasing of the pre-cracking age. Same trend has been reported (Granger, 2006). The gradient ratio with water recuring condition was higher than those with air recuring condition at all material. It indicates that water recuring condition is more effective in autogenous healing than air recuring condition. Comparing to normal concrete (NC), fly ash concrete and fly ash concrete with short fiber showed higher gradient ratio regardless of the pre-cracking age, and the convergent value of the gradient ratios also higher. The gradient ratios of fly ash concrete with short fiber were also higher than those of normal concrete, but lower than those of fly ash concrete without fiber. And fly ash concrete with short fiber in air condition had significant change comparing to the other case. One of the reasons seems to be that PE fiber does not have hydroxide (OH^-) and it could not enough to be nuclei for recovery during the recuring period. This will be considered in the next sub chapter.



(a) Normal Concrete (NC)



(b) Fly Ash Concrete (FC)



(c) Fly ash Concrete with Short Fiber (FC+Fib)

Figure 2.9 Effect of Pre-cracking Age on Autogenous Healing Ability

2.4 Modification of Recovery Index for Autogenous Healing Ability

2.4.1 Motivation and Objective

Effect of the recuring period and the pre-cracking age were investigated by the proposed index (Comparing to both the initial gradient of recured series and that of control series). Although typically reasonable results was deduced by the proposed index, but several problem were noted as follows; Two different specimens should be prepared, such as specimens of the recuring series and specimens of the control series. Because specimens are different, the gradient ratio should be calculated by the averaged value of each series, and it could not possible to consider the scatter of each case.

In this section, modified index, which can evaluate autogenous healing ability for each specimen, will be proposed.

2.4.2 Modified Index Using The 2nd and The 3rd loading

In contrast to the previous proposed index, the modified index uses the gradient just after the pre-cracking test, not to use the control series, as shown in **Figure 2.10**. The 2nd loading test was performed just after the pre-cracking test, and both tests were performed at m days. The initial gradient G_2 was calculated from the 2nd loading test, and an unloading point of the 2nd loading test was the same with that of the pre-cracking test. All specimens had recuring process during r days after the pre-cracking test and the 2nd loading test. The initial gradient G_3 was calculated from the 3rd loading test after the recuring. If the initial gradient G_3 of after the recuring is larger than the initial gradient G_2 of before the recuring, it means that pre-crack recovered during recuring process by autogenous healing ability. The gradient ratio of G_3 to G_2 was calculated for

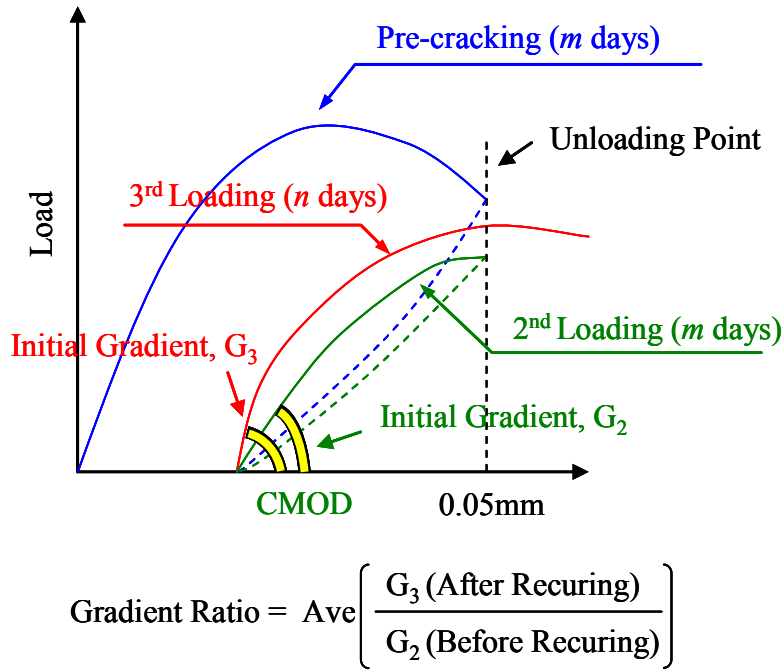


Figure 2.10 Comparison of Before and After Recuring

a quantitative comparison.

While modified index can directly compare G_2 and G_3 from the same specimen, ageing phenomena of an un-cracked part of specimens can affect to the 3rd loading test. However, a recured part seems to be usually weaker than an un-cracked part, and the initial behavior of the Load-CMOD curve mainly depends on the property of a recured part. Thus, a influence of ageing of un-cracked part can be disregardable in measurement of the initial gradient G_3 from the 3rd loading test.

2.4.3 Experimental Setup

Normal concrete was used to examine the applicability of modified index for investigation of autogenous healing ability. The water to cement ratio (W/C) was 45%, and an ordinary Portland cement with a density of 3.15g/cm^3 , sand with

Table 2.3 Mix Proportion of Normal Concrete for Modified Index

W/C (%)	Unit Content (kg/m ³)					
	Water	Cement	Sand	Gravel	AWR [†]	AEA [‡]
45	175	389	780	879	1.22	0.156

AWR[†] : Water Reducing Agent

AEA[‡] : Air Entraining Agent

Table 2.4 Experimental Program for Modified Index

Type	Case	Days after Casting						
		7		28		49		70
Recurring Period	7-28	Pre 2nd	→	3rd				
	7-49	Pre 2nd	→			3rd		
	7-70	Pre 2nd	→					3rd
Pre- cracking Age	7-28	Pre 2nd	→	3rd				
	28-49			Pre 2nd	→	3rd		
	49-70					Pre 2nd	→	3rd

Pre : The pre-cracking test (m days)

2nd : The 2nd loading test (m days)

3rd : The 3rd loading test (n days)

→ : Recuring in water or air condition during r days

surface-dry density of 2.51g/cm³, a coarse aggregate with surface-dry density of 2.58g/cm³ and the maximum size of 20mm were used, and these were the same with previous tests in Chapter 2.3. **Table 2.3** shows the mix proportion of normal concrete.

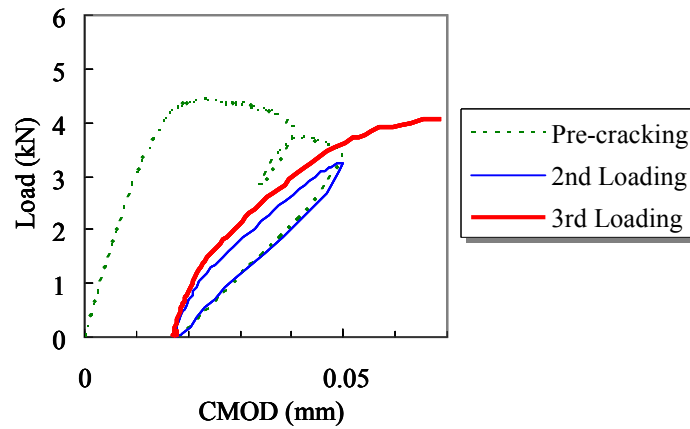
Table 2.4 shows the test program considering the recurring period and the pre-cracking age for modified index. The 7-28, 7-49, and 7-70 cases were prepared for the investigation of the effect of the the recurring period on

autogenous healing ability, and the 7-28, 28-49, and 49-70 cases were prepared for investigation of the effect of the pre-cracking age on autogenous healing ability, respectively. Three specimens were tested in each case. As described, each case had the pre-cracking test and the 2nd loading test at the same day (m days), after that specimens were recured in water or air condition up to the scheduled days (r days). The initial gradient G_2 can be calculated from the Load-CMOD curve of the 2nd loading. After the recuring, the 3rd loading test was performed, and the initial gradient G_3 was calculated. Each gradient ratio was calculated directly comparing to G_3 and G_2 .

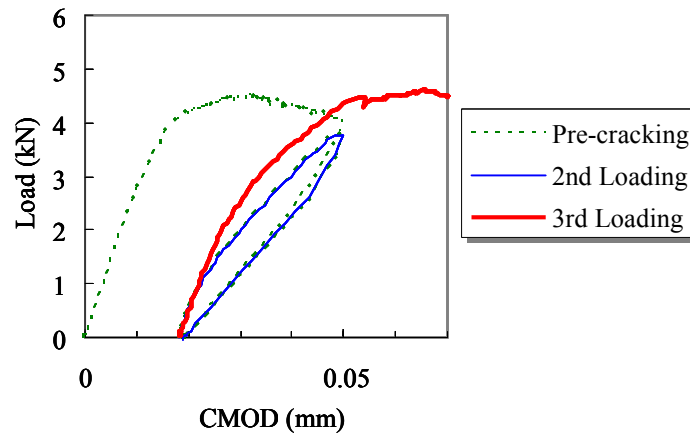
2.4.4 Experimental Results

(a) Effect of Recuring Period

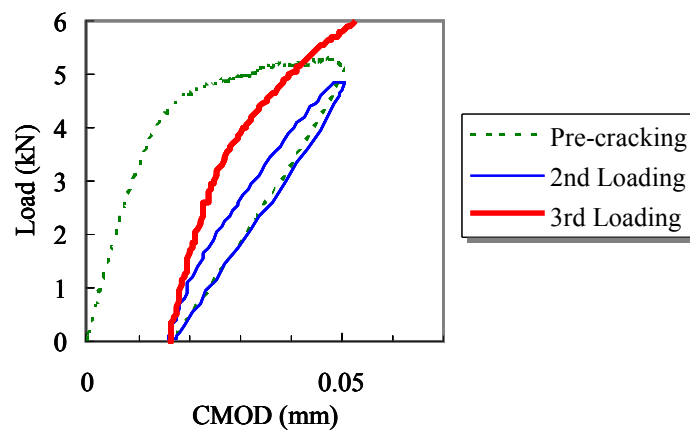
Figures 2.11 and **2.12** show the example of the Load-CMOD curve with the recuring period of 21 days, 42 days and 63 days in water and air recuring condition (the 7-28, 7-24, and 7-70 cases), respectively. The effect of the recuring period can be directly understood through the observation of G_2 and G_3 . Autogenous healing effect was observed in specimens of the 7-28 case (recured 21 days) with water recuring condition, and elongation of the recuring period is effective to obtain increase of the value of G_3 . With air recuring condition, the 7-28 and 7-49 cases provided the same of less gradient value comparing to G_2 . Fortunately, the 7-70 cases gave the recovered gradient up to G_2 .



(a) Example of 21days Recuring Period
(NC7-28-W3)

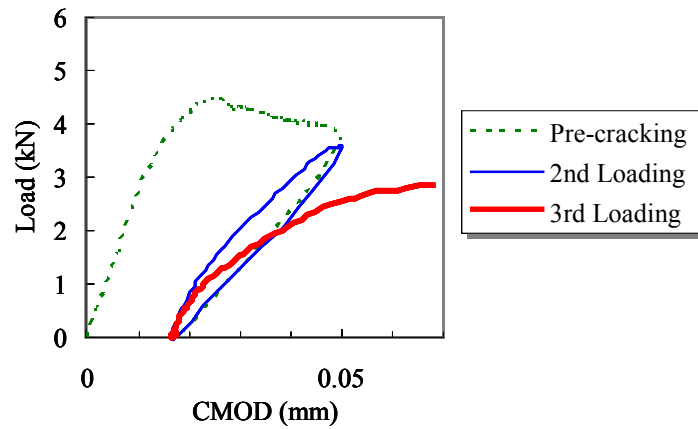


(b) Example of 42days Recuring Period
(NC7-49-W3)

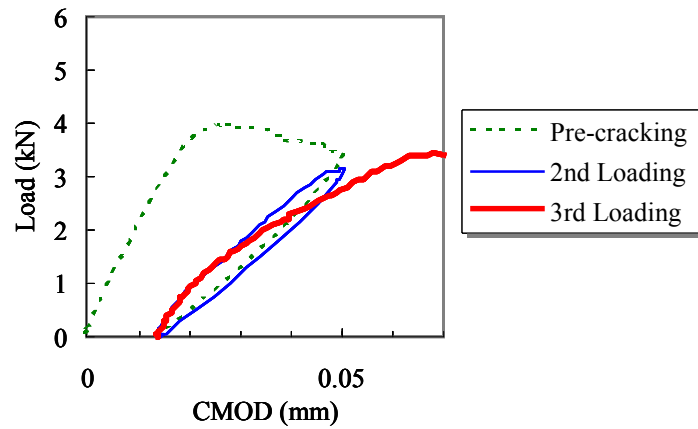


(c) Example of 63days Recuring Period
(NC7-70-W2)

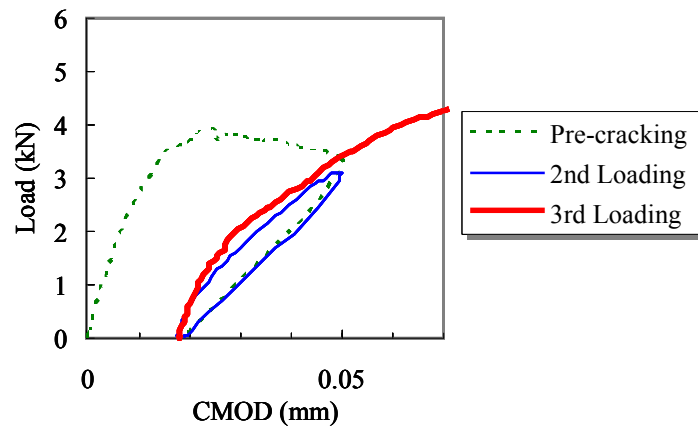
Figure 2.11 Example of Load-CMOD Curve of Different Recuring Period
with Water Recuring Condition



(a) Example of 21days Recuring Period
(NC7-28-A1)



(b) Example of 42days Recuring Period
(NC7-49-A2)



(c) Example of 63days Recuring Period
(NC7-70-A2)

Figure 2.12 Example of Load-CMOD Curve of Different Recuring Period
with Air Recuring Condition

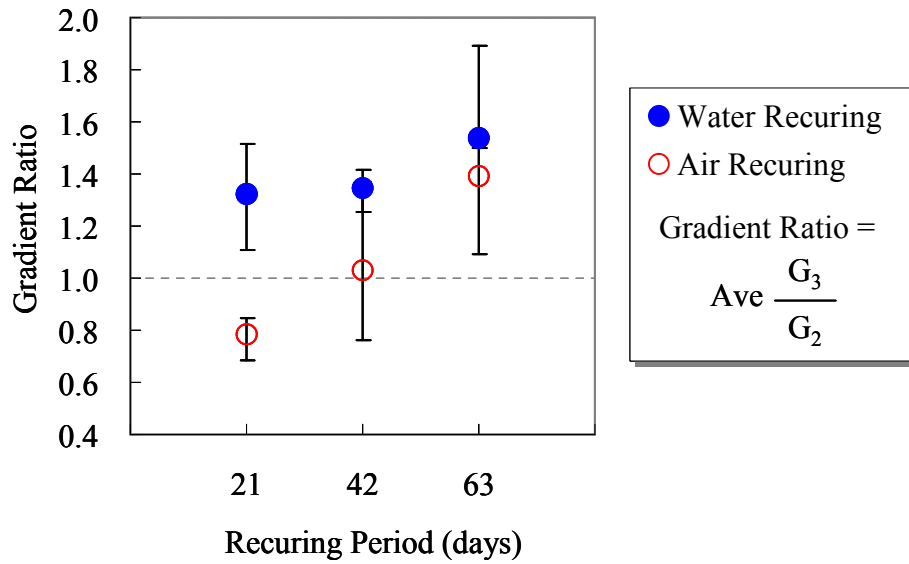
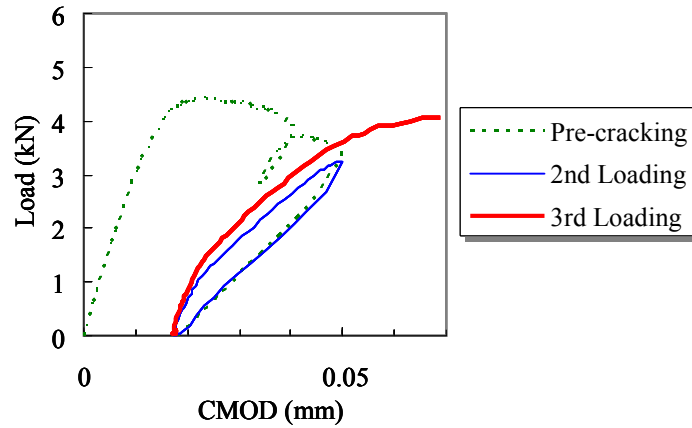


Figure 2.13 Effect of Recuring Period Evaluated Modified Index

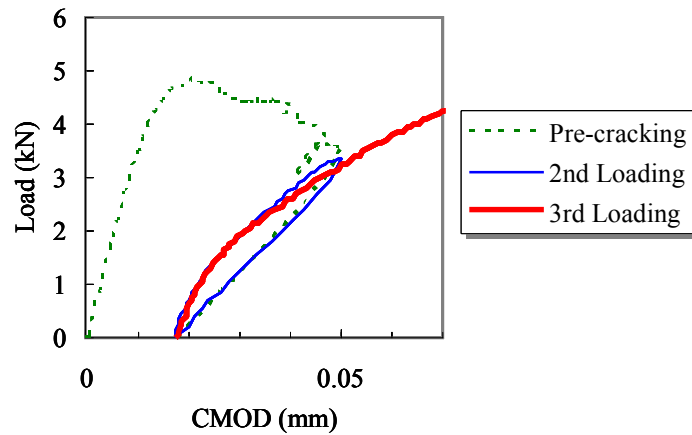
Figure 2.13 shows the gradient ratios depending on the recuring period evaluated by modified index. The gradient ratio increased with elongation of the recuring period, regardless of recuring condition. All the gradient ratios with water recuring condition values greater than 1.0, and they were also higher than those with air recuring condition at the same recuring period. With air recuring condition, 21 days seemed not to be enough for recovery, but the gradient ratios of recuring of 42 days and 63 days indicated that crack can be also recovered in air recuring condition with enough recuring period.

(b) Effect of the Pre-cracking Age

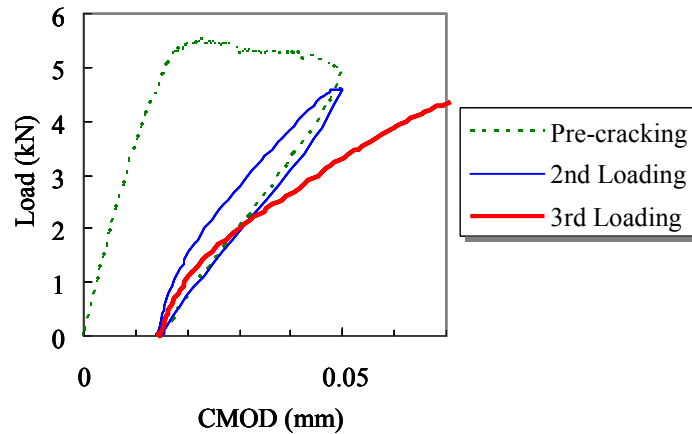
Figures 2.14 and **2.15** show an example of the Load-CMOD curve of 7 days, 28 days and 49 days of the pre-cracking age with water and air recuring condition (the 7-28, 28-49, and 49-70 cases), In contrast to results of the recuring period, autogenous healing effect of the 3rd loading test decreased with delay of the pre-cracking age. In addition, difference of water recuring condition is more prominent than those in air recuring condition. And later behavior of the Load-CMOD curve was also changed with delay of the pre-cracking age, but insignificant change was observed in air recuring condition. These indicated that some factors influenced to autogenous healing, such as re-hydration of un-hydrated cement and pozzolanic reaction, was more sensitive to the existence of water during recuring process.



(a) Example of Pre-cracking Age of 7days
(NC7-28-W3)

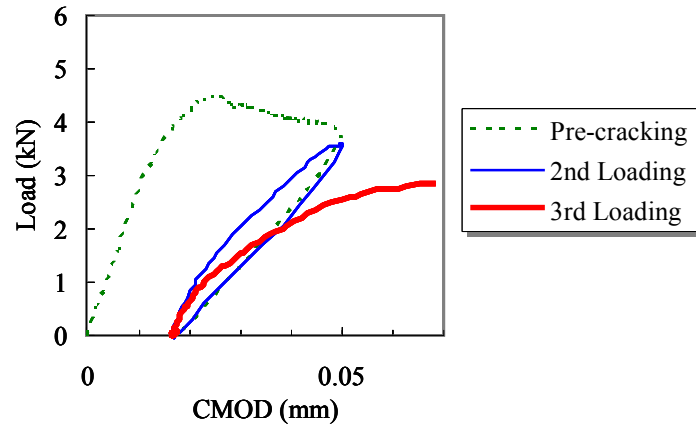


(b) Example of Pre-cracking Age of 28days
(NC28-49-W3)

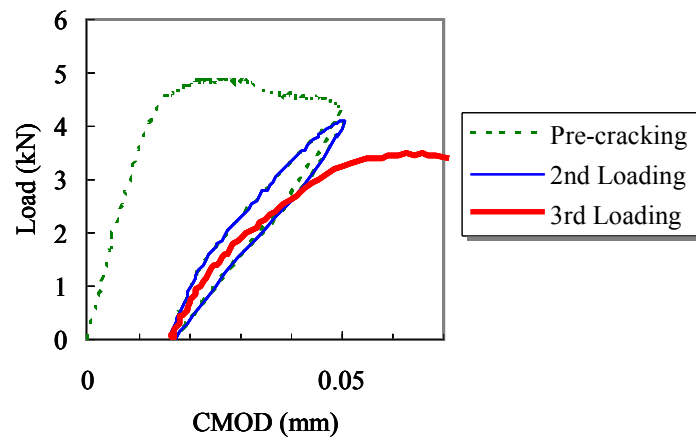


(c) Example of Pre-cracking Age of 49days
(NC49-70-W2)

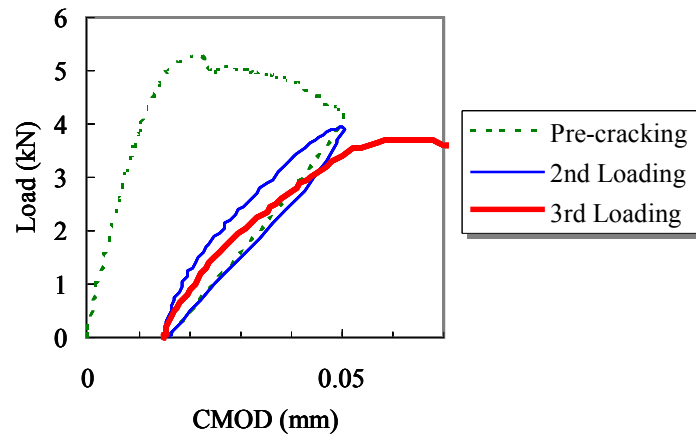
Figure 2.14 Example of Load-CMOD Curve of Different Pre-cracking Age
with Water Recuring Condition



(a) Example of Pre-cracking Age of 7days
(NC7-28-A1)



(b) Example of Pre-cracking Age of 28days
(NC28-49-A2)



(c) Example of Pre-cracking Age of 49days
(NC49-70-A3)

Figure 2.15 Example of Load-CMOD Curve of Different Pre-cracking Age
with Air Recuring Condition

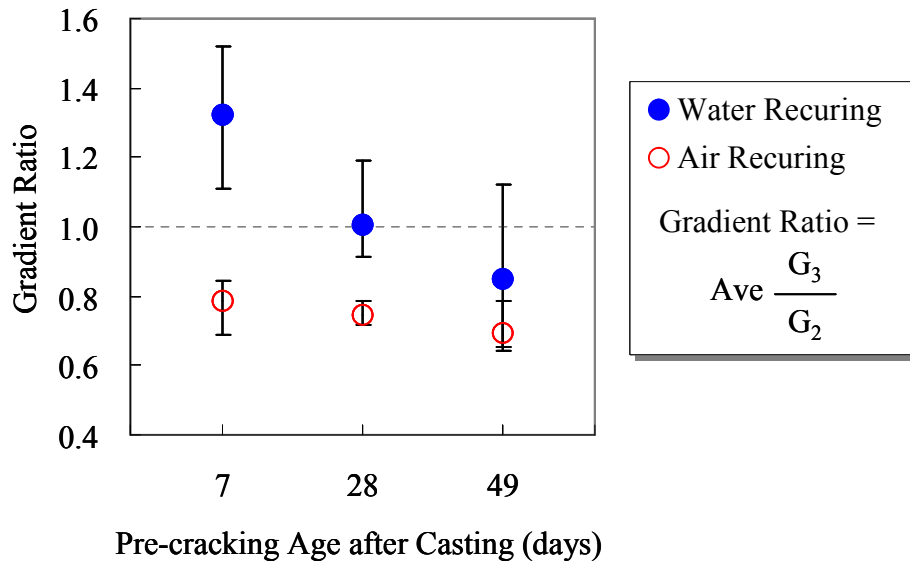


Figure 2.16 Effect of Pre-cracking Age Evaluated Modified Index

Figure 2.16 shows the gradient ratios depend on the pre-cracking age evaluated by modified index. The gradient ratio decreased with delay of the pre-cracking age, regardless of recuring conditions, and the gradient ratios in water recuring conditions showed more prominent change than those in air recuring condition. All cases under the air recuring condition didn't recover to the original level. In water recuring condition, the specimens of the 7-28 and 28-49 cases showed recovery tendency, but those of the 49-70 case didn't over the original level.

These two results evaluated by modified index coincided with results evaluated by previous index. However, the modified index compared with before and after the recuring in the same specimen directly, thus spurious effect from different specimen can be disregarded. With distribution data of the gradient ratios, it made the result more creditable.

2.5 Experimental Cause Analysis of Recovery of Initial Gradient

The recovery of the initial gradient due to autogenous healing was investigated in previous test. But there were a question which area was damaged by the pre-cracking test, and how much area was recovered by recuring. Two methods were used for observation to answer this question. They confirmed mainly influencing area by autogenous healing ability, and can help why the initial gradient changes.

2.5.1 Specimen

The same specimen with the same mix proportion was used to investigate the same damage situation. Normal concrete specimens, as shown in **Figure 2.1**, were prepared with mix proportion as shown in **Table 2.4**. Used material properties were also the same with previous tests. All specimens were demoulded at 24 hours after casting and cured in 20°C water.

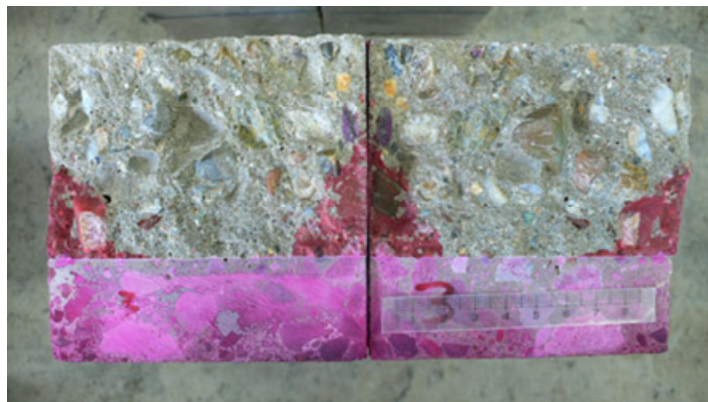
2.5.2 Ink Injection

Crack depth can be observed by ink injection to opened cracks. After the pre-cracking test, and damage level of CMOD was 0.05mm, which was the same as previous tests. A cellophane paper was attached to both sides of specimen to prevent ink leak. Red ink was injected from notch, and specimens were leave enough time to permeate. The reloading was conducted to observe the fracture surface, and damage level was confirmed to observe a dyed part of fracture surface. Normally, a crack part was not even to depth direction, so the averaged crack depth was calculated by equation (2.1).

$$\text{averaged Crack Depth} = \text{Dyed Area} / \text{Width of specimen} \quad (2.1)$$



(a) Pre-cracking at 7days of Age



(b) After Recuring in Water condition
during 21days



(c) After Recuring in Air condition
during 21days

Figure 2.17 Example of Dyed Crack Area

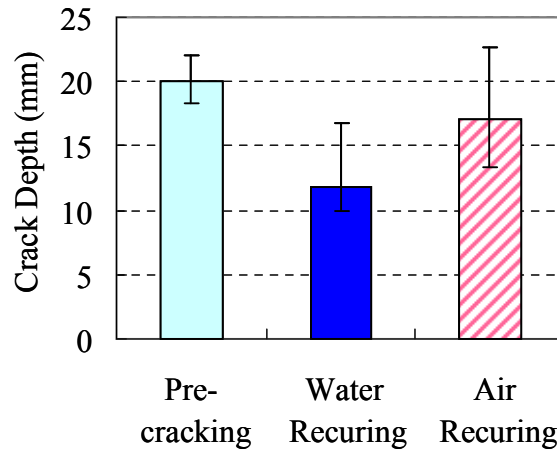


Figure 2.18 Averaged Crack Depth of Each Case

Figure 2.17 shows an example of dyed crack area of after the pre-cracking test, after water recuring and after air recuring, respectively. The pre-cracking test was performed at 7 days after casting. After 21 days recuring, the averaged crack depth become smaller, regardless of recuring conditions. In particular, in water recuring condition, closing of cracked part was observed. Dyed both side part of specimen seemed to be influenced by shrinkage during ink injection (Swartz and Refai 1989).

Figure 2.18 shows the averaged crack width of each case. The averaged crack width after the pre-cracking test was about 20mm. The averaged crack width with water recuring condition was calculated as about 12mm, but as previously described, central crack depth was almost zero as shown in **Figure 2.17-(b)**. The averaged crack depth with air recuring condition also became generally smaller to about 17mm.

2.5.3 Location of Crack Tip and Its Movement Due to Autogenous Healing

In order to monitor a propagated crack and its recovery due to autogenous healing, four strain gauges (length: 30mm) were attached on the ligament of the

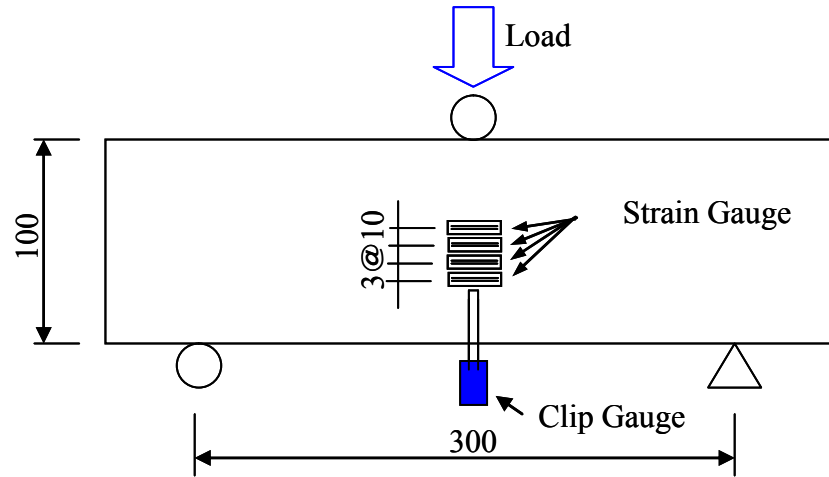


Figure 2.19 Four Strain Gauges for Estimation of Crack Tip

concrete specimen for three-point bending test, as shown in **Figure 2.19**. Induced damage level in the pre-cracking test was the same as the previous tests (CMOD of 0.05mm). The pre-cracking test and the 2nd loading test were conducted at m days, and the 3rd loading test was performed at n days.

Figure 2.20 shows the relation between load and the estimated crack depth in water recuring condition, and **Figure 2.11** also shows that in air recuring condition. Note that, the location having the strain of 100μ was assumed to be a crack tip, and the distance from the notch to the crack tip was defined as the crack depth.

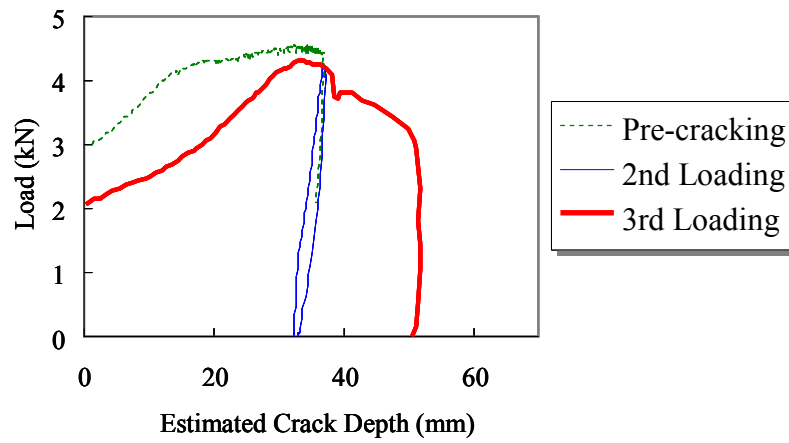
In the pre-cracking test, cracking load (the section of Y axis) was almost 3kN, and the crack propagated to about 30mm that is similar to the results of ink injection method. In particular, a slightly higher cracking load was attained in the case of the pre-cracking test at 28 days because of enough curing time comparing to the case of the pre-cracking test at 7 days.

Regarding the 3rd loading test, the shape of the Load-Estimated crack depth

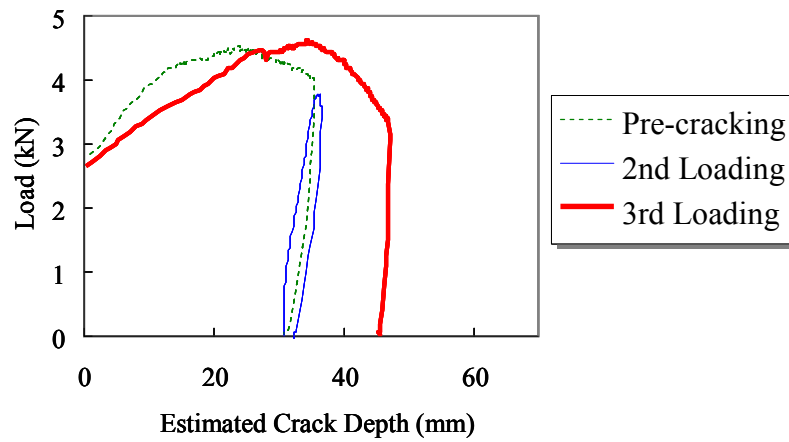
curve was affected by the autogenous healing ability. Comparing to the 7-28 and 7-49 cases in water recuring condition (**Figure 2.20**-(a) and (b)), the increasing rate of the curve for the 7-28 case was larger than that of the 7-49 case, and it means the induced crack by the pre-cracking test was healed due to longer recuring period. It means that resistance against the crack propagation after the recuring became higher. Regarding the 28-49 case, the shape of the curve was different from the above cases, and the estimated crack depth became larger in lower loading level because of lower resistance against the crack propagation. The pre-cracking test was conducted at 28 days, and autogenous healing ability was reduced comparing to those of the 7-28 and 7-49 cases.

Regarding the air recuring condition, the shape of the curve of 3rd loading test was similar to that of the 28-49 case in water recuring condition, because autogenous healing ability in the air recuring condition is not significant, as described before.

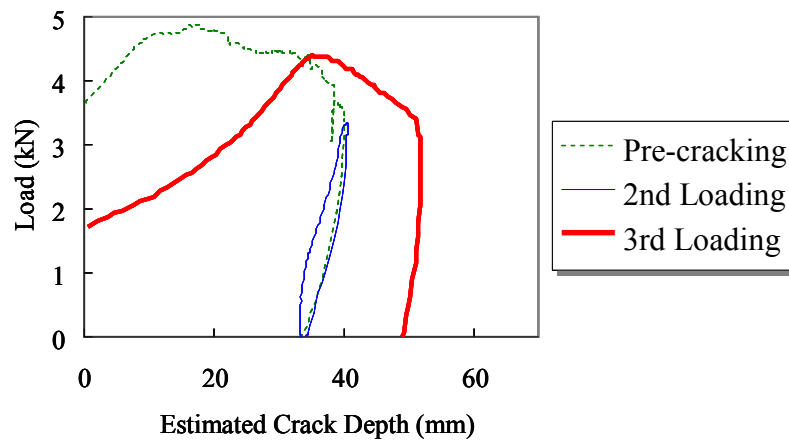
Through this investigation, higher autogenous healing ability reduced the crack propagation rate in low loading level, and lower autogenous healing ability accelerated the crack propagation in low loading level. This phenomenon indicated that the effect of autogenous healing on cracking behavior was significant at initial state of the 3rd loading test, and the proposed index using the gradient could be appropriate for the evaluation of autogenous healing ability.



(a) 7-28 case

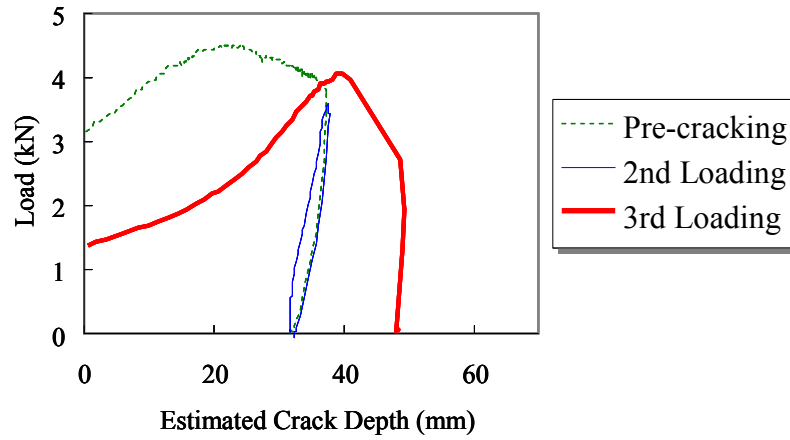


(b) 7-49 case

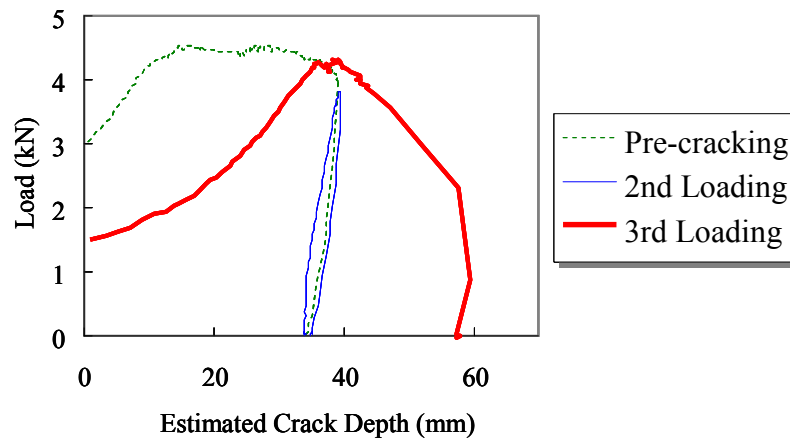


(c) 28-49 case

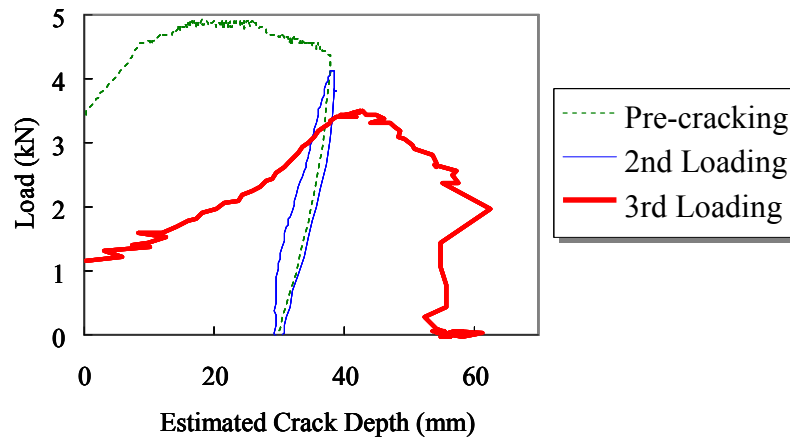
Figure 2.20 Relation with Load and Estimated Crack Depth
with Water Recuring Condition



(a) 7-28 case



(b) 7-49 case



(c) 28-49 case

Figure 2.21 Relation with Load and Estimated Crack Depth
with Air Recuring Condition

2.6 Summary

The proposed test methods and index can classify the ability of autogenous healing in various kinds of concrete (NC, FC and FC+Fib), and following concludes can be obtained.

- (1) Fly ash included in concrete affect to increase of autogenous healing ability, and it seemed to be induced from increase of un-hydrated cement by fly ash. Addition of fiber showed insignificant effect.
- (2) Autogenous healing ability increased with increasing of the recuring period, regardless of recuring condition.
- (3) Autogenous healing ability depended on the pre-cracking age, and it seemed to be affected by the rate of un-hydrated cement in the same age.
- (4) Two methods were proposed in this chapter, such as comparison of recured specimen and non-recured specimen (first index), and comparison of before and after the recuring of the same specimen (modified index). Both showed creditable results to investigate autogenous healing ability, but modified index was more efficient.

3. Evaluation of Autogenous Healing of Concrete through Modified Recovery Index

3.1 Introduction

In this chapter, the applicability of the proposed index was investigated by using various kinds of cementitious composites. In particular, the effect of specimens size, contents of short fiber and recuring temperature on autogenous healing ability were evaluated by the proposed index (modified index in Chapter 2.4).

3.2 Effect of Specimen Size on Autogenous Healing Ability

3.2.1 Experimental Program

A Used material was fly ash concrete, which showed significant autogenous healing ability in the previous chapter 2.3. Mix proportion of the fly ash concrete was shown in **Table 3.1**. The water to cement ratio (W/C) was 45%, and an ordinary Portland cement with a density of 3.15g/cm^3 , a coarse aggregate with a maximum size of 20mm and surface-dry density of 2.58g/cm^3 , and sand with surface-dry density of 2.51g/cm^3 were used. A fly ash (the Type II specified in JIS A 6210), which has a density of 2.38g/cm^3 , was used.

Three sizes of specimen were adopted to compare the effect of specimen size on autogenous healing, such as FC100, FC200, and FC300, as shown in **Figure 3.1**, and four specimens were prepared for each case. The FC100 specimen had the same size as the test in previous chapter, but specimen sizes of the FC200 and FC300 specimens had two and three times of that, thus each specimen size were $100\times100\times400\text{mm}$, $200\times200\times800\text{mm}$, and $300\times300\times1200\text{mm}$, respectively, and loading span of all specimens was three quarters of specimens length. In addition, the depths of notch were 33mm in the FC100 specimen, 66mm in the FC200 specimen and 100mm in the FC300 specimen, which were one third of the specimen depth. All specimens was demoulded at 24 hours after casting, and cured in curing room at temperature of 20°C and relative humidity

Table 3.1 Mix Proportion of Fly Ash Concrete

W/C (%)	Unit Content (kg/m^3)					
	Water	Cement	Sand	Gravel	Fly ash	AE
45	175	389	624	879	137	0.97

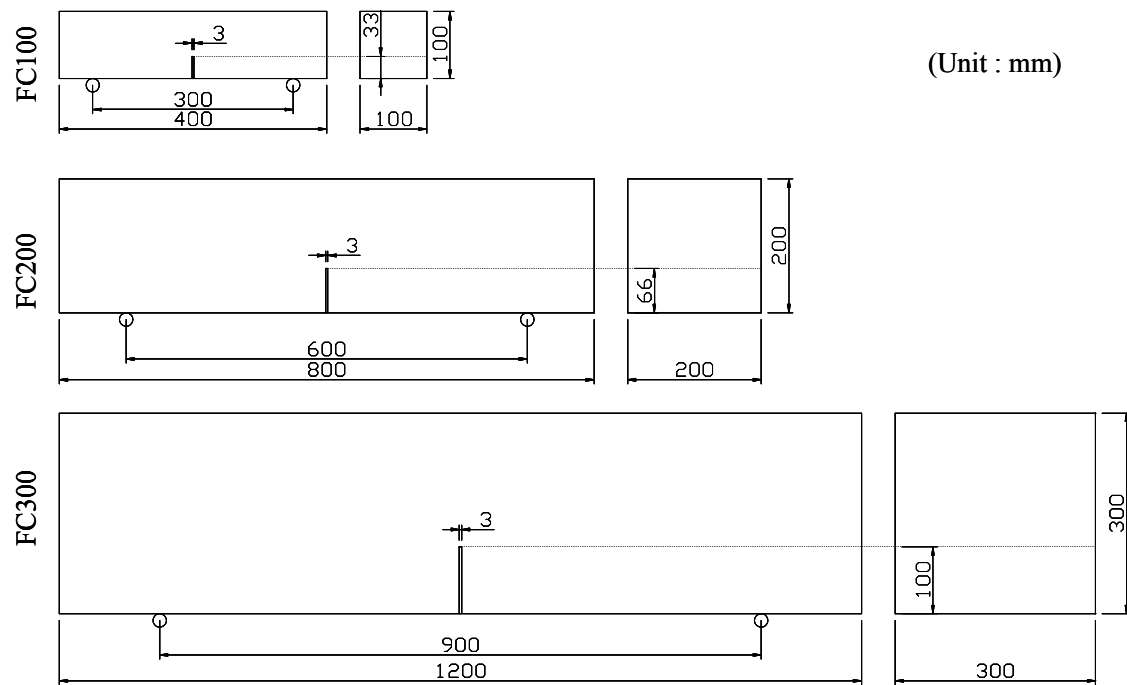


Figure 3.1 Shapes of Each Specimen Size

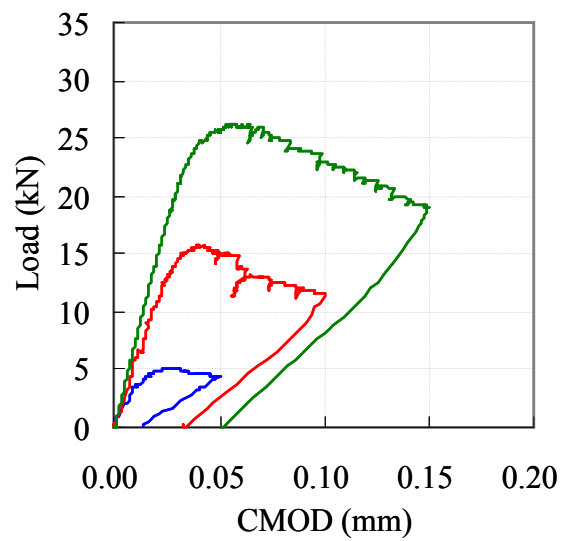
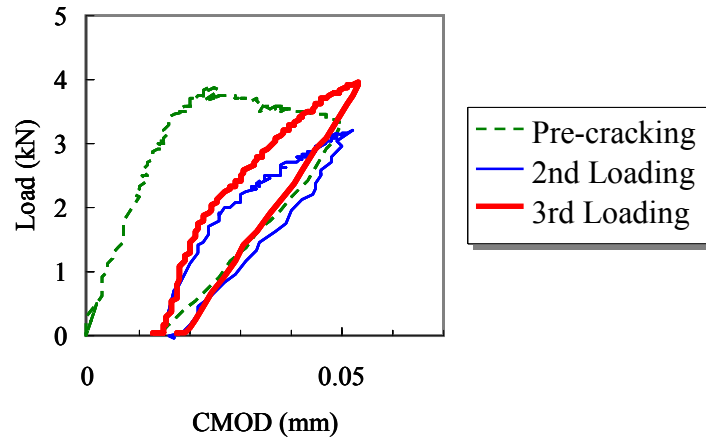


Figure 3.2 Different Load-CMOD Curves of Each Specimen Size

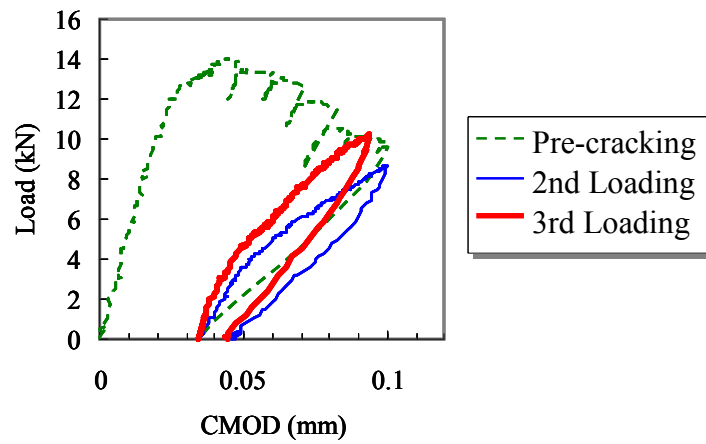
of 70~80%. The pre-cracking was performed at the age of 28 days. Three-point bending tests were conducted for each specimen size. The unloading points were 0.05mm in the case of the FC100 specimen, 0.10mm in the case of the FC200 specimen and 0.15mm in the case of the FC300 specimen. **Figure 3.2** shows the Load-CMOD curves of each specimen size. Unloading point for the pre-cracking test was 70~80% to maximum load in softening region. The 2nd loading test was performed until unloaded point, and the initial gradient G_2 was calculated. Water and air recuring condition were applied to the FC100 and FC200 specimens, but only air recuring condition was applied to the FC300 specimen. The recuring period was 56 days. After the recuring, the 3rd loading test was performed, and the initial gradient G_3 was calculated.

3.2.2 Experimental Results

Figures 3.3 and **3.4** show an example of the Load-CMOD curves of each specimen size with water and air recuring condition, respectively. A mechanical response represented by the Load-CMOD curves of each specimen size was similar each other regardless recuring condition, and residual CMOD of the FC200 and FC300 specimens was about two and three times larger than that of the FC100 specimen. Recuring tendency of the initial gradient was observed in both specimen sizes with water recuring condition. The strength recovery tendency of latter part of Load-CMOD curve was also observed in water recuring condition, and it was supposed to be influenced by an aging effect of un-cracked part. Regarding air recuring condition, the initial gradients of the 3rd loading test decreased compare to those of the 2nd loading test.

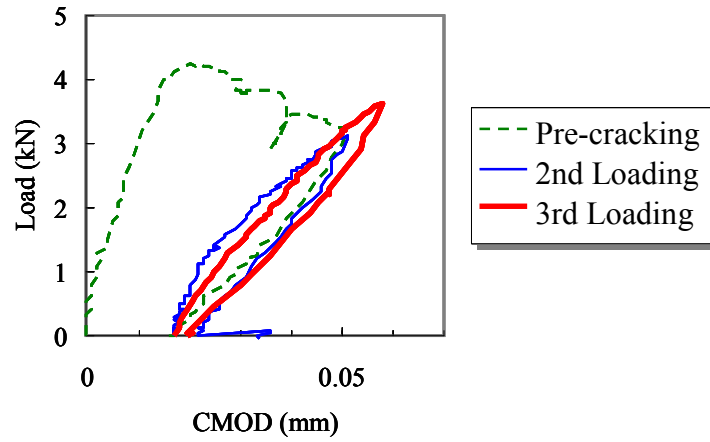


(a) Example of FC100 (FC100-W1)

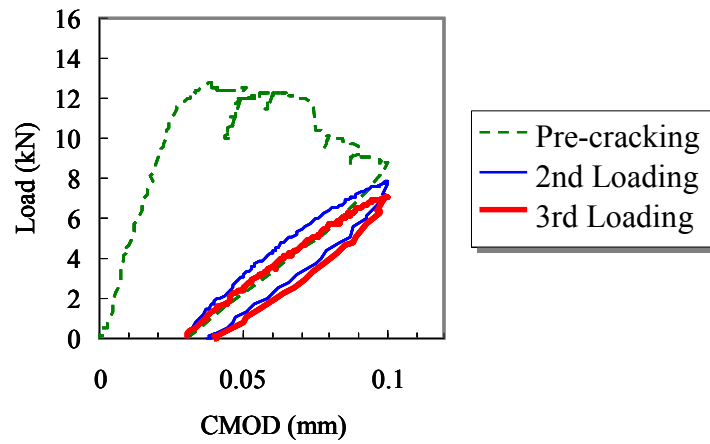


(b) Example of FC200 (FC200-W4)

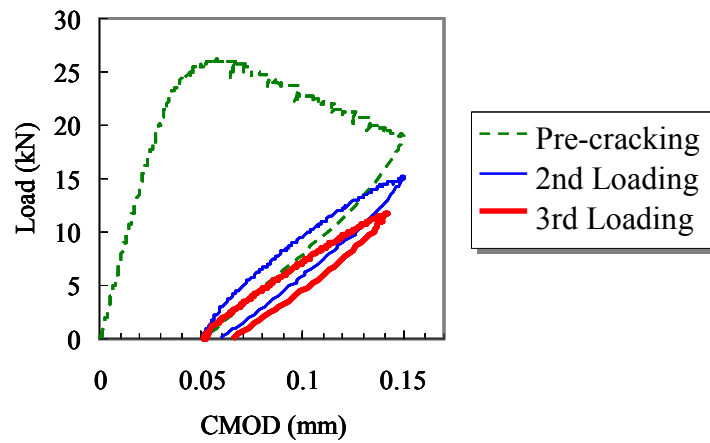
Figure 3.3 Example of Load-CMOD Curves of Each Specimen Size
with Water Recuring Condition



(a) Example of FC100 (FC100-A3)



(b) Example of FC200 (FC200-A3)



(c) Example of FC300 (FC300-A2)

Figure 3.4 Example of Load-CMOD Curves of Each Specimen Size with Air Recuring Condition

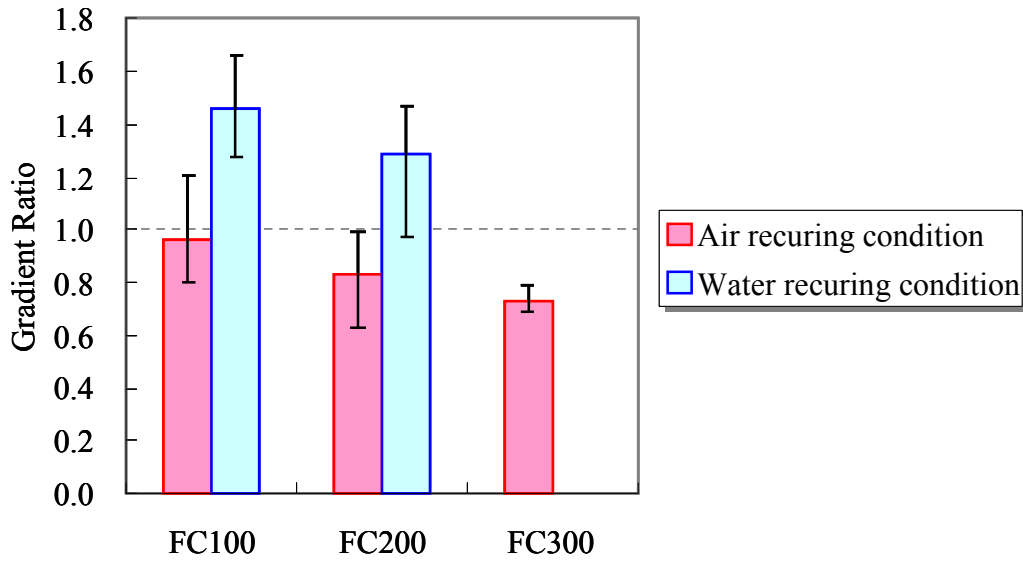


Figure 3.5 Gradient Ratios of Each Specimen Size

Figure 3.5 shows the gradient ratios of each specimen size. Firstly, the gradient ratios with water recuring condition had higher value than those with air recuring condition. Regarding size effect, autogenous healing ability decreased with increasing of specimen size, regardless of recuring condition. Although the ratio of propagated crack length to specimen depth is the same each other, specific residual crack width seems to be different. It seems that a limit crack width for autogenous healing ability can be defined for each material.

3.3 Effect of Short Fiber Type on Autogenous Healing

3.3.1 Experimental Program

In Chapter 2.3, it was clarified that PE fiber was not effective for improvement of autogenous healing ability. In this section, two kinds of fiber, such as Polyethylene fiber (PE) and Polyvinylalcohol fiber (PVA), were prepared for the investigation of effect of short fiber type on autogenous healing. **Figure 3.6** shows the sample of each fiber. PVA fiber has hydroxide (OH) that is different from PE fiber, and it is expected that PVA fiber with hydroxide can become to be nuclei for fixation of CaCO_3 and pozzolanic reaction product.

An ordinary Portland cement with a density of 3.15g/cm^3 , a coarse aggregate with a maximum size of 20mm and surface-dry density of 2.58g/cm^3 , and sand with surface-dry density of 2.51g/cm^3 were used. A fly ash (the Type II



(a) Polyethylene Fiber (PE)



(b) Polyvinylalcohol Fiber (PVA)

Figure 3.6 Sample of PE and PVA fiber

Table 3.2 Mix Proportions of Fly Ash Concrete with Different Short Fiber

Case	W/C (%)	s/a (%)	Volume Fraction of Fiber (%)	Unit Content (kg/m^3)						Additive (cc/m^3)
				Water	Cement	Sand	Gravel	Fly Ash	Fiber	SP†
PE	45	47	0.25	175	389	879	618	137	2.43	0.97
PVA	45	47	0.19	175	389	879	618	137	2.43	0.97

SP† : Superplasticizer

specified in JIS A 6210), which has a density of 2.38g/cm^3 , was used. The mix proportions of each fiber are shown in **Table 3.2**. Physical properties of each fiber are shown in **Table 3.3**. Length of each fiber was 4mm, and the content of fiber was 2.43kg/m^3 . Five specimens were prepared in each case.

Table 3.4 shows the test program in this study, and the 7-28, 28-49, 49-70 and 91-112 cases were prepared. Four cases having different pre-cracking age, and the same recuring period (21 days) were investigated. All specimens were demoulded at 24 hours after the casting, and cured in 20°C water. The

Table 3.3 Properties of Fibers

Content	PE	PVA
Length	4mm	4mm
Diameter	0.012mm	0.040mm
Density	0.97g/cm^3	1.30g/cm^3
Young's Modulus	88GPa	41GPa
Tensile Strength	2700MPa	1560MPa

Table 3.4 Test Program Considering Fiber Difference

Case	Days after casting									
	7		28		49		70	91		112
7-28	Pre 2nd	Water → Air	3rd							
28-49			Pre 2nd	Water → Air	3rd					
49-70					Pre 2nd	Water → Air	3rd			
91-112								Pre 2nd	Water → Air	3rd

Pre : The pre-cracking test (m days)

2nd : The 2nd loading test just after the pre-cracking test (m days)

3rd : The 3rd loading test after the recuring (n days)

Water
→
Air : Recuring in water and air condition during r days

pre-cracking test was performed at m days after the casting, and the 2nd loading test was also performed at m days just after the pre-cracking test. The initial gradient G_2 was calculated from the 2nd loading test. Specimens had recuring under water or air conditions. All series had the same recuring period (21 days) and the 3rd loading test was performed at n days. The initial gradient G_3 from the 3rd loading test was compared with the initial gradient G_2 from the 2nd loading test to evaluate autogenous healing ability.

3.3.2 Experimental Results

Figures 3.7 and 3.8 show the example of the Load-CMOD curves of PE fiber and PVA fiber. The tendency of recovery was observed more in water recuring condition, and the Load-CMOD curves of the 3rd loading test were measured under that of the 2nd loading in air recuring condition. The difference between PE and PVA fibers was observed in air recuring condition. Only the 7-28 case of PE fiber has shown the trend of recovery, and significant decrease of the Load-CMOD curves was observed in other cases. The Load-CMOD curves of PVA fiber with air recuring condition also decreased, but there was gradual reduction with delay of the pre-cracking age.

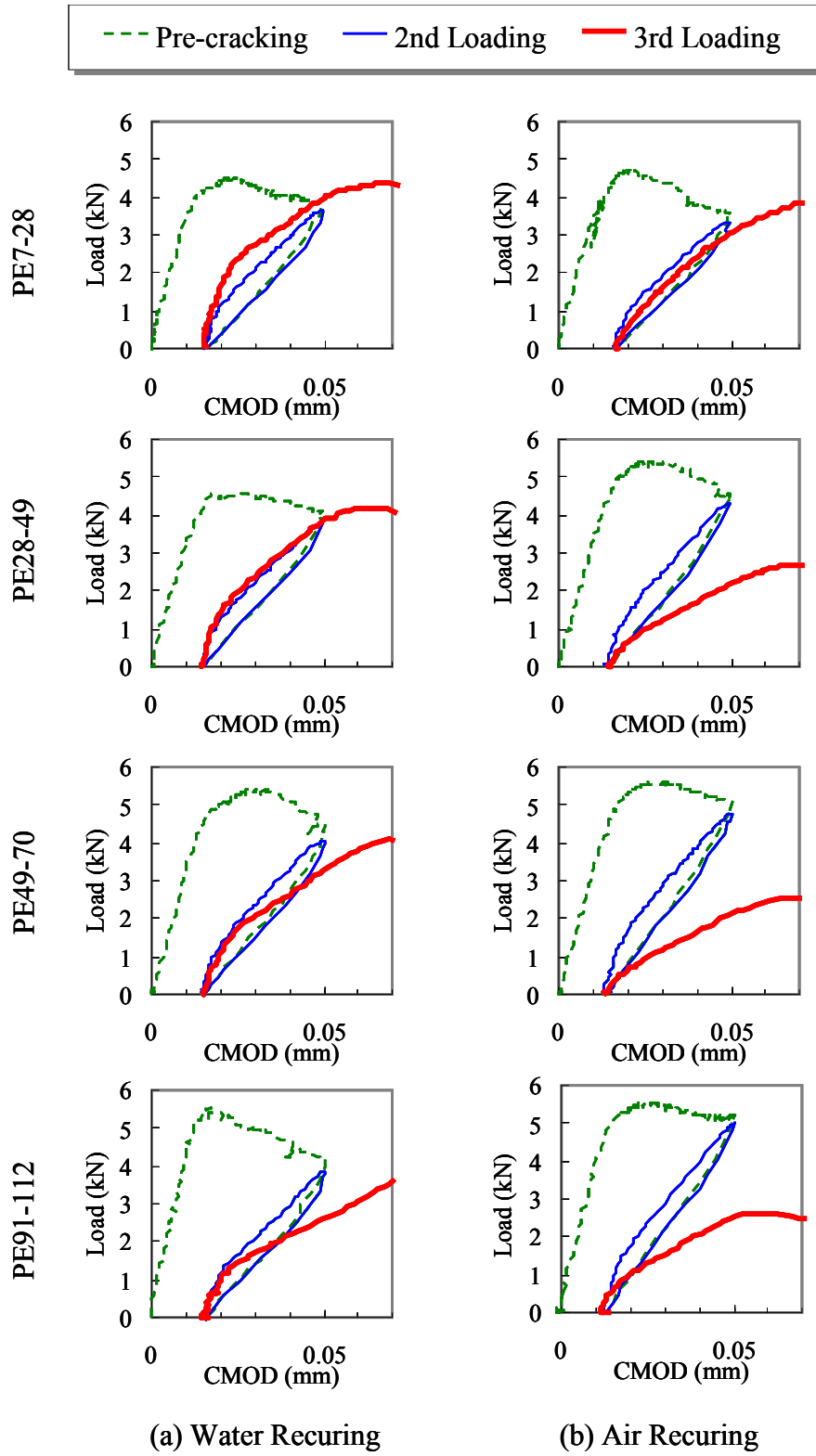


Figure 3.7 Example of Load-CMOD Curves of PE Fiber

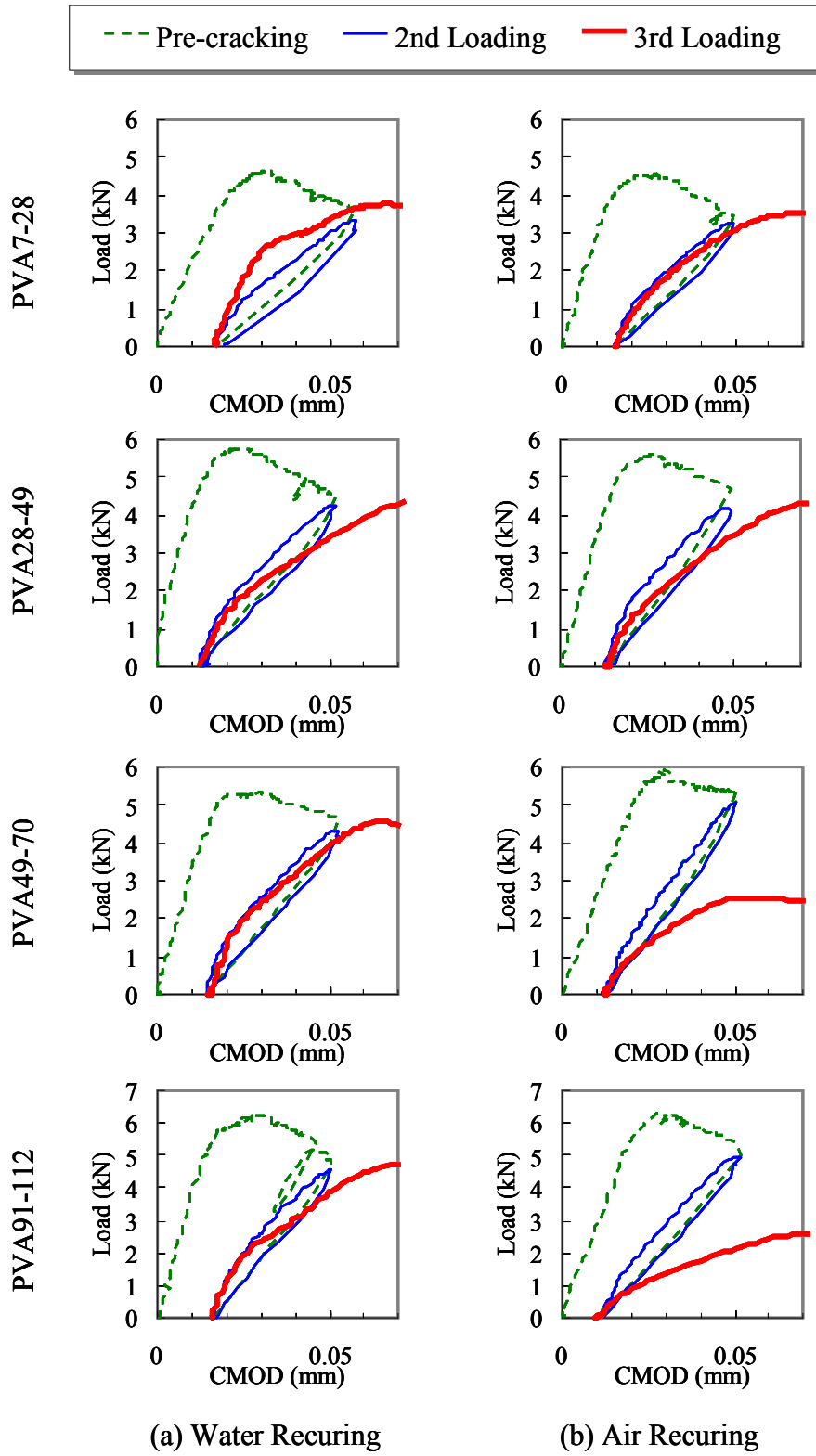
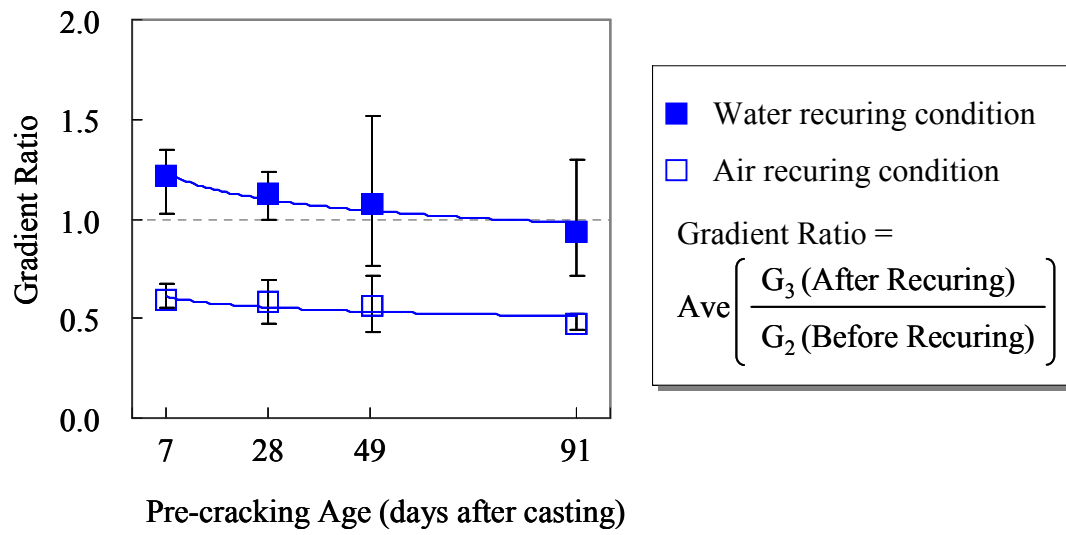
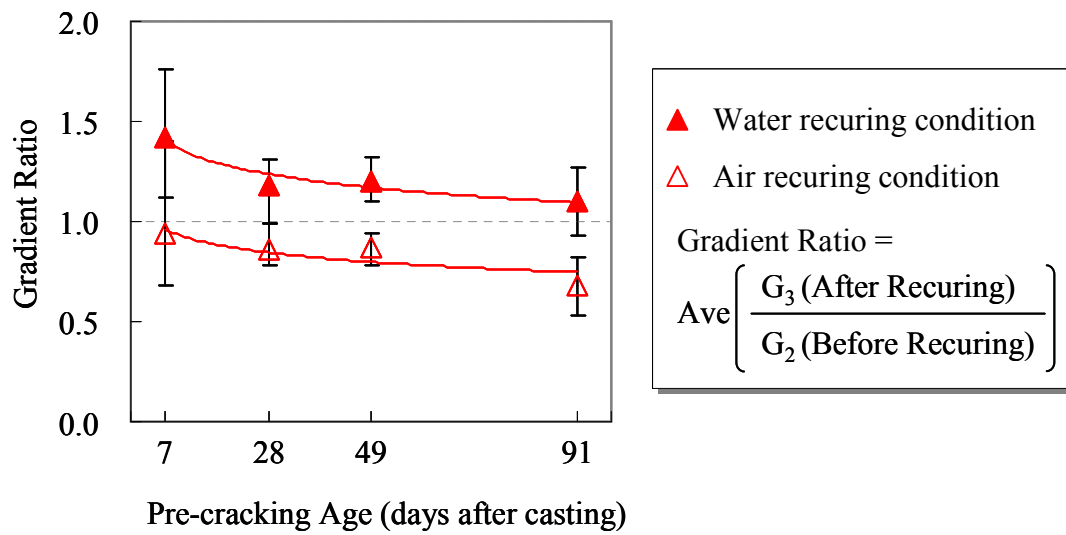


Figure 3.8 Example of Load-CMOD Curves of PVA Fiber

Figure 3.9 shows the gradient ratios of different pre-cracking age. The gradient ratio was decreased with delay of the pre-cracking age, and water recuring conditions provided higher recovery than air recuring conditions, regardless of types of fibers. A slight difference was observed on difference of fiber types. The gradient ratios of PVA fiber was higher than those of PE fiber in both water and air recuring conditions, even if the volume fraction of fiber in PVA fiber was lower than that in PE fiber case. It seems that hydroxide (OH⁻) of PVA fiber contributes precipitation of CaCO₃ and regeneration of re-hydrated cement easier than PE fiber. Some other points of these results were the gradient ratio in air recuring condition of both cases had were less than 1.0, and it means the specimens did not recover but deteriorate during air recuring condition. Some reasons, such as shrinkage in air condition, stress concentration on the pre-cracked edge or non-closed crack due to exist of fiber and fragments, can be supposed. Further study and discussion should be needed.



(a) Effect of Pre-cracking Age of PE Fiber



(a) Effect of Pre-cracking Age of PVA Fiber

Figure 3.9 The Gradient Ratios of PE and PVA Fiber

3.4 Effect of Curing temperature on Autogenous Healing Ability

3.4.1 Experimental Program

It is well known that thermal curing condition accelerates the chemical reaction of hydration, and thus it affects to increase in strength of concrete with the same curing period. But, it also reported that a higher temperature during early age makes hydration products poorer in physical nature and lead to a lower strength due to more porosity (Neville, 1998). Thermal curing condition also affects to the reaction of fly ash, as shown in **Figure 3.10**. Curing period for about 100 days is required to obtain the reaction rate of 20% in the case of 20°C. However, high temperature curing with 40°C reduce the curing period up to a week to obtain the reaction rate of 20%. Autogenous healing depends on chemical reaction on the crack surface, and it could be supposed that thermal curing condition affect to the autogenous healing ability. The purpose of this

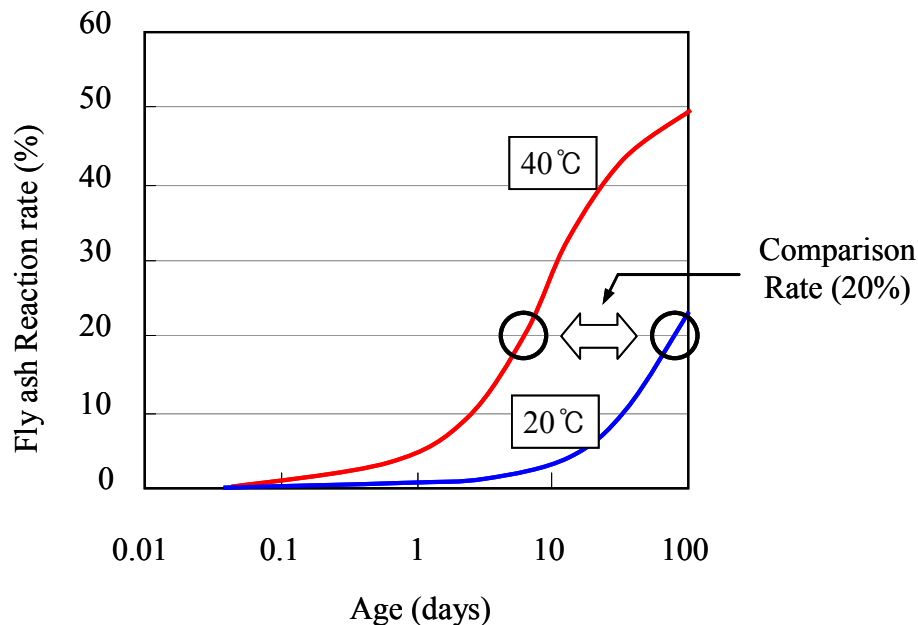


Figure 3.10 Fly Ash Reaction Rate of 20°C and 40°C Curing Condition (JCI-C79 2011)

study is to investigate that higher temperature accelerates the autogenous healing ability of the fly ash concrete basically.

Table 3.5 shows mix proportions of normal concrete (NC) and fly ash concrete (FC). A normal concrete was prepared for comparison. Two kinds of test were prepared, as three-point bending test and compressive test. Autogenous healing ability was evaluated from the gradient ratio using three-point bending test, and four rectangular specimens with size of 400×100×100 were prepared for each case. Compressive test was performed to confirm the development of concrete strength with different curing conditions. For the compressive strength tests, three specimens with size of $\Phi 100 \times 200$ were prepared for each age. There were four cases to compare thermal effect, as shown **Table 3.6**. All specimens were demoulded at 24 hours after casting, and cured in 20°C water.

The NC20 and FC20 cases had the pre-cracking test and the 2nd loading test at the age of 28 days. The initial gradient G_2 was obtained from the 2nd loading test. After that, both specimens of the NC20 and FC20 cases recured for 63 days in 20°C water condition to be reaction rate of 20%. After the recuring, specimens for the NC20 and FC20 cases were under the 3rd loading test, and the initial gradient G_3 was calculated. The NC40 and FC40 cases had also the

Table 3.5 Mix Proportions of Normal and Fly Ash Concrete

Case	W/C (%)	s/a (%)	Unit Content (kg/m ³)					Additive (cc/m ³)
			Water	Cement	Sand	Gravel	Fly ash	AEA [†]
NC	45	47	170	377	780	903	-	0.97
FC	45	47	170	377	716	903	58	0.97

AEA[†] : Air Entraining Agent

Table 3.6 Experimental Program for Thermal Effect

Temp	Case	Days after casting			
		28		35	91
20°C	NC20	Pre / 2nd	63 days in 20°C water →		3rd
	FC20	Pre / 2nd	63 days in 20°C water →		3rd
40°C	NC40	Pre / 2nd	7 days in 40°C water →	3rd	
	FC40	Pre / 2nd	7 days in 40°C water →	3rd	
Compressive Test		C1			
		20°C in 28 days + 40°C in 7 days		C2	
		20°C in 28 days + 20°C in 63 days			C3

Pre : The pre-cracking test (28 days)

2nd : The 2nd loading test just after the pre-cracking test (28 days)

3rd : The 3rd loading test after the recuring (35 or 91 days)

Cn : Compressive loading test.

→ : Recuring in 40°C water during 7 days or in 20°C water during 63 days

pre-cracking test and the 2nd loading test at the age of 28 days, and the initial gradient G_2 was obtained. But, recuring condition for those was different from the NC20 and FC20 cases. Recuring condition of NC40 and FC40 was 7 days and in 40°C hot water. Note that the fly ash reaction rate was 20%. After the recuring, the 3rd loading test was performed, and the initial gradient G_3 was calculated. The gradient ratios of G_3 to G_2 on each case were calculated, and the thermal effect was investigated through comparison with 63 days in 20°C water cases (NC20, FC20) and 7 days in 40°C hot water cases (NC40, FC40).

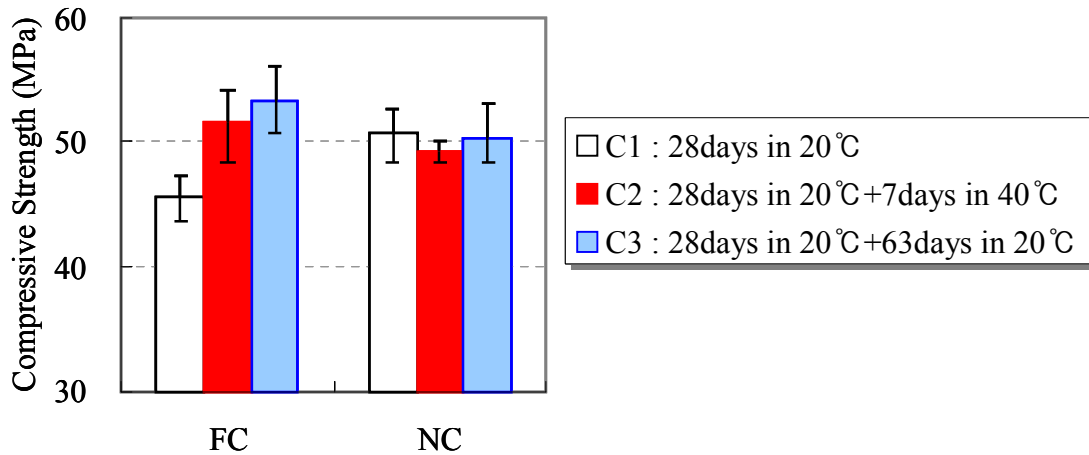


Figure 3.11 Compressive Strength of Each Recuring Condition

3.4.2 Experimental Results

Figure 3.11 shows the compressive strength of the C1 (28 days), C2 (35 days) and C3 (91 days) compressive test. Compressive strengths of the C2 test was almost same degree with that of the C3 test. There was insignificant difference between normal concrete and fly ash concrete except for the early age. As a result, hydration of cement and reaction of fly ash seemed to be slightly accelerated by thermal curing condition.

Figures 3.12 and **3.13** show the example of the Load-CMOD curves of each recuring condition of fly ash concrete (FC) and normal concrete (NC), respectively. The behaviors of the 3rd loading test with 63 days in 20°C recuring condition indicate recovery by autogenous healing effect. But in 7 days in 40°C recuring condition, the initial part of the 3rd loading test showed less recovery trend. This phenomenon was observed both fly ash concrete (FC) and normal concrete (NC).

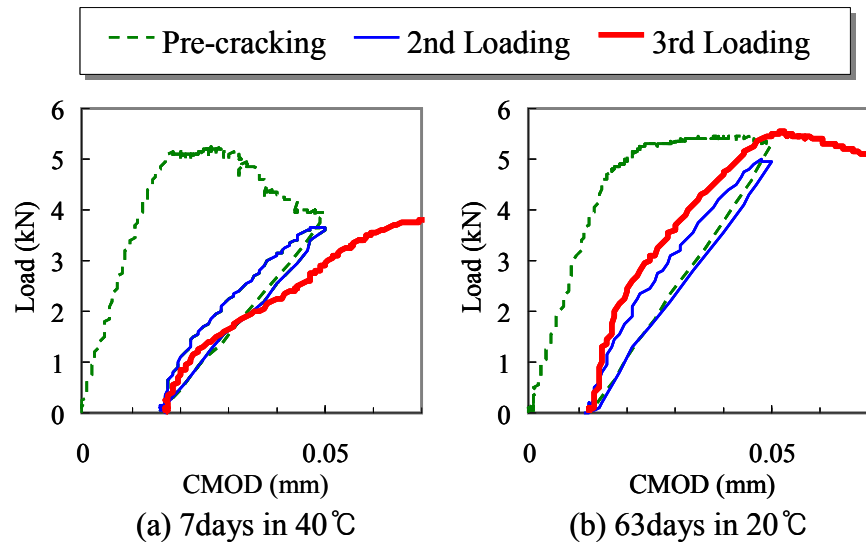


Figure 3.12 Example of Load-CMOD Curves of Fly Ash Concrete

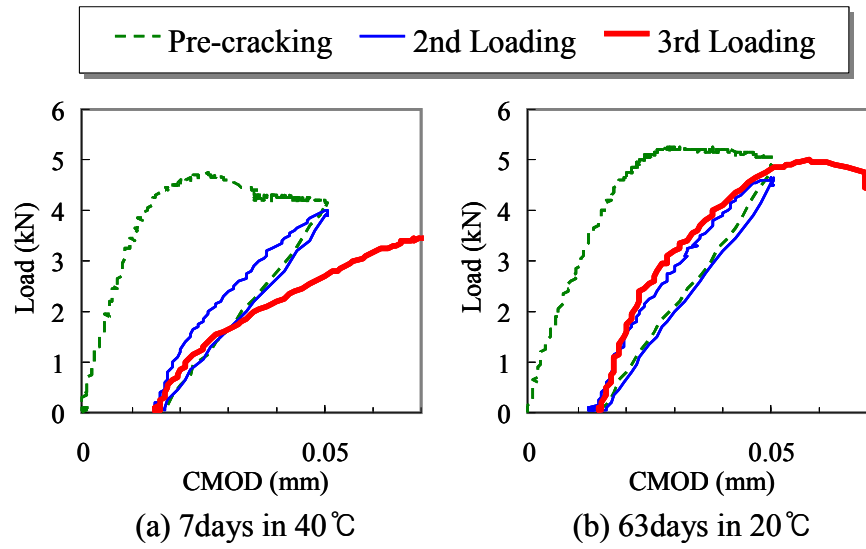


Figure 3.13 Example of Load-CMOD Curves of Normal Concrete

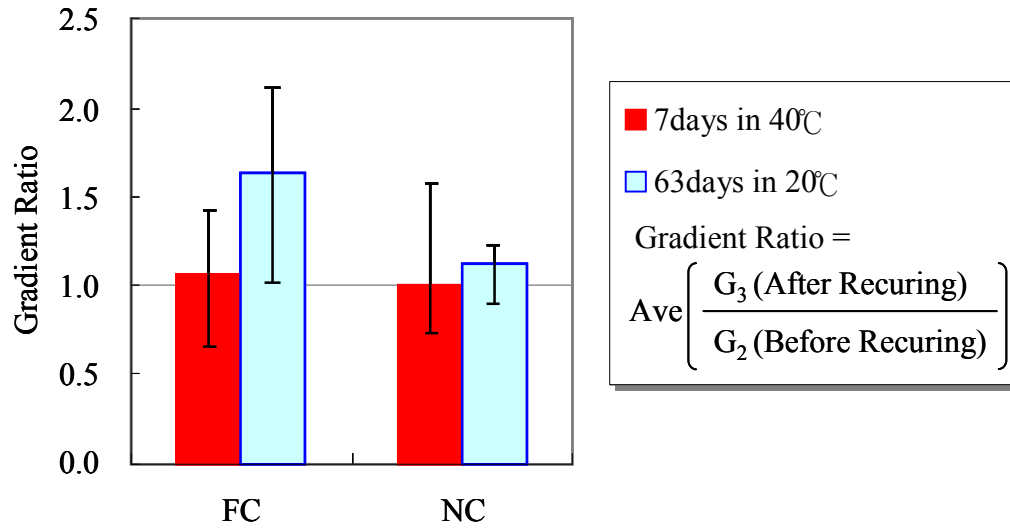


Figure 3.14 Gradient Ratios of Each Recuring Conditions

Although the compressive strength was shown almost the same degree between the 7 days in 40°C case and the 63 days in 20°C case, the trend represented by gradient ratio indicated different results, as shown in **Figure 3.14**. The gradient ratios of the specimens with 63 days in 20°C water recuring case were over 1.0, regardless of concrete, and fly ash concrete showed significant increase of the gradient ratio. But, the gradient ratios of the specimens with 7 days in 40°C hot water were about 1.0. It was clarified recuring period is more effective than thermal acceleration on autogenous healing ability.

3.5 Summary

The modified index proposed in previous chapter, which used the initial gradient was used for investigation of effect of specimen size, fiber type, and thermal recuring on autogenous healing ability, and following conclusions can be obtained:

- (1) Autogenous healing ability decreased with increasing of specimen size, although the ratio of crack propagation length to specimen depth was the same.
- (2) The effect of short fiber type, such as Polyethylene fiber (PE) and Polyvinylalcohol fiber (PVA), on autogenous healing ability was investigated. PVA fiber showed higher healing ability than PE fiber, It seems that the presence of hydroxide (OH^-) of PVA fiber helps to nucleate for deposition of CaCO_3 and re-hydration of un-hydrated cement efficiently.
- (3) Two water recuring conditions were investigated, such as 7 days in 40°C hot water and 63 days in 20°C water, which were expected to be the same reaction rate of fly ash in calculation. Although the acceleration of chemical reaction due to thermal curing was observed in compressive strength, the gradient ratio of longer recuring period (63 days in 20°C water) was higher than that of thermal recuring condition (7 days in 40°C hot water). It was indicated that autogenous healing ability is more dependent on the recuring period than chemical acceleration.

4. Evaluation of Autogenous Healing through Acoustic Emission

4.1 Introduction

Acoustic Emission (AE) technique was used for investigation of autogenous healing in this chapter. In the first part of this study, the AE technique was applied to the plain concrete beam, and AE sources location and the averaged frequency of each case was investigated by three-point bending test. The initial gradient was also investigated to compare with AE test results. In the second part of this study, RC beam test was conducted. The different recoveries of several cracks were evaluated by the gradient ratio, and the application of the gradient ratio to RC beam test was investigated with AE technique.

4.2 Acoustic Emission

Acoustic Emission (AE) is commonly defined as transient elastic wave within a material, caused by the release of localized stress energy. The frequency of elastic wave is ranging from kHz to MHz. AE sensors can detect the weak wave form, which is corresponding to the occurrence time of defects or cracks. AE technique can be classified into passive methods because the input of the wave form is not required. On the other hand, there are some active methods such as the ultrasonic method and the impact each method, which required a input of wave form.

AE technique can estimate the crack location. The wave propagates radial direction, and there is time difference in each sensor due to difference distances from source location. The location of crack was calculated by this time difference, as shown in **Figure 4.1**. The detailed calculation process was as follows;

The fundamental basis for the location calculation is just the simple time-distance relation implied by the velocity of the elastic wave. The absolute arrival time, t , of a hit in an event can combine with the velocity, v , of the sound wave to yield the distance, d , from the sensor to the source.

$$d = v \times t \quad (4.1)$$

The distance between two points depends on the geometry of the problem. The majority of the location modes are a variation of two dimensional source

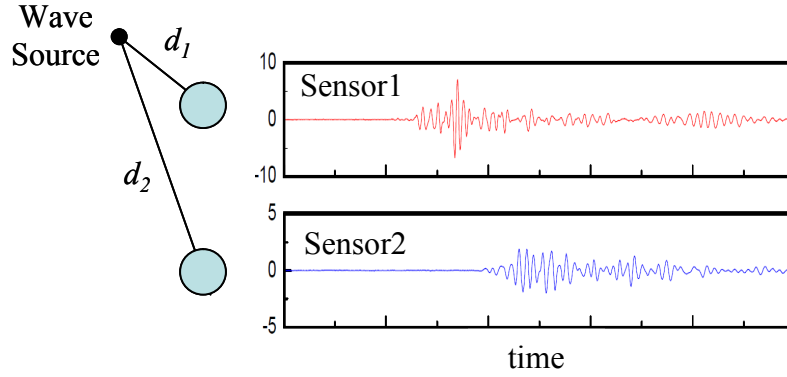


Figure 4.1 Fundamental Basic of Acoustic Emission (AE) Method

locations in a plane, although in many cases the 2D plane will wrap around a three dimensional object. For two points in a flat plane, the distance equation is just the pythagorean theorem expressed in Cartesia coordinates:

$$d = \sqrt{(x_2 - x_1)^2 + (y_2 - y_1)^2} \quad (4.2)$$

This calculation is complicated by the lack of knowledge of the exact time the event originated. To get around that problem, all the times are considered relative to the first hit in the event. Each arrival time difference implies a difference in distance to the sensor relative to the distance to the first hit sensor. For the second hit sensor relative to the first hit sensor, a difference equation can be written as:

$$t_2 - t_1 = (d_2 - d_1)/v \quad (4.3)$$

The distance equation (4.2) can be combined with the difference equation (4.3) to yield:

$$t_2 - t_1 = \left[\sqrt{(x_2 - x_S)^2 + (y_2 - y_S)^2} - \sqrt{(x_1 - x_S)^2 + (y_1 - y_S)^2} \right] / v \quad (4.4)$$

where x_S and y_S are the unknown coordinates of the source. This equation contains two unknowns and cannot be solved by itself. To get a second equation with the same two unknowns, the third hit is added to the event producing analogous equation:

$$t_3 - t_1 = \left[\sqrt{(x_3 - x_S)^2 + (y_3 - y_S)^2} - \sqrt{(x_1 - x_S)^2 + (y_1 - y_S)^2} \right] / v \quad (4.5)$$

These simultaneous equations can then be solved for x_S and y_S , although the algebra is fairly complex. If possible source location is limited in 2D Planar location, multiple regression analysis is not needed. The answer of x_S and y_S directly indicate the source location.

If there are additional hits added to the event, there is a question of how to use the extra information. A better approach would be to average the data somehow to produce a single location. Multiple regression analysis does just that, although it does not actually average the results of multiple three hit calculations directly. Rather it searches for the location that best fits all the all the available data. Each additional hit basically adds an extra equation to the set of simultaneous equations given above as (4.4) and (4.5). This can be generalized as:

$$t_i - t_1 = \left[\sqrt{(x_i - x_S)^2 + (y_i - y_S)^2} - \sqrt{(x_1 - x_S)^2 + (y_1 - y_S)^2} \right] / v \quad (4.6)$$

If one defines

$$\Delta t_i = t_i - t_1 \quad (4.7)$$

one can write:

$$\Delta t_i = \left[\sqrt{(x_i - x_S)^2 + (y_i - y_S)^2} - \sqrt{(x_1 - x_S)^2 + (y_1 - y_S)^2} \right] / v \quad (4.8)$$

Equation (4.7) and (4.8) give two ways of calculating the Δt of the i th sensor. Using the known arrival times of the hits, equation (4.7) calculates the observed time difference, $\Delta t_{i,obs}$. For a given set of source location coordinates, equation (4.8) defines the calculated time difference, $\Delta t_{i,calc}$. Multiple regression analysis is a general purpose algorithm that minimizes the difference between two quantities which in this case are the observed and calculated Δt values. To do that a quantity called χ^2 is calculated. In this case, it is defined as defined as a sum across all sensors in the event:

$$\chi^2 = \sum (\Delta t_{i,obs} - \Delta t_{i,calc})^2 \quad (4.9)$$

This quantity is also called the fit value and is dependent on the x,y coordinates of the source location. The sum is recalculated for each potential source location. Assuming no error in the data, χ^2 will have a value of 0 at the source location. The location code searches for the values of x_s and y_s that minimize the value of χ^2 . The process is an iterative search, because it is not possible to directly write down simple equations for the values of x_s and y_s that minimize χ^2 . The search is performed using one of 2 algorithms, either a Simplex search or Powell's Method. The math gets more complicated when extended to three dimensions, but the approach is still basically the same.

4.3 Investigation by Means of Three-point Bending Test

4.3.1 Experimental Setup

Two kinds of concrete were prepared, such as normal concrete and fly ash concrete, and mix proportions of each concrete are shown in **Table 4.1**. The water to cement ratio (W/C) was 45%. An ordinary Portland cement with a density of 3.15g/cm^3 , sand with surface-dry density of 2.51g/cm^3 , a coarse aggregate with surface-dry density of 2.58g/cm^3 were used. A fly ash (the Type II specified in JIS A 6210), which has a density of 2.38g/cm^3 , was used for fly ash concrete.

Figure 4.2 shows the shape of specimen and the AE sensor location. Six AE sensors were attached on both sides of specimen to measure three dimensional crack locations. Sensor location was selected to detect the AE source effectively. A notch at the midpoint of specimen, which have a depth of 33mm (one third of specimen depth) and a thickness of 3mm, was induced. All specimens were demoulded at 24 hours after casting, and cured in 20°C water. The pre-cracking test was performed at the age of 28 days, and the 2nd loading test was performed just after the pre-cracking test. Unloading point of both the pre-cracking test and the 2nd loading test was CMOD of 0.05mm. After that, all

Table 4.1 Mix Proportions of Normal and Fly Ash Concrete

Case	W/C (%)	s/a (%)	Unit Content (kg/m^3)					Admixture (cc/m^3)
			Water	Cement	Sand	Gravel	Fly ash	AEA†
NC	45	47	170	377	780	903	-	0.97
FC	45	47	170	377	716	903	58	0.97

AEA† : Air Entraining Agent

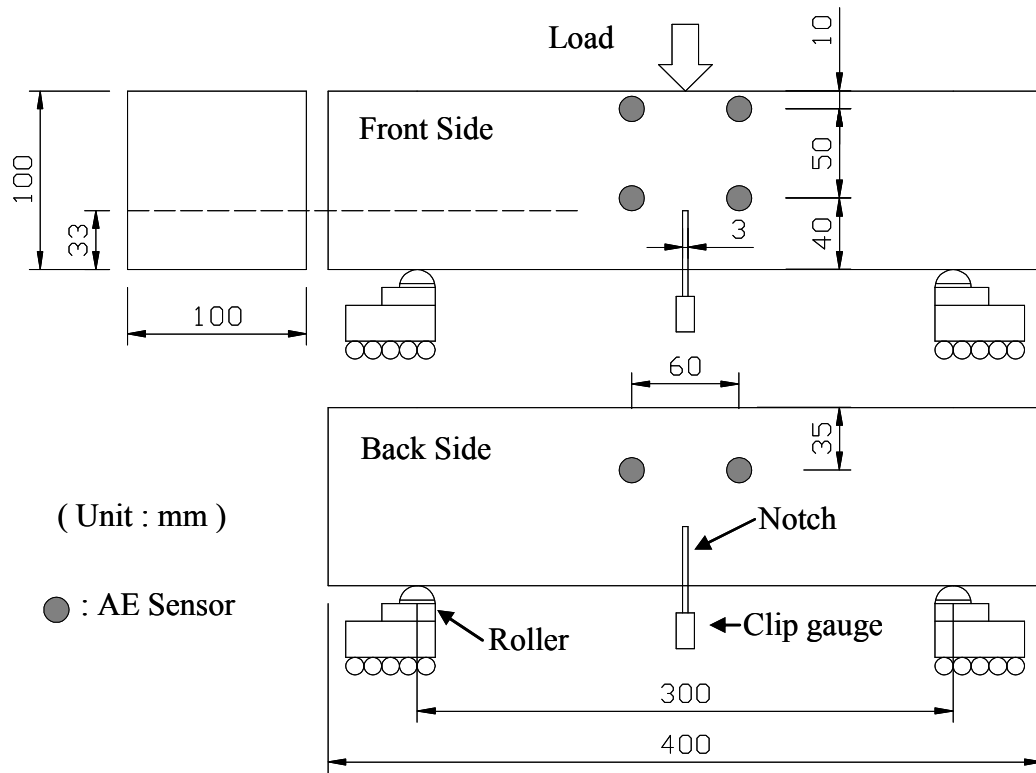


Figure 4.2 Shape of Specimen and AE Sensor Location

specimens were recured in water condition for 28 days, and the 3rd loading test was performed after the recuring.

AE sources location and the averaged frequency were calculated from AE device at the pre-cracking test, the 2nd loading test, and the 3rd loading test. The detected AE signal was magnified to 35dB by a pre-amplifier, and also magnified to 45dB by a main amplifier. The threshold value of 40dB was used in this study. The frequency range of acquisition is set from 1kHz to 400kHz. And the initial gradient G_2 and G_3 were calculated from the 2nd loading test and the 3rd loading test, and the gradient ratio was calculated.

4.3.2 Experimental Results

(a) The Gradient Ratio

Figure 4.3 shows an example of the Load-CMOD curves of each material, and the recovery tendency in stiffness could be observed between before and after the recuring. **Figure 4.4** shows the gradient ratio of each concrete, and it indicates that the initial gradient of the 3rd loading test after the recuring was recovered due to autogenous healing. These results were the same trend as the results of previous three-point bending test in Chapter 2 and 3.

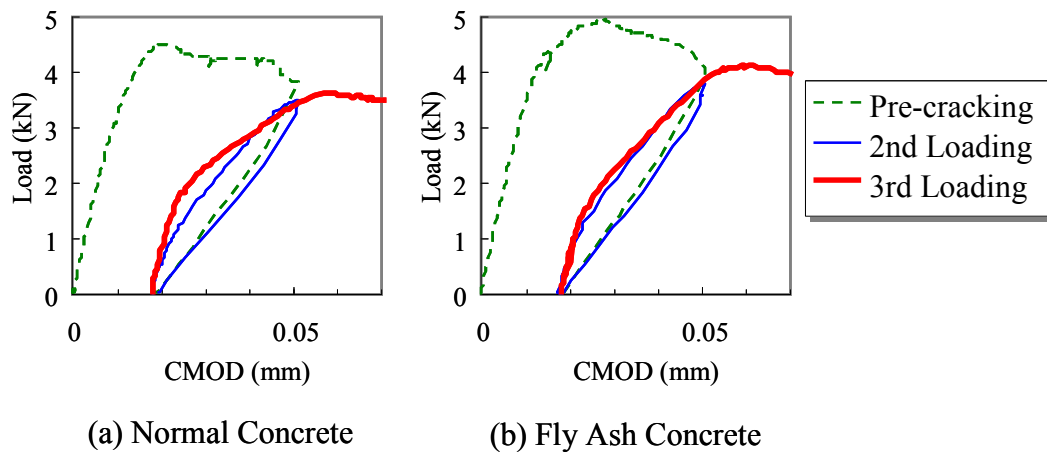


Figure 4.3 Example of Load-CMOD Curves of Each Concrete

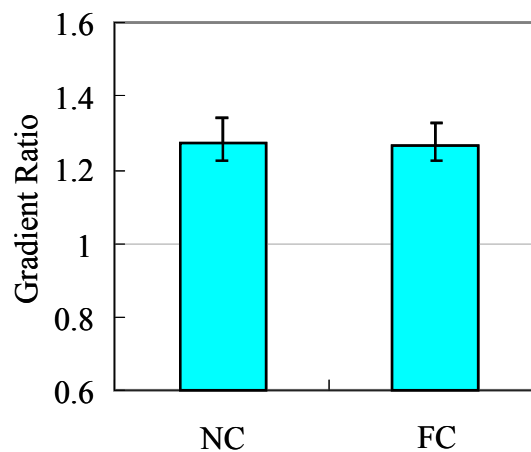


Figure 4.4 Gradient Ratio of Each Concrete

(b) AE Source Location

Figures 4.5 and **4.6** show the AE sources location of normal concrete and fly ash concrete during the pre-cracking test, the 2nd loading test, and the 3rd loading test, respectively. Many cracks were observed in front of the induced notch tip at the pre-cracking test. Several AE sources were also detected at the 2nd loading test. However, a few AE sources were also detected at the 3rd loading test after water recuring, although the gradient ratios showed the recovery tendency.

(c) Averaged Frequency of AE Test

Figures 4.7 and **4.8** show the averaged frequencies of the detected AE on normal concrete and fly ash concrete during the pre-cracking test, the 2nd loading test, and the 3rd loading test. The averaged frequencies during the pre-cracking test were over 100 kHz regardless of concretes. The averaged frequency during the 2nd loading test was similar to those during the pre-cracking test. But, those of the 3rd loading test became noticeably lower comparing to the pre-cracking test and the 2nd loading test.

These result indicated that the release fracture energy of generated products due to autogenous healing was lower comparing to that of bulk concrete. However, the gradient ratios showed recovery tendency, and it seems to be cause that the gradient ratios related with recovery of adhesive strength of whole crack part. Consequently, it seems that the gradient ratio has more sensitivity to detect the recovery of not enough recovered area than AE technique.

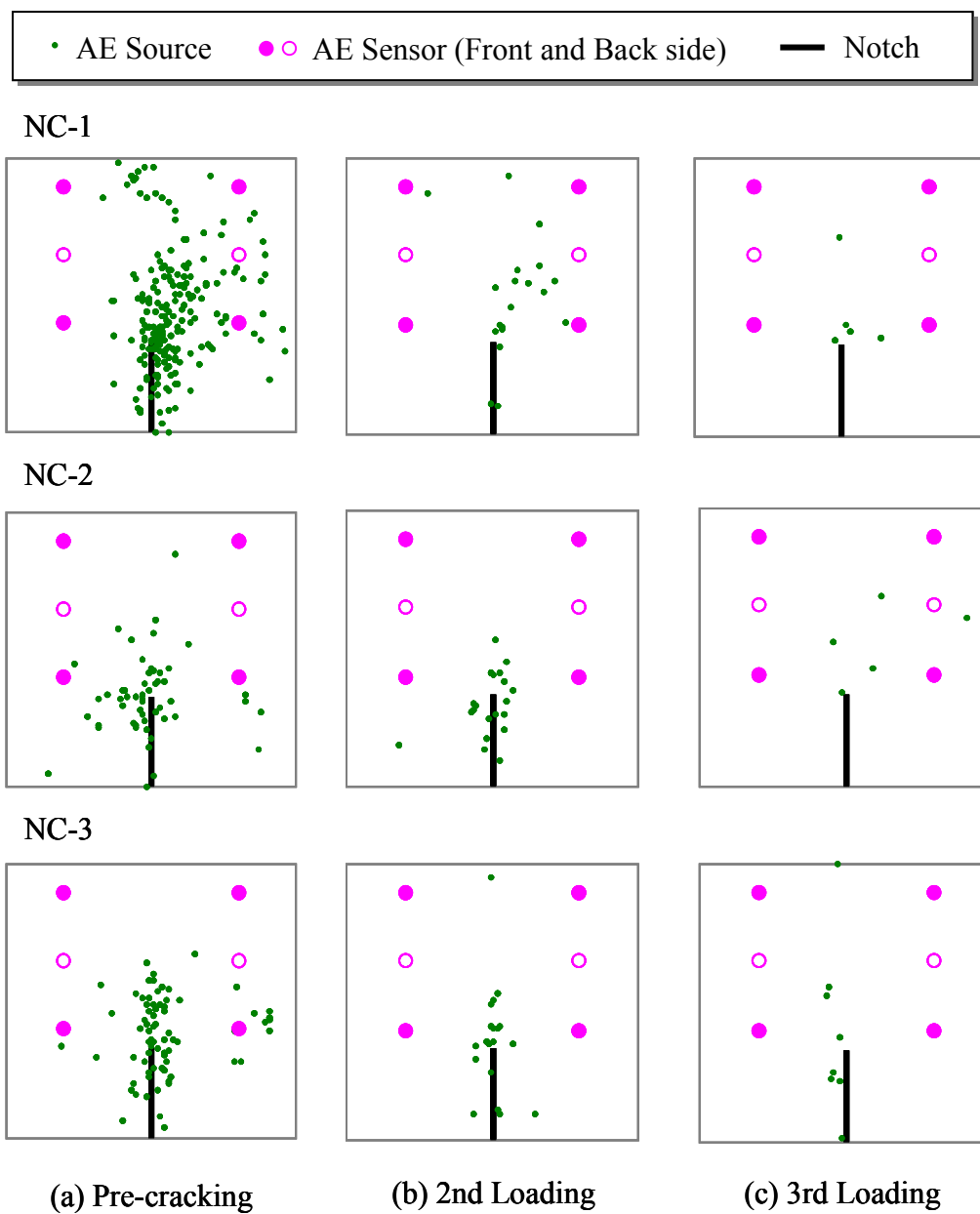


Figure 4.5 AE Sources Location of Normal Concrete

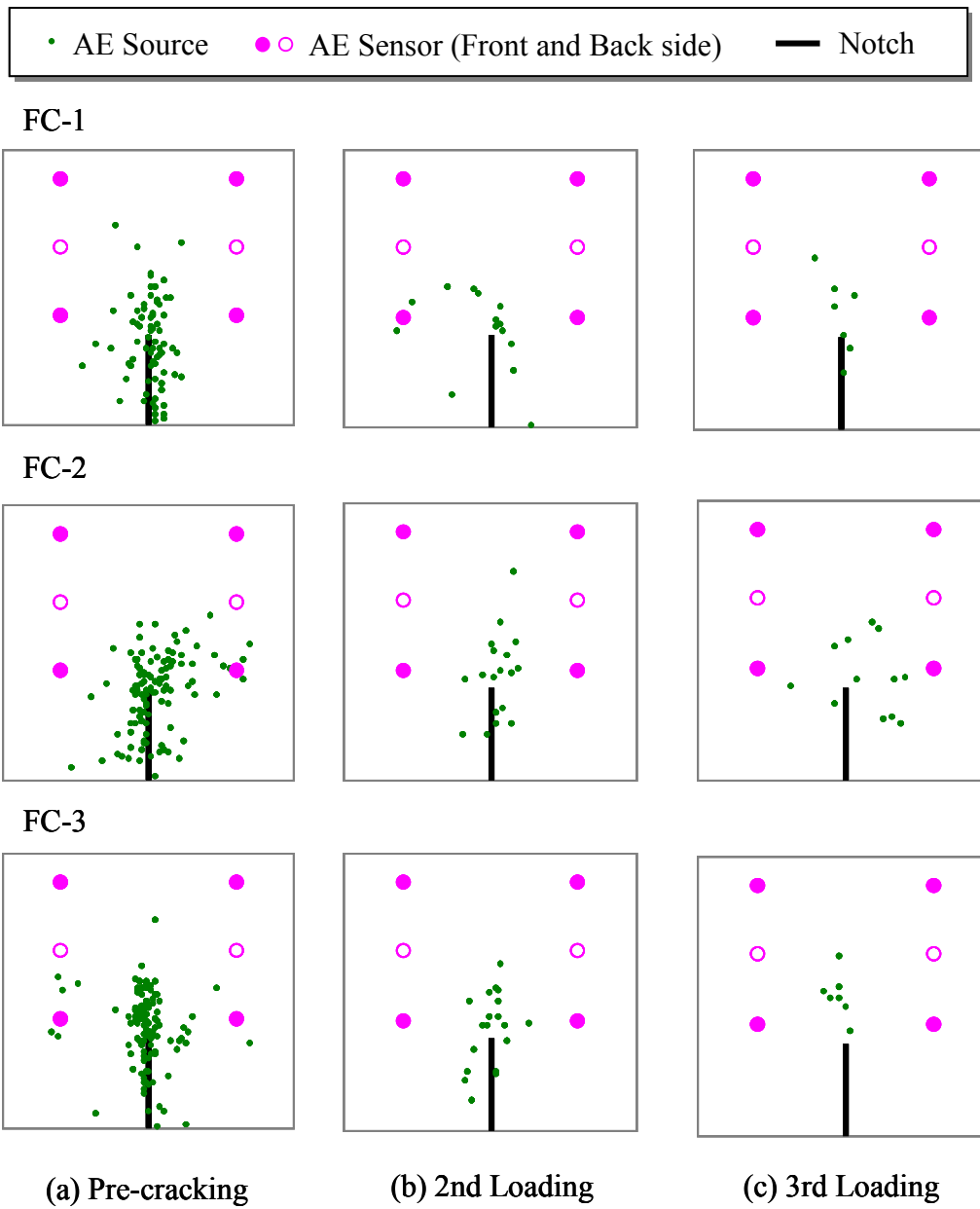


Figure 4.6 AE Sources Location of Fly Ash Concrete

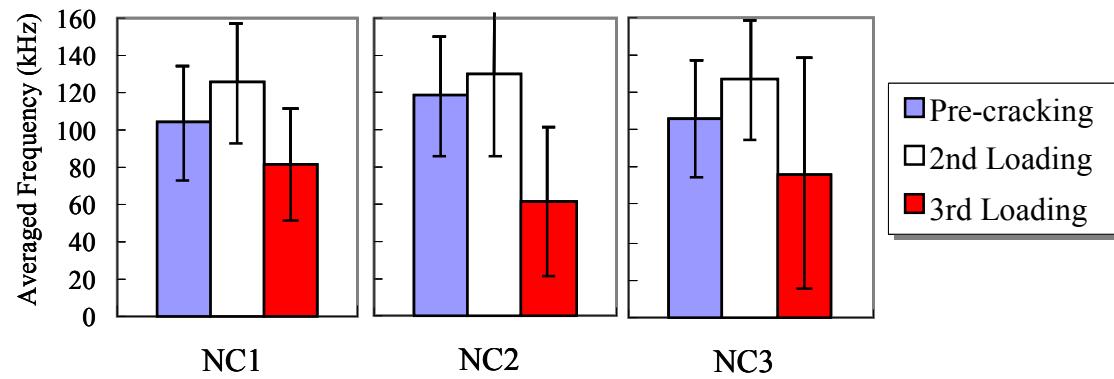


Figure 4.7 Averaged Frequencies of Normal Concrete

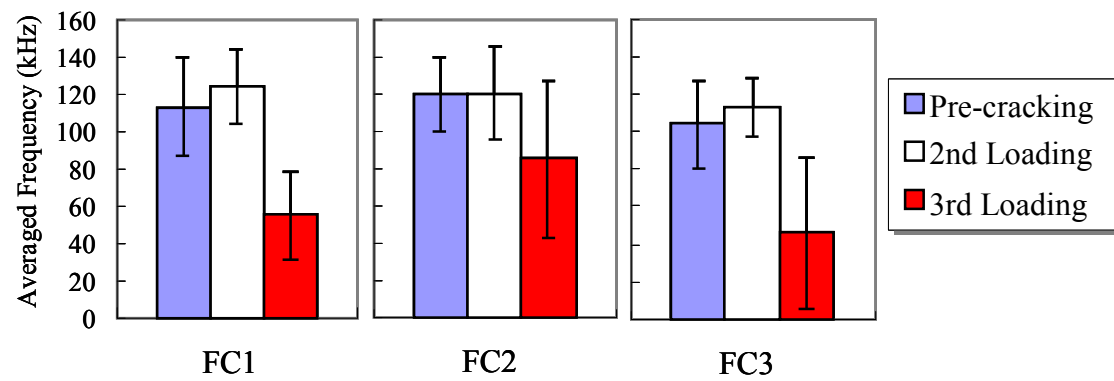


Figure 4.8 Averaged Frequencies of Fly Ash Concrete

4.4 Investigation by Means of Flexural Test for RC Beam

4.4.1 Experimental Setup

Two kinds of concrete were prepared, such as normal concrete and fly ash concrete, and mix proportions of each material is the same as the previous three-point bending test, as shown in **Table 4.1**. The water to cement (W/C) ratio was 0.45, and used material properties was same with previous test.

Four-point bending test was conducted, and **Figure 4.9** shows the shape of specimen. Cross section of the specimen was 100×200mm, and loading span was 1400mm. Two D13 rebars were placed at the bottom part of section, and six stirrup rebar (D6) were located in the shear span of specimen with intervals of 100mm. Four PI gauges were attached to this bottom area, and it measured each the crack opening. The Load-Displacement relationship was measured. **Figure 4.10** shows the experimental setup.

All specimen were demoulded at 24 hour after casting, and moist curing was conducted in constant curing room with relative humidity of 70~80% and temperature of 20°C. The pre-cracking test was performed at the age of 28 days,

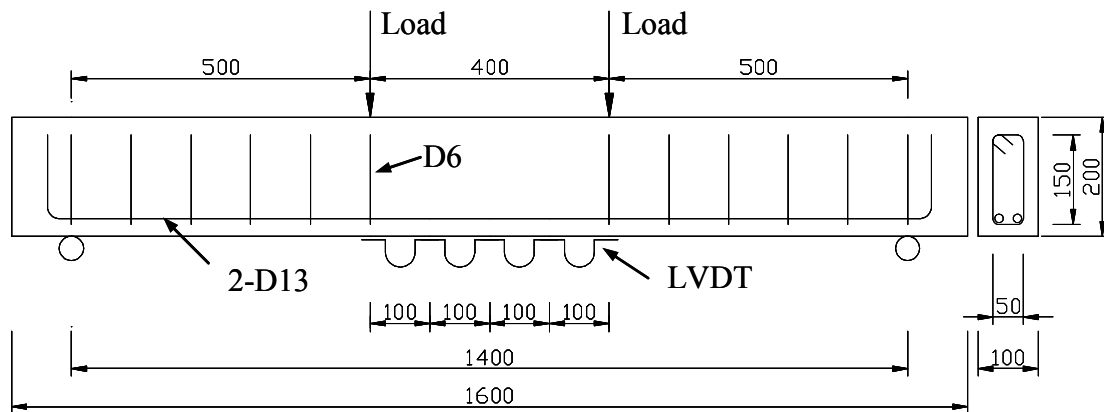


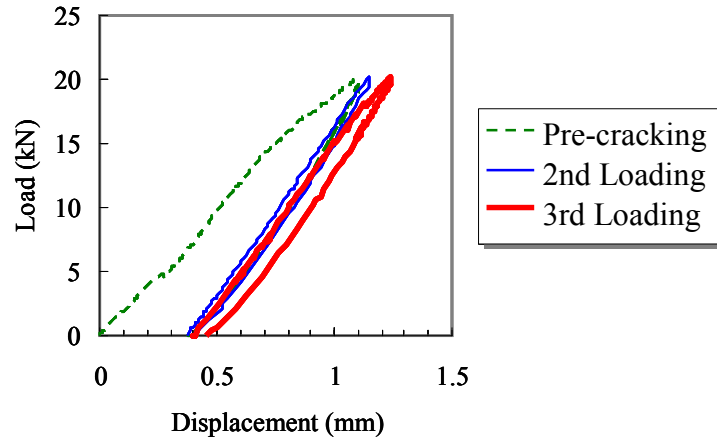
Figure 4.9 Shape of Specimen for RC Beam



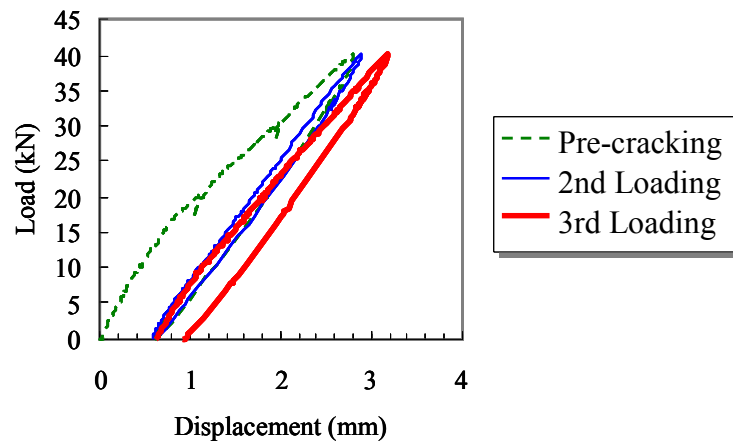
Figure 4.10 Experimental Setup of RC Beam Test

and two damage levels were adopted (20kN and 40kN). Thus, four cases were prepared with different concrete, such as the NC20, NC40, FC20, and FC40 cases. The 2nd loading test was also performed just after the pre-cracking test to compare the behaviors before and after the recuring. After that, all specimens were recured in 20°C water condition. The 3rd loading test was performed after the recuring for 28 days. To compare the before and after the recuring, autogenous healing ability on RC beam level specimen was evaluated. **Figure 4.11** shows the Load-Displacement curve of each load case.

Figure 4.12 shows the location of AE sensors. The monitoring area was selected (200×50mm). Six AE sensors were attached to both sides of specimen order to detect AE source three dimensionally.



(a) 20kN Case



(b) 40kN Case

Figure 4.11 Example of Load-Displacement Curve of Each Load Case

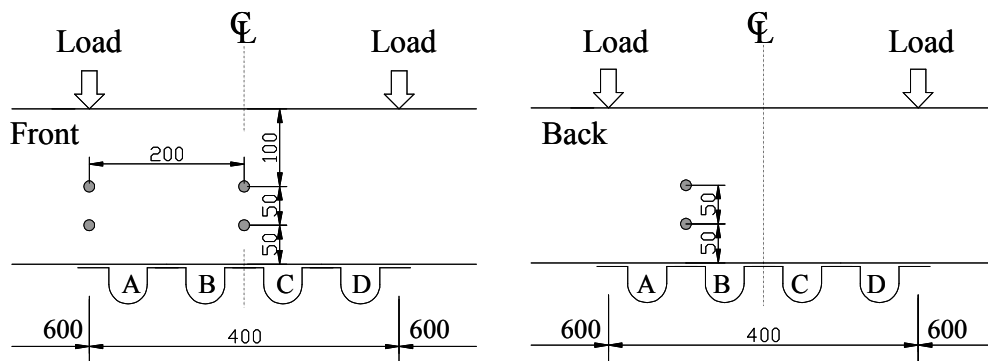


Figure 4.12 AE Sensor Location of RC Beam Test

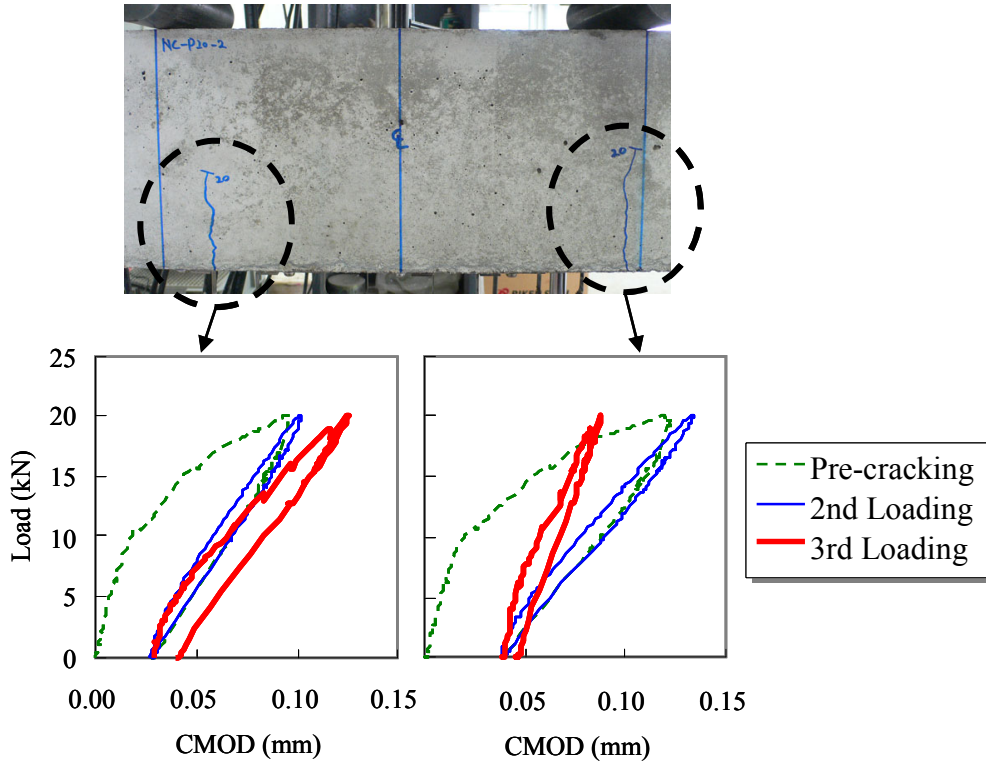


Figure 4.13 Different Load-CMOD Behavior of Each Crack

The Load-CMOD curves for each crack can be measured. In three-point bending test, the gradient ratio was easily used to evaluate autogenous healing ability of specimen, because only one controlled crack was occurred by induced notch. However, there were several cracks were occurred in RC beam, and the damage level could not be control constantly, and it caused the different recovery level to each crack. For example, two cracks in the same beam specimen show different Load-CMOD behavior after the recuring, as shown in **Figure 4.13**. In this part of study, each gradient ratio was comparing with the detected crack by AE technique, and the application of the gradient ratio to evaluate autogenous healing ability of RC beam test was investigated.

4.4.2 Experimental Results

Figures 4.14, 4.15, 4.16, and 4.17 show the AE sources location of each case during the pre-cracking test, the 2nd loading test, and the 3rd loading test. And, below of the AE sources location shows the gradient ratio of each crack and the residual crack width.

In the discussion of gradient ratios of the RC beam, the weakest value should be focused, because mechanical response depends on the weakest point mainly. Regarding 20kN case with less damage, fly ash concrete (FC20) provided higher gradient, which corresponds to autogenous healing ability. However, in the 40kN case with severe damage, both concretes gave the gradient value of 1.0 or less. In the pre-cracking test, the maximum crack width of 40kN case was over 0.1mm, and the wider crack width was out of range on the autogenous healing ability of these contents

Number of the detected AE source in the pre-cracking test was larger than these of the 2nd and the 3rd loading test. It was a similar result to the result of three-point bending test. However, relative many AE sources were detected in some parts during the 3rd loading test. There was no AE sensor in right side from center of the specimen, thus only the gradient ratio of cracks occurred in measuring by A and B parts could be able to compare with AE results. The gradient ratio was normally higher in the area where many AE source were detected area. It seems that some crack was more recovered to be detect by AE sensor, thus the gradient ratio of this part showed also higher.

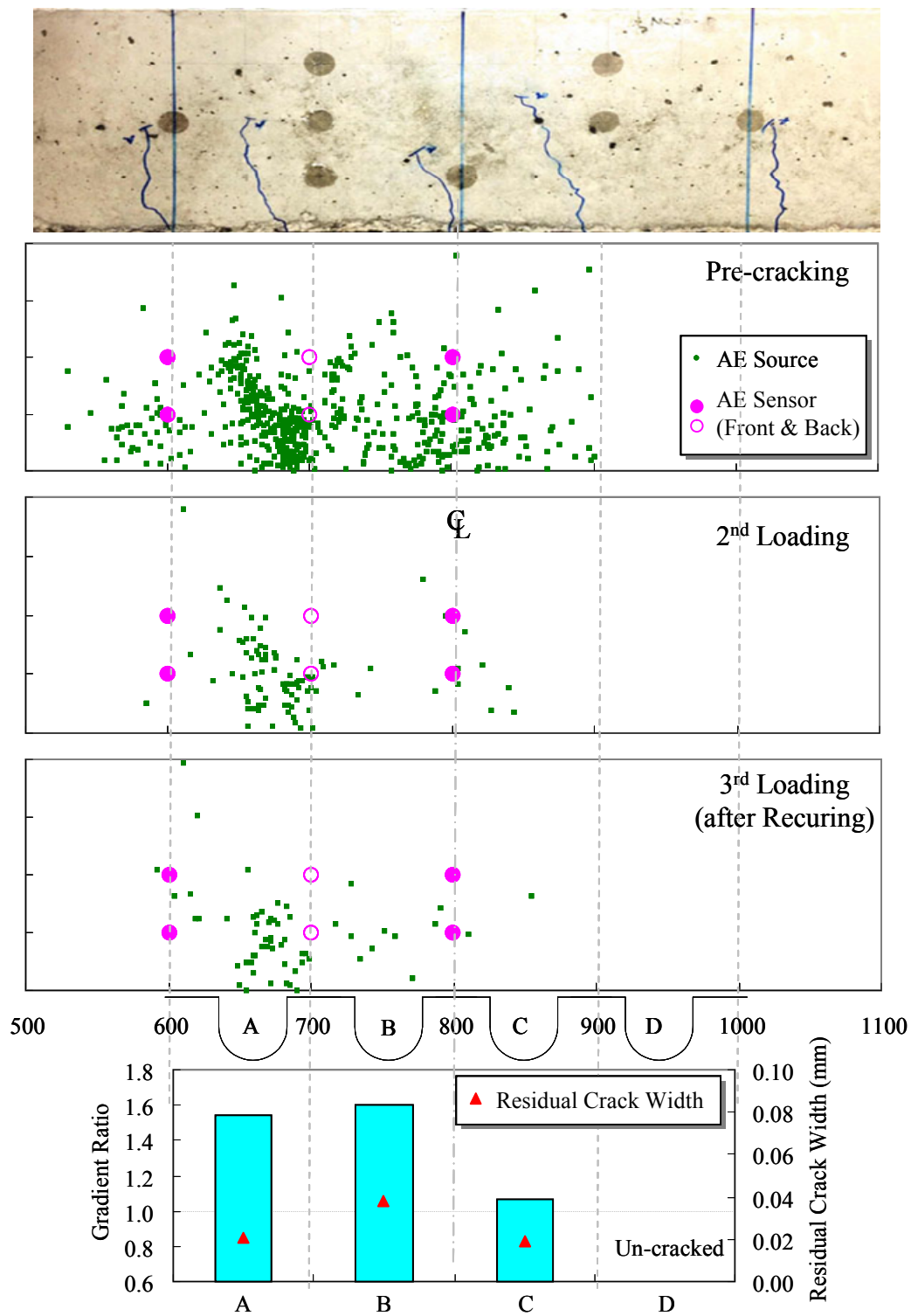


Figure 4.14 AE Sources Location (Upside) and Gradient Ratio and Residual Crack Width (Downside) of NC20 Case

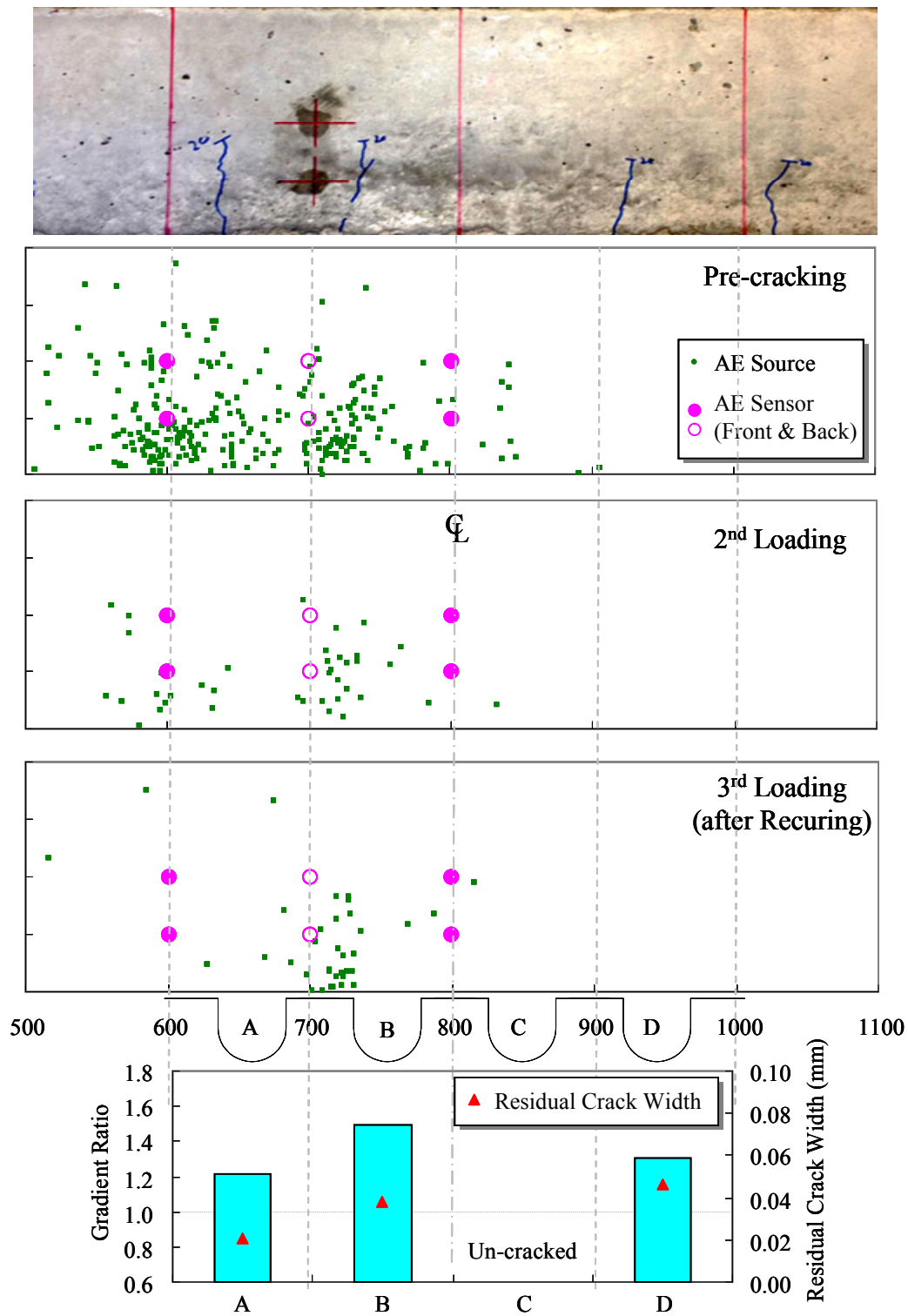


Figure 4.15 AE Sources Location (Upside) and Gradient Ratio and Residual Crack Width (Downside) of FC20 Case

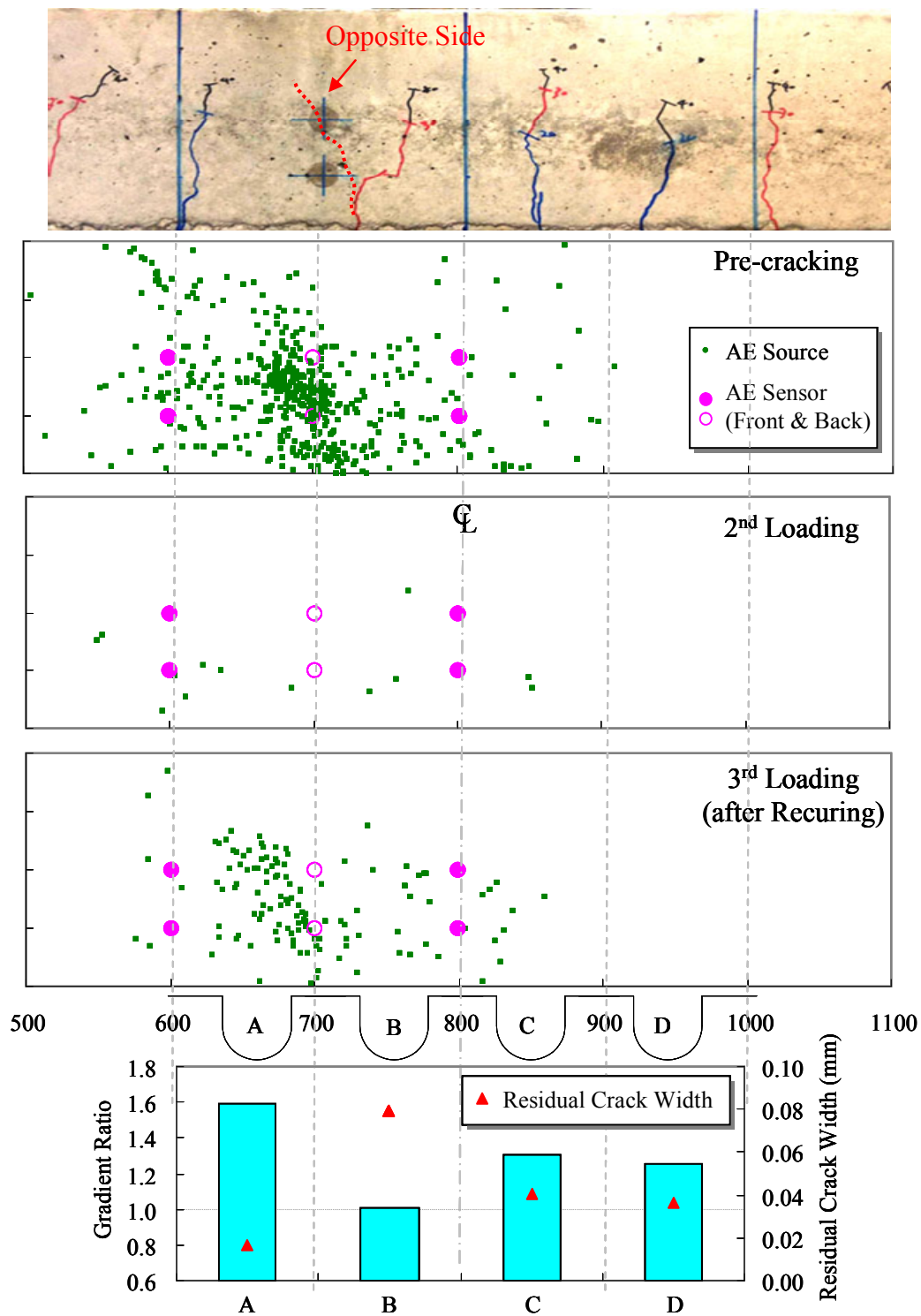


Figure 4.16 AE Sources Location (Upside) and Gradient Ratio and Residual Crack Width (Downside) of NC40 Case

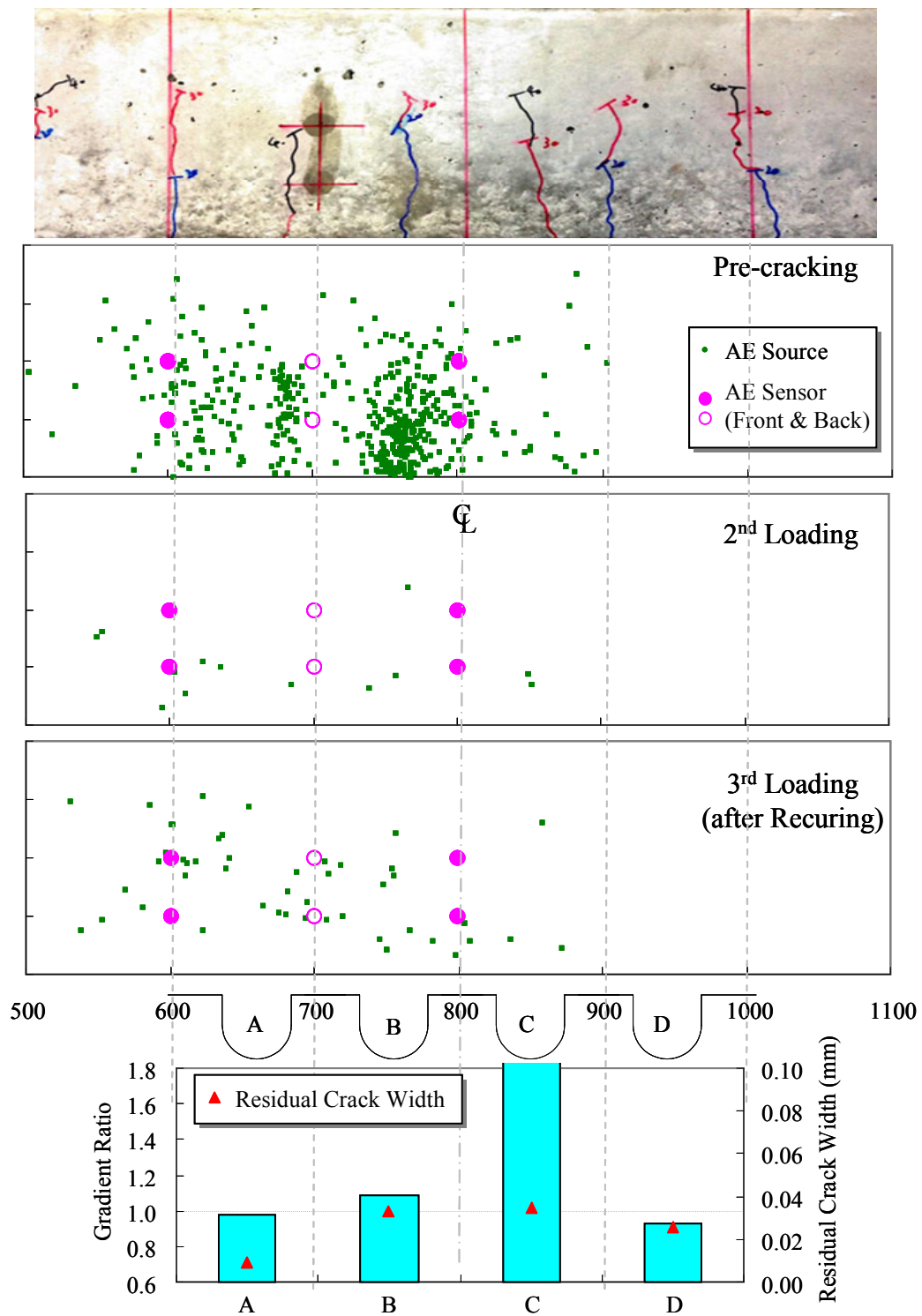


Figure 4.17 AE Sources Location (Upside) and Gradient Ratio and Residual Crack Width (Downside) of FC40 Case

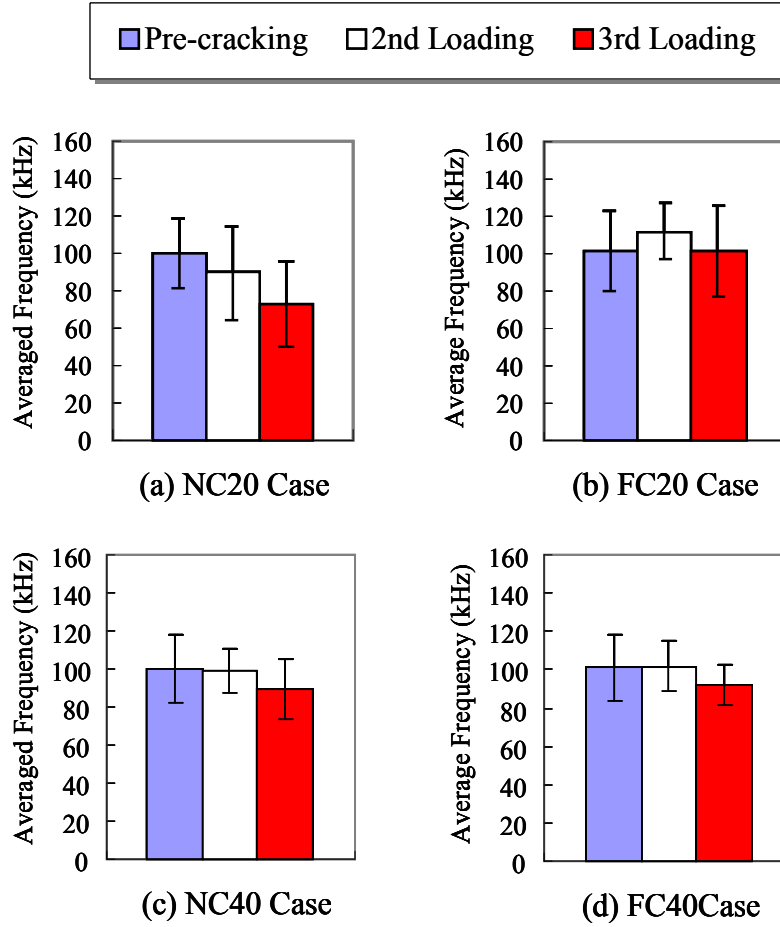


Figure 4.18 Averaged Frequencies of Each Case

Figure 4.18 shows the averaged frequencies of each case. The averaged frequency during pre-cracking was about 100kHz, and that during the 2nd loading test showed a similar level. The averaged frequency during the 3rd loading test presented lower values comparing to the previous test, but the decreasing was not significant comparing to that of the three-point bending test. It indicates the release fracture energy of re-opening crack was lower than those of bulk concrete, although relatively many AE source were also detected during the 3rd loading test.

4.5 Summary

Acoustic Emission (AE) technique was used for investigation of autogenous healing ability in this chapter. It was applied to three-point bending test and the RC beam test, and following conclusion can be obtained.

- (1) In the three-point bending test, a few AE source were detected during the 3rd loading test comparing to the pre-cracking test and the 2nd loading test. The averaged frequency of the 3rd loading test was also lower than others. It indicates the released fracture energy of generated products due to autogenous healing was lower than that of bulk concrete. However, the gradient ratio showed recovery tendency. It seems that the gradient ratio has more sensitivity to detect the recovery of not enough recovered area than AE technique.
- (2) Each gradient ratio of RC beam test showed different recovery. It seems to be caused by the different damage level during the pre-cracking test. Mechanical response depends on the weakest point mainly is also a reason.
- (3) In the RC beam test, a few AE sources were detected during the 3rd loading test, and the averaged frequency of the 3rd loading test was also lower than others. It was a similar results with those of the three-point bending test. However, some part showed relative many detected AE source with high gradient ratio. It seems that some crack was more recovered during recuring process.

5. Evaluation of Autogenous Healing Ability on UHP-SHCC

5.1 Introduction

Ultra High Performance Strain Hardening Cementitious Composites (UHP-SHCC) is a new strain hardening cementitious composite with a dense matrix. This material combines excellent protective performance with a significantly higher tensile strength and strain hardening at tensile strength, and it can be controlled fine cracks. Silica fume, which is mixed in UHP-SHCC, causes pozzolanic reaction, and this gave advantages for autogenous healing in addition to the phenomena due to high ratio of un-hydrated cement in UHP-SHCC. This chapter evaluates autogenous healing ability of UHP-SHCC in protective performance point of view. By using air and water permeability test, the change of protective performance of UHP-SHCC was investigated, such as before and after pre-cracking, and with different recuring period. And the repeatability of the autogenous healing of UHP-SHCC was confirmed.

5.2 Protective Performance

Various kinds of recoveries are reported, such as strength, stiffness of member (Schlangen et al. 2006), water tightness (Reinhardt and Jooss 2003) etc. However, Strain Hardening Cementitious Composite has higher strain capacity in tension, and increase in strength after cracking was observed during significant strain. Although mechanical properties exhibit still increasing after crack occurrence, the protective performance is deteriorated because gaps of cracks make water or air easy to flow. Generated products of autogenous healing can filled the gaps of crack during recuring, and protective performance can be recovered. In this chapter, recovery of protective performance of UHP-SHCC due to autogenous healing was focused on.

5.2.1 Ultra High Performance - Strain Hardening Cementitious Composite

A new strain hardening cementitious composite, Ultra High Performance Strain Hardening Cementitious Composites (UHP-SHCC), has a dense matrix, a significantly higher tensile strength and strain hardening under tensile loading

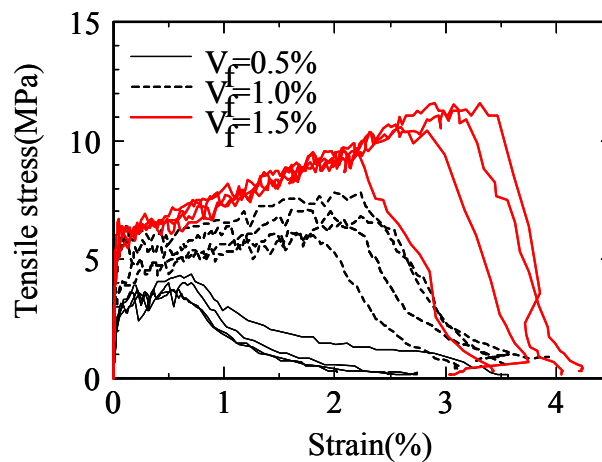


Figure 5.1 Example of Tensile Stress-Strain Response
with Difference Fiber Content (Kamal 2008)

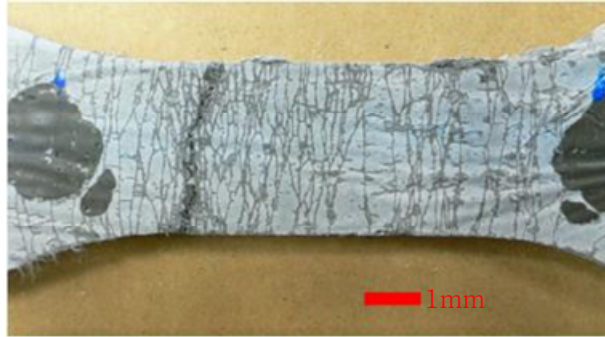


Figure 5.2 Multiple Fine Crack of UHP-SHCC

(Kunieda 2007, 2011, Kamal 2008) as shown in **Figure 5.1**. The multiple fine cracks of UHP-SHCC are less than $30\mu\text{m}$ width, and crack width of each crack should be almost constant. And the number of cracks increased as increasing the damage level represented by nominal tensile strain. **Figure 5.2** shows the multiple fine cracks of UHP-SHCC under uniaxial tensile test. This constant and fine crack is proper circumstance that generated products due to autogenous healing fill the gaps.

A chemical characteristic of UHP-SHCC also has advantage for autogenous healing. Water to binder ratio of UHP-SHCC is significantly lower than that of other concretes, silica fume that causes pozzolanic reaction was also mixed to UHP-SHCC. It can be expected that re-hydration of un-hydrated cement and pozzolanic reaction help autogenous healing more efficiently.

5.3 Recovery of Protective Performance due to Autogenous Healing

5.3.1 Specimens

Table 5.1 shows the mix proportion of UHP-SHCC used for uniaxial test. Low heat Portland cement with density of 3.14g/cm^3 was used, and silicafume with density of 2.2g/cm^3 replaced to cement of 15 %. Quartz sand with density of 2.68g/cm^3 and less than 0.5mm in diameter was used as the fine aggregate. High strength polyethylene (PE) fiber with density of 0.97g/cm^3 , tensile strength of 2700MPa, and elastic modulus of 88GPa was used, and the diameter and length of the PE fiber were 0.012mm and 6mm, respectively. Superplasticizer (poly-carbonic acid type) was used to enhance the workability of the material, and air reducing agent was also used.

Figure 5.3 shows the shape of the specimen. A measure surface was $150 \times 200\text{mm}$ to consider of enough measuring area for air and water permeability tests, and thickness was 30mm. Two D6 rebars (SD295, f_y : 407MPa) were placed in the specimen to control the crack formation. Another three D10 rebars (SD295A) were embedded in both of end sides of the specimen to hold the specimen by a testing machine. All rebars location was considered not to influence to the permeability tests.

Table 5.1 Mix Proportion of UHP-SHCC for Uniaxial Test

Fiber volume $V_f(\%)$	W/B	Unit contestn (kg/m^3)						
		Water	Cement	Silica fume	Sand	SP [†]	ARA [‡]	Fiber
1.5	0.22	340	1313	232	155	15.4	0.062	14.6

SP[†] : Superplasticizer

ARA[‡] : Air reducing agent

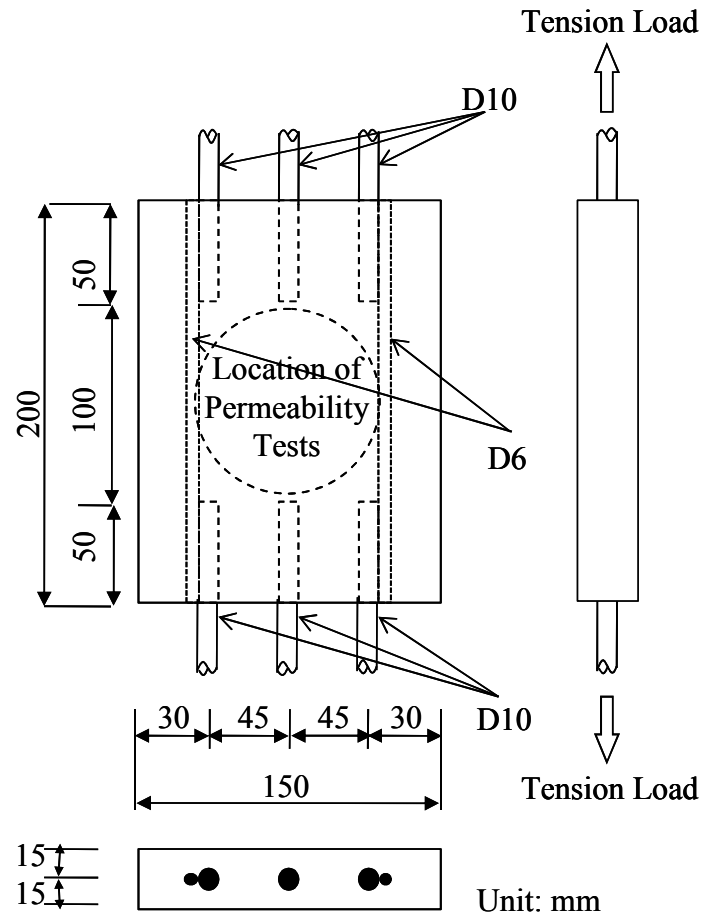


Figure 5.3 Shape of Uniaxial Tensile Specimen

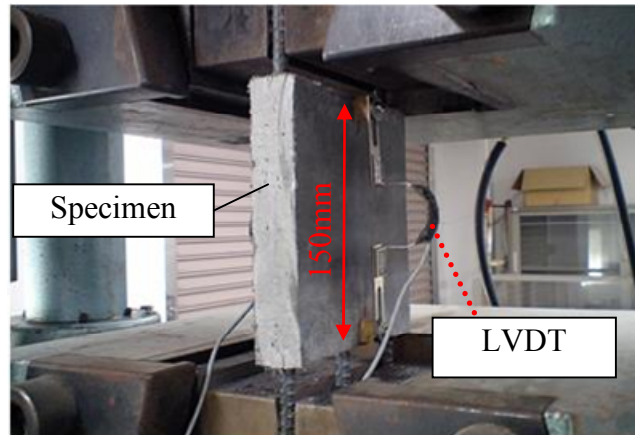


Figure 5.4 Uniaxial Tensile Test Setup

Cracks were induced by uniaxial tensile test. The strain was monitored by LVDT, which was fixed on both surfaces of specimens, and the measurement length was 150mm. Universal Testing Machine used for the the pre-cracking test and the reloading test. **Figure 5.4** shows the test setup of uniaxial tensile test.

5.3.2 Air Permeability Test

A sensitive index related to required performance should be selected for evaluation autogenous healing ability. A protective performance, such as a water permeability test, was usually used for SHCC type materials with multiple fine cracks, because of high sensitivity on durability issues (Reinhardt, 2006 and Yingzi, 2003). Although the material has higher strength and higher strain capacity after cracking, the protective performance is decreased by cracking, and could be increased by autogenous healing effect.

Air permeability test was conducted using the Torrent Permeability Test (TPT), proposed by Torrent (Torrent, 1992). **Figure 5.5** shows the Torrent Permeability Tester device. The device consists of a chamber, a vacuum pump, a

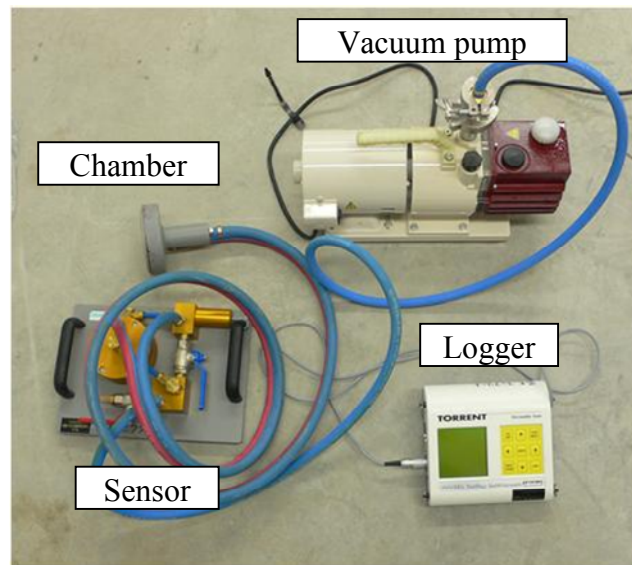


Figure 5.5 Torrent Permeability Tester

pressure sensor, and a logger. To prevent misleading lead to spurious ingress of air along the skin, there are two chambers; outer chamber and inner chamber. After the desired level of vacuum has been attained, pump just act on the outer chamber, and a logger records the history of change of inner chamber. A spurious ingress from concrete surface is evacuated by outer chamber, and uniaxial air flow can be measured through the pressure of the both chambers, as shown in **Figure 5.6**. Air permeability coefficient is calculated by equation given in (5.1)

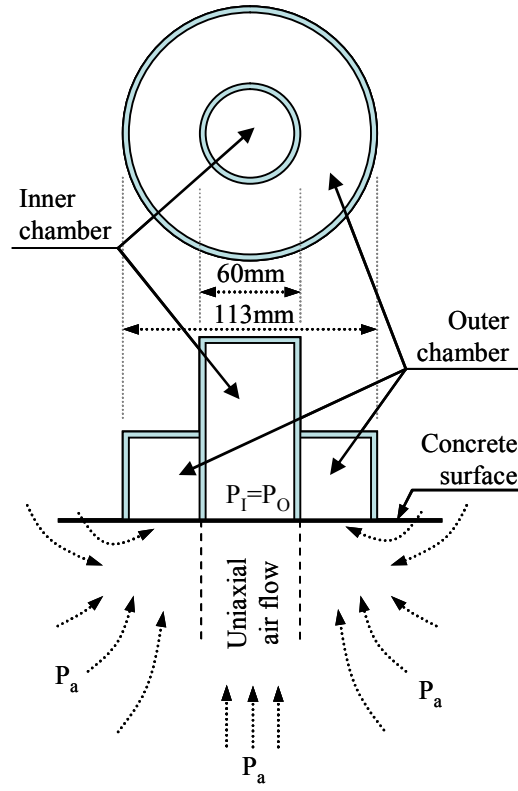


Figure 5.6 Conceptual Diagram of the Chamber

$$k = 4 \left(\frac{V_c (dP_I / dt)}{A (P_a^2 - P_I^2)} \right)^2 \frac{\mu P_a}{\epsilon} \int_{t_0}^t \left(1 - \left(\frac{P_I}{P_a} \right)^2 \right) dt \quad (5.1)$$

where,

k : coefficient of permeability to air (m^2)

V_c : volume of inner chamber (m^3)

P_I : pressure in inner chamber (N/m^2)

P_a : atmospheric pressure (N/m^2)

μ : dynamic viscosity of air (N/m^2)

ϵ : empty porosity of the concrete

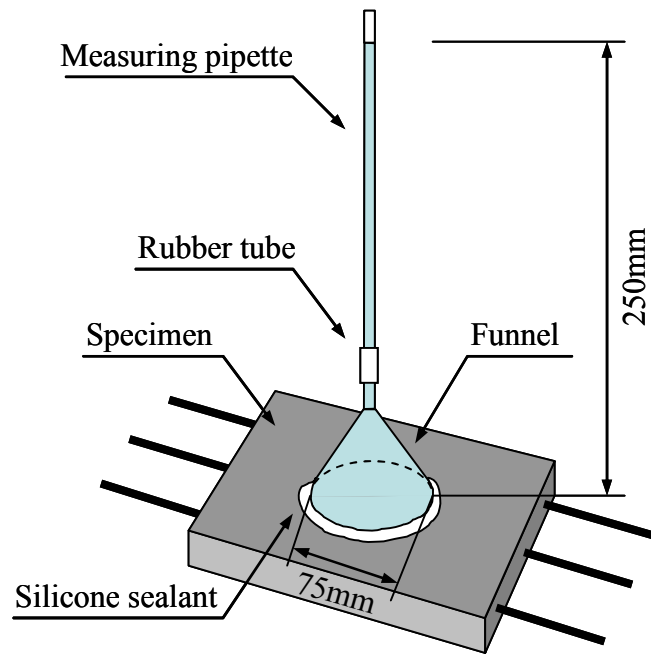


Figure 5.7 Water Permeability Test Setup

5.3.3 Water Permeability Test

Water permeability test was used in this chapter, which is specified in the testing method of surface penetrant (JSCE-K571-2004), as shown in **Figure 5.7**. The measuring section was located at center of the specimen, which was the same position with the location for the air permeability test. A caliber funnel having the size of 75mm in diameter was attached to the surface of the specimen, and connected with measuring pipette by a rubber tube. An interface between the funnel and the surface of specimen was sealed with a silicone sealant. Water was poured until 250mm head of pipette, and the change of water head was measured. The amount of water per an hour was calculated, and it was defined as water permeation in this study.

5.3.4 Experimental Program

The outline of the experimental procedures is schematically illustrated in **Figure 5.8**. The specimens were demoulded at 24 hours after casting, and cured in water in a constant temperature room with 20°C. Air permeability tests and water permeability tests were performed at the age of 32~35 days, before the pre-cracking test. Then, the pre-cracking test induced cracks to specimens. Air permeability tests and water permeability test were performed again just after the pre-cracking to measure the damage level, and specimens were recured in water or air condition. Recovery of protective performance was investigated by measuring air permeability test and water permeability test for 20 days, 90 days and 360 days after the pre-cracking test. All specimen were dried about 6 hours before permeability test in curing room (20°C and RH 70~80%), and water permeability test was performed after air permeability test in all sequences.

Four cases were prepared, such as the 0.1W, 0.1A, 0.2W, and 0.2A cases.

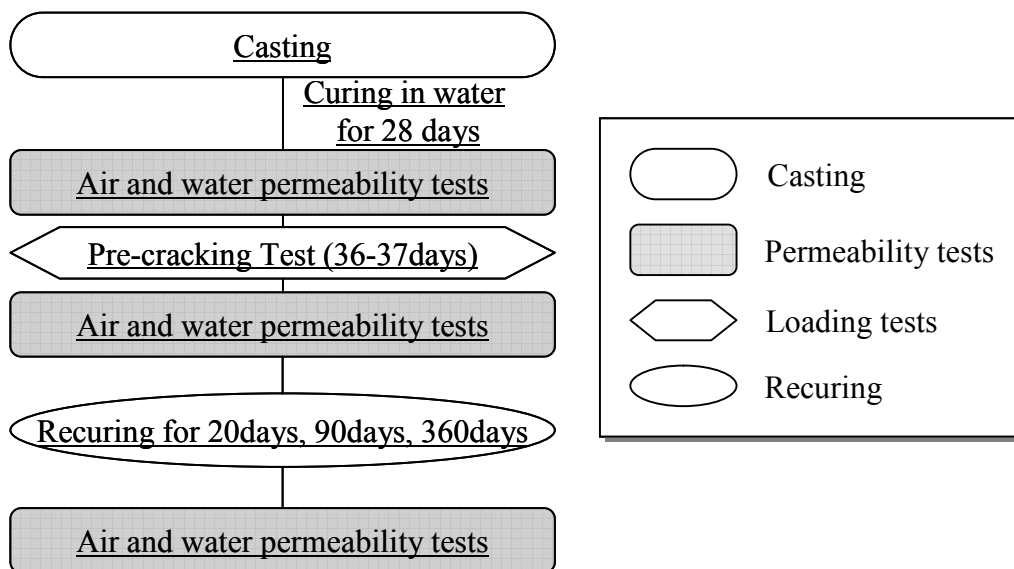


Figure 5.8 Experimental Procedures of Permeability Test

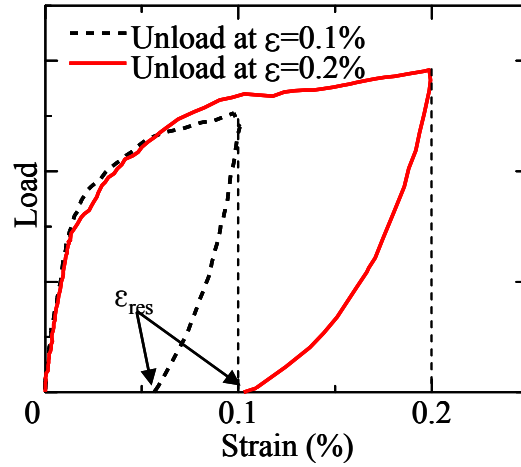
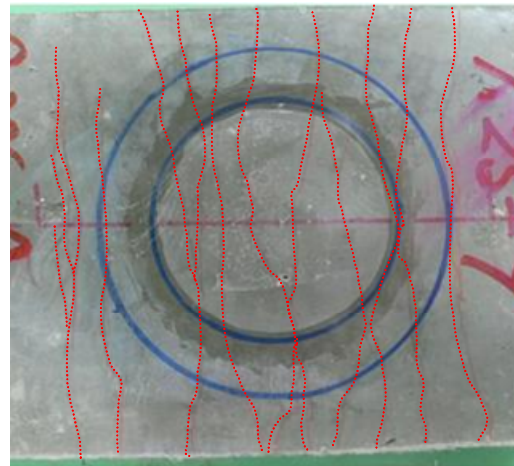


Figure 5.9 Schematic Image of Load-Strain Curves



(a) 0.1% strain case



(b) 0.2% strain case

Figure 5.10 Example of Induced Cracks

The first number means the damage level, and the character after number means recuring condition. For example, 0.1W means that damage level was strain of 0.1% and recured in water condition. And, the control specimens with no damage were also prepared to compare, such as NW and NA. Three specimens were prepared for each case. **Figure 5.9** shows schematic image of the Load-Strain curves of the each load case, and typical crack patterns are shown in **Figure 5.10**.

5.3.5 Experimental Results

(a) Averaged Crack Widths

The averaged crack width \overline{w} was calculated by equation (5.2) using the measured residual strain and observed number of cracks, and **Table 5.3** tabulates the detailed data after the pre-cracking of each case.

$$\overline{w} = \frac{\epsilon_{res} \times \Delta l}{n} \quad (5.2)$$

where,

\overline{w} : averaged crack width

ϵ_{res} : residual strain

Δl : measurement length (150mm)

n : number of cracks in measurement length

Table 5.2 Induced Residual Strains and Averaged Crack Widths

Case	Pre-cracking Test		
	Residual strain (%) ϵ_{res}	Number of cracks n	Averaged crack width (μm) \overline{w}
0.1W-1	0.051	6	12.7
0.1W-2	0.051	5	15.2
0.1W-3	0.052	5	15.5
0.1A-1	0.057	6	14.2
0.1A-2	0.052	6	12.9
0.1A-3	0.051	7	10.9
0.2W-1	0.091	9	15.1
0.2W-2	0.096	14	10.3
0.2W-3	0.114	16	10.7
0.2A-1	0.116	15	11.6
0.2A-2	0.108	15	10.8
0.2A-3	0.081	14	8.7

Several cracks were observed in the measurement area. Although the damage level was different between the 0.1% strain and 0.2% strain cases, there was no significant difference in the averaged crack width, which is material nature of UHP-SHCC.

(b) Results of Air Permeability Tests

Figure 5.11 shows air permeability coefficients of each specimen before the pre-cracking, just after the pre-cracking and after the recuring for 20 days, 90 days and 360 days. Firstly, densification of matrix in UHP-SHCC with increasing of the age was confirmed by air permeability coefficients of control case with no damage. Air permeability coefficient became smaller with increase of curing period.

Air permeability coefficient of 0.1% strain case and 0.2% strain case was similar level with control cases before the pre-cracking test. It became dramatically larger by the pre-cracking test, and was over 0.1. However, air permeability coefficients became smaller, and it was noticeable in water recuring condition. In water recuring condition, air permeability coefficients recovered to the almost original level for 20 days of recuring, after that, it became smaller than those before the pre-cracking test. In air recuring condition, air permeability coefficients became smaller with increasing of the recuring period, but change rate was slower compared to those with water recuring condition. The main cause for recovery of resistance against air permeability seems to be generated products due to re-hydration of un-hydrated cement, calcium carbonate and pozzolanic reaction, with increasing of the recuring period. There was insignificant difference between 0.1% strain and 0.2% strain case, and it seems

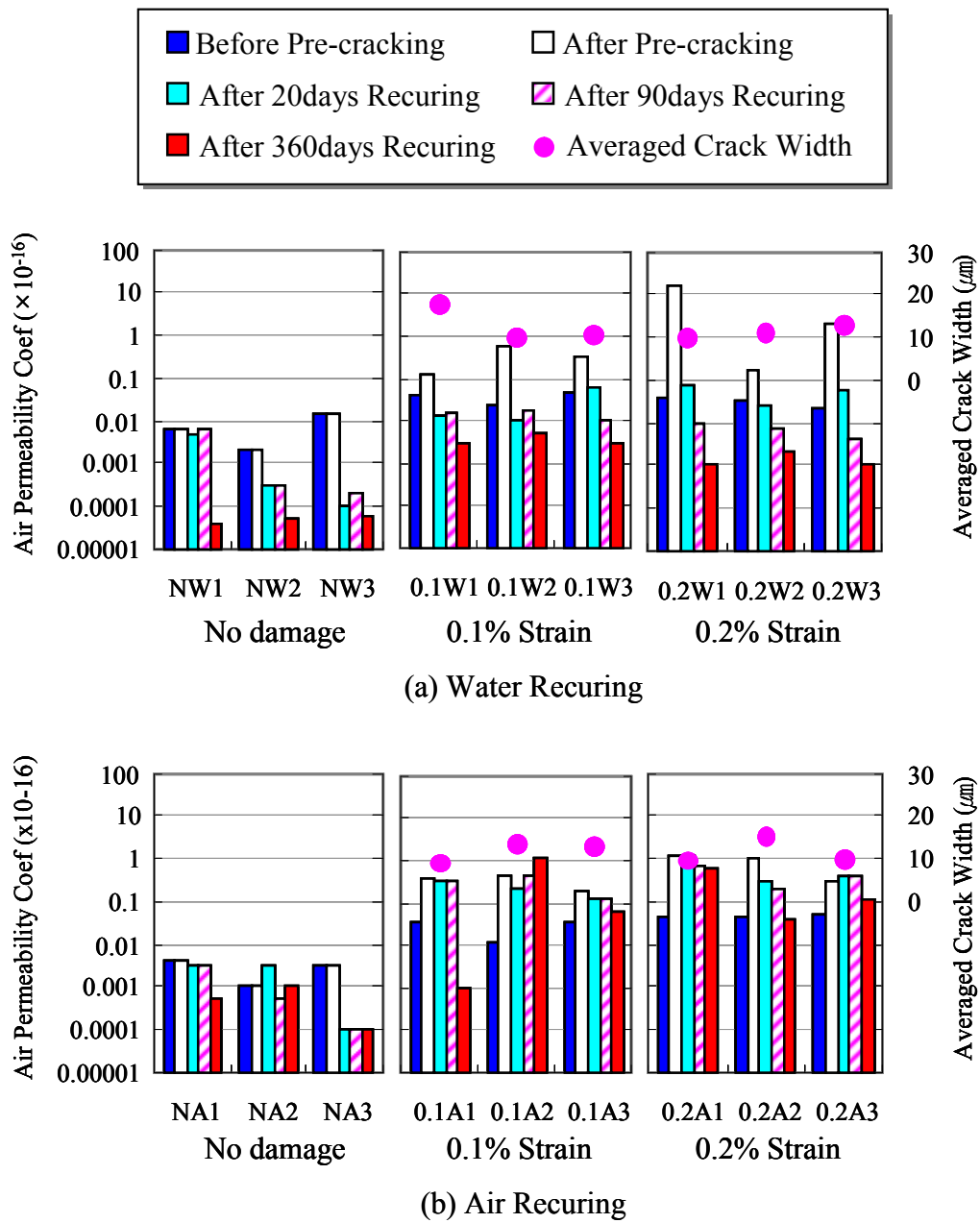


Figure 5.11 Results of Air Permeability Tests

to be related to the averaged crack width.

The quality grading of concrete by air permeability tests was proposed by Torrent (1992), and it defines that less than 0.1 of air permeability coefficient is good quality concrete, and less than 0.01 is very good concrete. In this point of view, these results indicate that recovered UHP-SHCC by autogenous healing has enough quality in terms of protective performance.

(c) Results of Water Permeability Tests

Figure 5.12 shows water permeation of each specimen, before the pre-cracking, just after the pre-cracking and after the recuring for 20 days, 90 days and 360 days. In control case with no damage, water permeation became smaller with increase of curing period. It seems that densification of matrix in UHP-SHCC accelerates to decrease of water permeation with increase of curing period.

Water permeation of 0.1% strain case and 0.2% strain case before the pre-cracking test showed similar level with those of control case, but it became dramatically larger after the pre-cracking test. In water recuring condition, water permeation recovered to the almost original level for 20 days recuring, and became smaller with increasing of the recuring period. Water permeation with air recuring condition also became smaller, but it was not significant decreasing. This result was similar to that of air permeability coefficients, and it can be concluded that these indices have a similar sensitivity to the recovery of protective performance on autogenous healing of UHP-SHCC

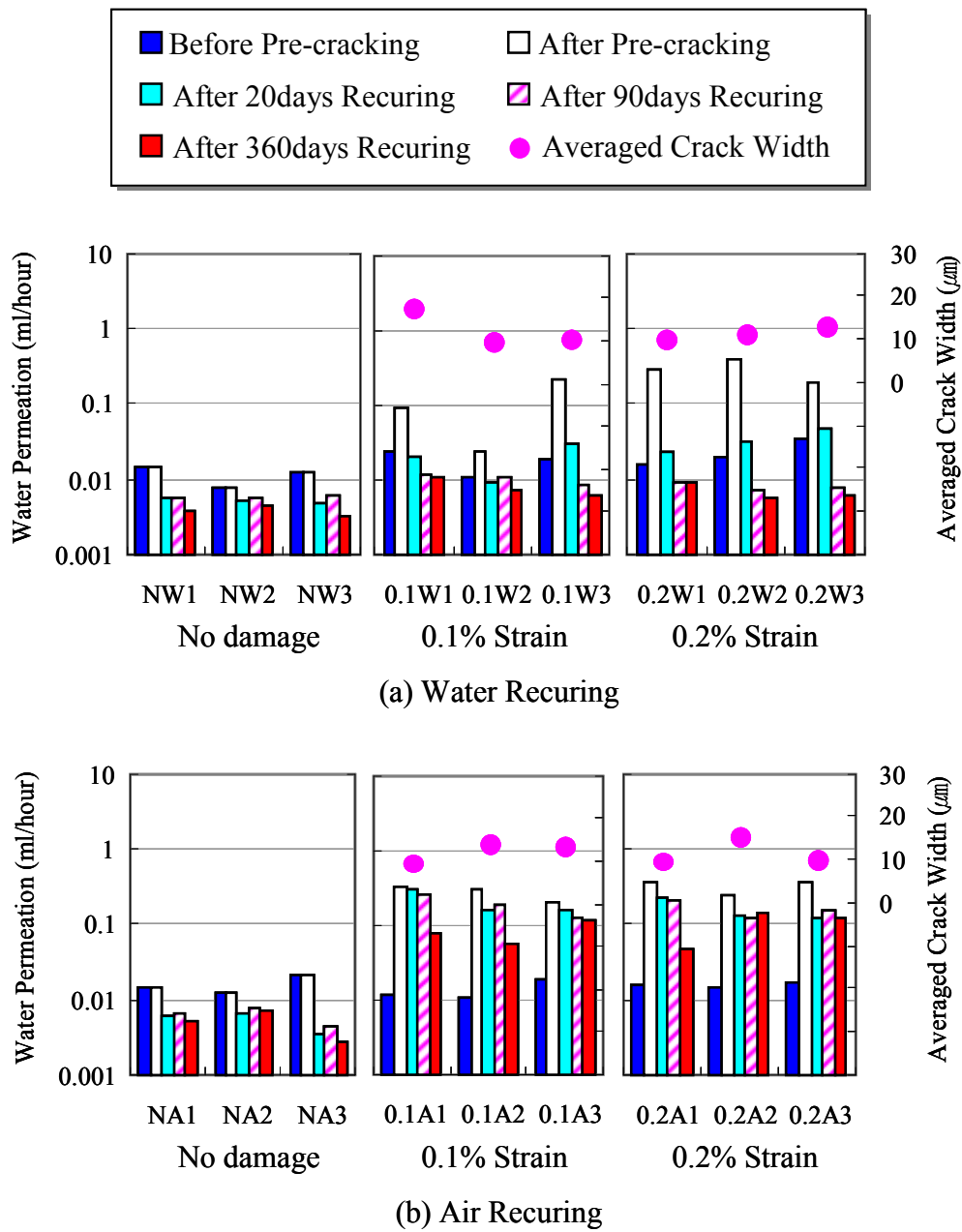
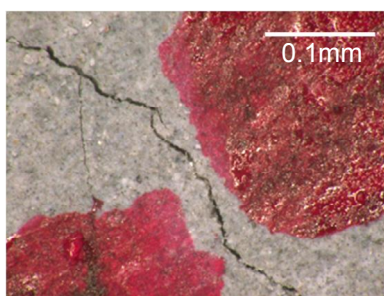


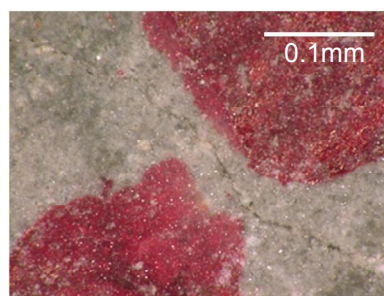
Figure 5.12 Results of Water Permeability Tests

(d) Observation of Crack Part and Material

Figure 5.13 shows the example of crack recovery by using a microscope. Opened crack were filled with new products for 20 days of recuring, which seems to be due to re-hydration of un-hydrated cement, formation of calcium carbonate, and pozzolanic reaction. **Figure 5.14** shows the Scanning Electronic Microscope (SEM) image of cracked part, and the products filling cracks can be observed. It seems that the products are slightly coarse comparing to the bulk matrix. **Figure 5.15** illustrates the results of Energy Dispersive X-ray (EDX) analysis, and Ca and Si can be detected at crack part. And **Figure 5.16** illustrates the back scattered electron image of UHP-SHCC at the age of 407 days. Light gray part shows an un-hydrated cement. Through the image, half of cement (about 49%) remains without hydration in the material after 407 days. These images can explain what was generated due to autogenous healing.



(a) Before Recuring



(b) After 20days Recuring

Figure 5.13 Details of Cracks Before and After Recuring
Observed by Using Microscope (Water Recuring Condition)

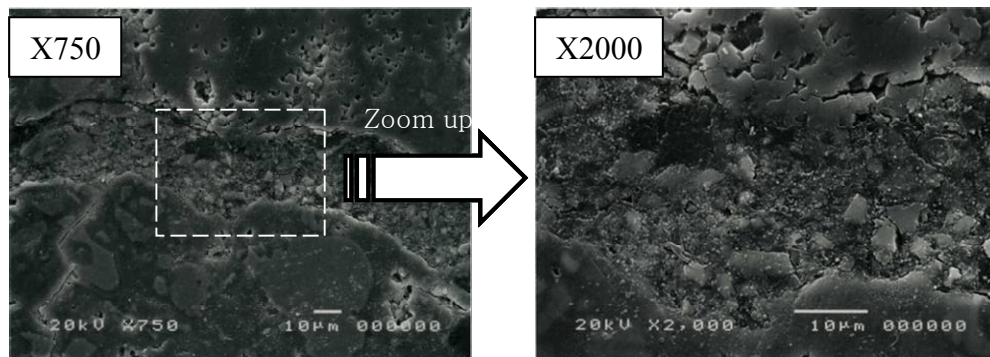


Figure 5.14 Image of Cracked Part by SEM
(Water Recuring Condition)

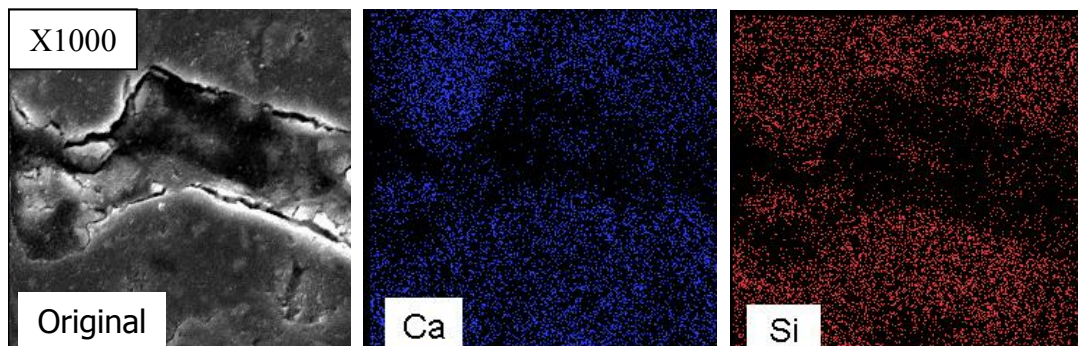


Figure 5.15 Image of Cracked Part by EDX Spectrometry
(Water Recuring Condition)

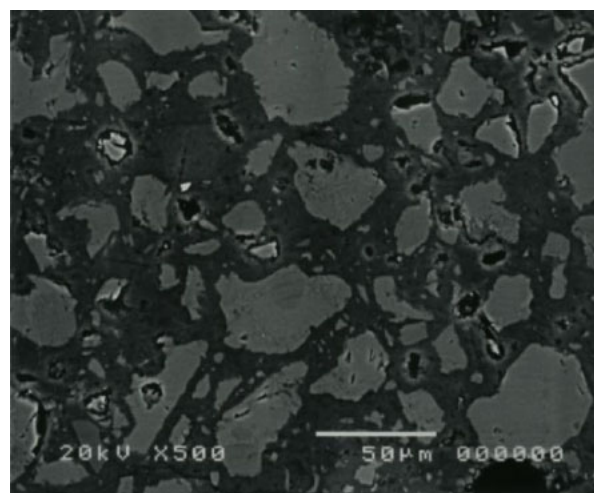


Figure 5.16 Back Scattered Electron Image of UHP-SHCC
(407 day after casting, Hydration ratio: 51.4%)

5.4 Repeatability of Autogenous Healing of UHP-SHCC

5.4.1 Experimental Program

The shape of specimens for repeated cycles was the same as that in the previous test, as shown in **Figure 5.3**. Mix proportion was also the same, as shown in **Table 5.1**, and used material had the same properties.

The twice loading-recuring were totally carried, and the outline of the experimental procedures is schematically illustrated in **Figure 5.18**. All specimens were casted and cured in 20°C water during 28 days. Before the pre-cracking test, air and water permeability test were performed to measure the permeability of specimens without any damage. Then air and water permeability tests were also performed after the pre-cracking test to ensure the damage level. After that, the 1st recuring process was performed. Water or air recuring conditions were prepared for each case, and the recuring period (28 days) was the same. Air and water permeability test before and after the reloading test were carried out, which followed the previous procedure. Recovery degree by autogenous healing through the 1st recuring process could be evaluated with air and water permeability test

The 2nd recuring process was performed, and the recuring period was also adopted for 28 days. Lastly, air and water permeability test was performed to evaluate the recovery degree by autogenous healing during the 2nd recuring process.

There were four cases having different damage levels were prepared; 0.1W, 0.1A, 0.2W, and 0.2A. The first number means the damage level in strain of the pre-cracking test, and the character after number means recuring condition,

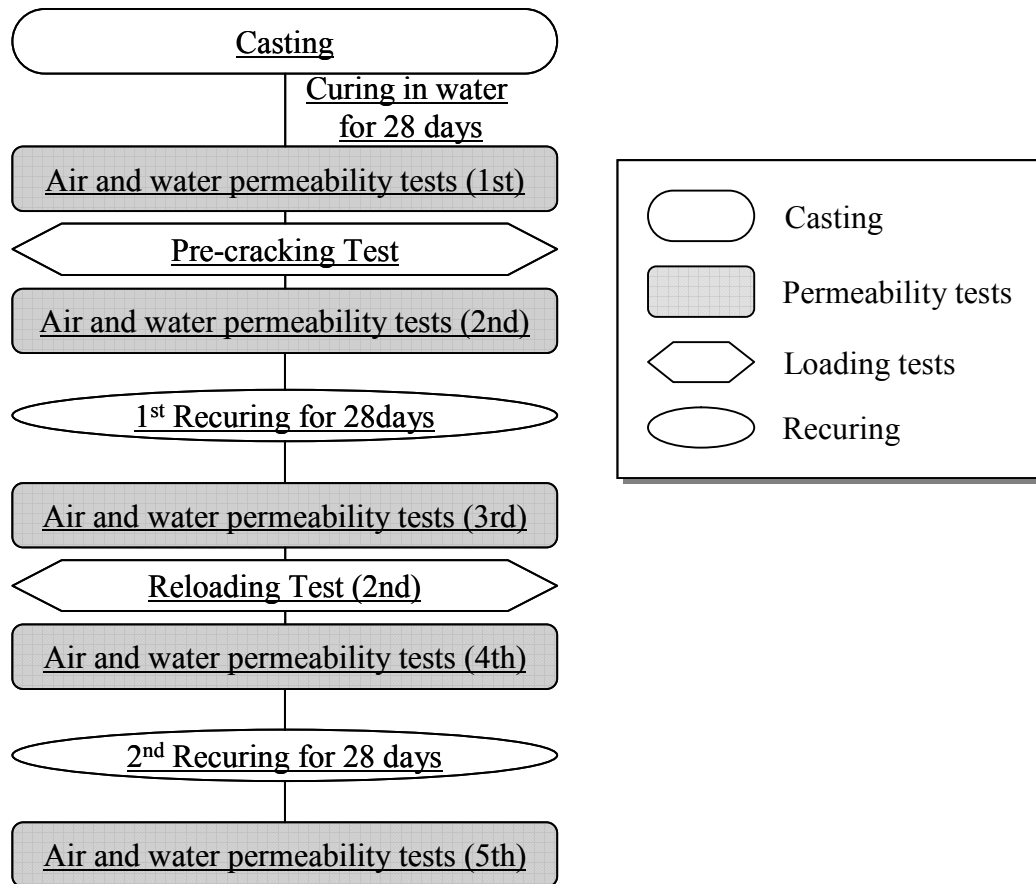


Figure 5.17 Experimental Procedures of Permeability Test under Repeated Loading-Recuring Cycle

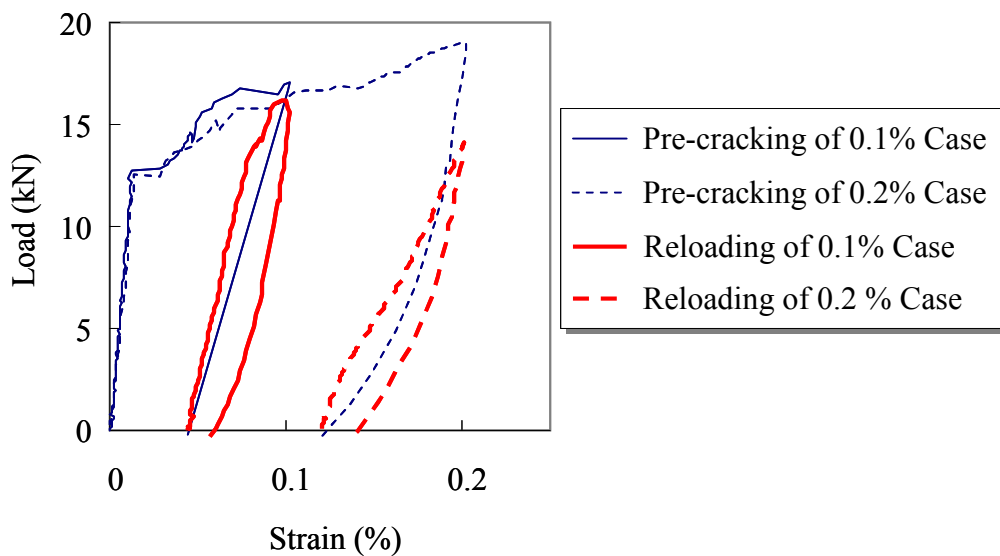


Figure 5.18 Example of Load-Strain Curves of Each Case under Repeated Loading-Recuring Cycle

for example, 0.1W means that damage level was strain of 0.1% and recured in water condition. The strain was monitored by LVDT, which was fixed on both surfaces of specimens, and the measurement length was 150mm. Universal Testing Machine was used for the pre-cracking test and the reloading test. An unloading point of the reloading test was same with the pre-cracking test. **Figure 5.19** shows the example of the Load-Strain curves obtained from the pre-cracking test and the reloading test of each case.

5.4.2 Experimental Results

(a) Averaged Crack Widths

Averaged crack \bar{w} was calculated by equation (5.2) using the measured residual strain and observed number of cracks, and **Table 5.3** tabulates the detailed data after the pre-cracking of each case. Residual strains of 0.2% strain case were about two times larger than those of 0.1% strain case. But, there was insignificant difference between the averaged crack widths of 0.1% strain case and those of 0.2% strain case, because the numbers of cracks of 0.2% strain case were also two times larger than those of 0.1% strain. This is one of the unique characteristic of UHP-SHCC because the total displacement is associated with occurring of multiple fine cracks mainly. After the reloading test, residual strain increased and slight increase of number of cracks was observed in some cases, although the damage level was same with the pre-cracking test. The averaged crack width also increased, but not so much due to increase of number of crack in some cases. There was not significant difference between recuring in water condition and in air condition.

Table 5.3 Residual Strains and Averaged Crack Widths

Case	Pre-cracking Test			2nd Loading Test		
	Residual strain (%) ϵ_{res}	Number of cracks n	Averaged crack width (μm) \bar{w}	Residual strain (%) ϵ_{res}	Number of cracks n	Averaged crack width (μm) \bar{w}
0.1W-1	0.058	3	28.9	0.065	4	24.4
0.1W-2	0.049	3	24.7	0.061	4	22.9
0.1W-3	0.027	2	20.4	0.069	4	25.9
0.1W-4	0.039	2	29.4	0.075	3	37.5
0.1A-1	0.036	3	18.0	0.053	3	26.5
0.1A-2	0.045	3	22.3	0.06	3	30.0
0.1A-3	0.046	3	23.1	0.062	4	23.3
0.1A-4	0.030	2	22.9	0.067	4	25.1
0.2W-1	0.088	8	24.4	0.153	8	28.7
0.2W-2	0.100	8	22.9	0.154	8	28.9
0.2W-3	0.124	7	25.9	0.144	7	30.9
0.2W-4	0.127	8	37.5	0.148	8	27.8
0.2A-1	0.096	7	20.6	0.159	7	34.1
0.2A-2	0.119	7	25.5	0.141	7	30.2
0.2A-3	0.122	7	26.1	0.166	7	35.6
0.2A-4	0.107	6	26.8	0.148	7	31.7

(b) Results of Air Permeability Tests

Figure 5.19 shows air permeability coefficients in each specimen. Firstly, air permeability coefficients of all specimens showed almost the same level as the pre-cracking test (1st test). However, the values were dramatically increased due to the pre-cracking test (2nd test), and in particular, 0.2% strain case exhibited the out of range in the measuring device, which was shown as a blank in the graph. Although the averaged crack widths were almost the same level, the damage in the 0.2% strain case represented by the air permeability was different

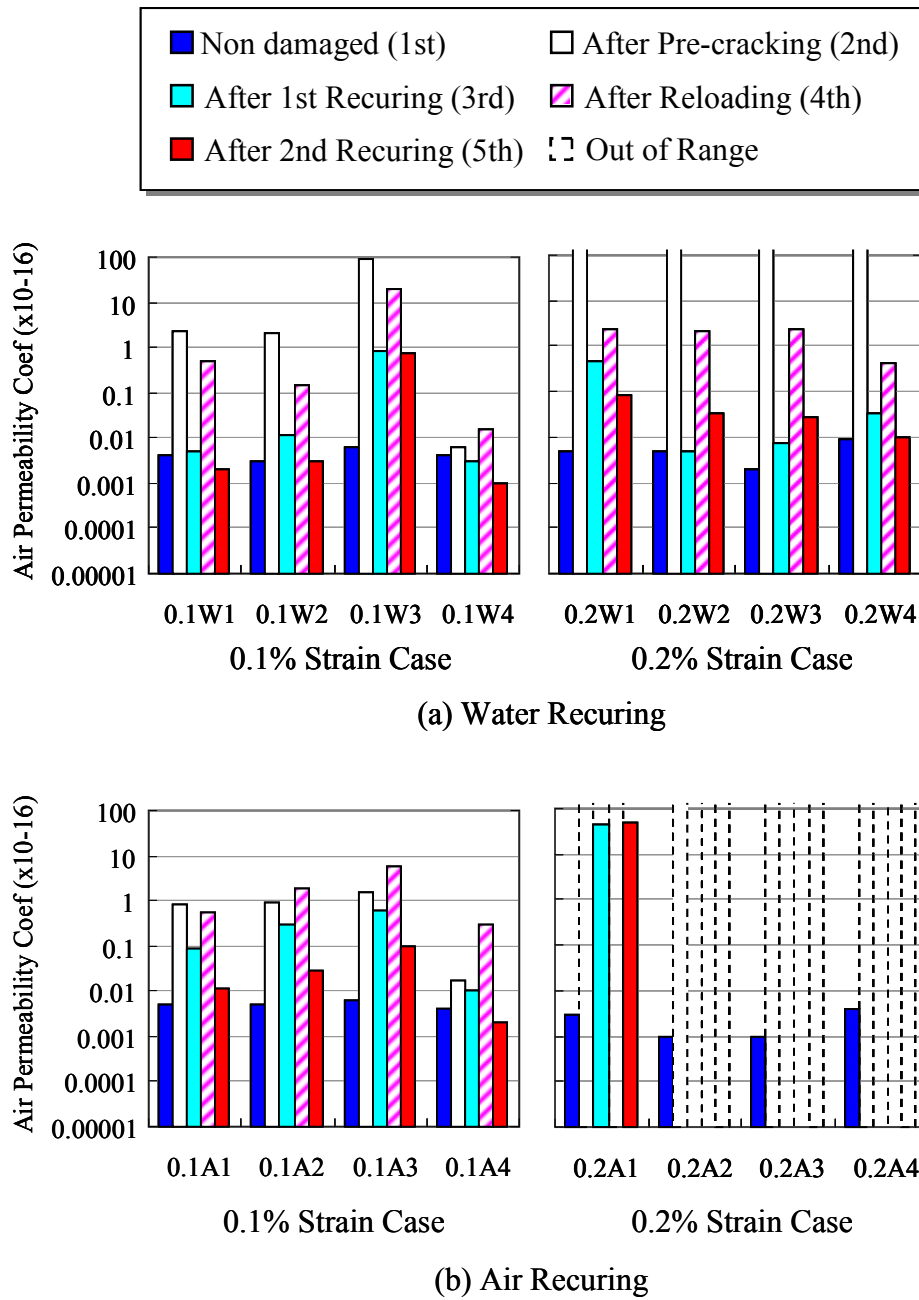


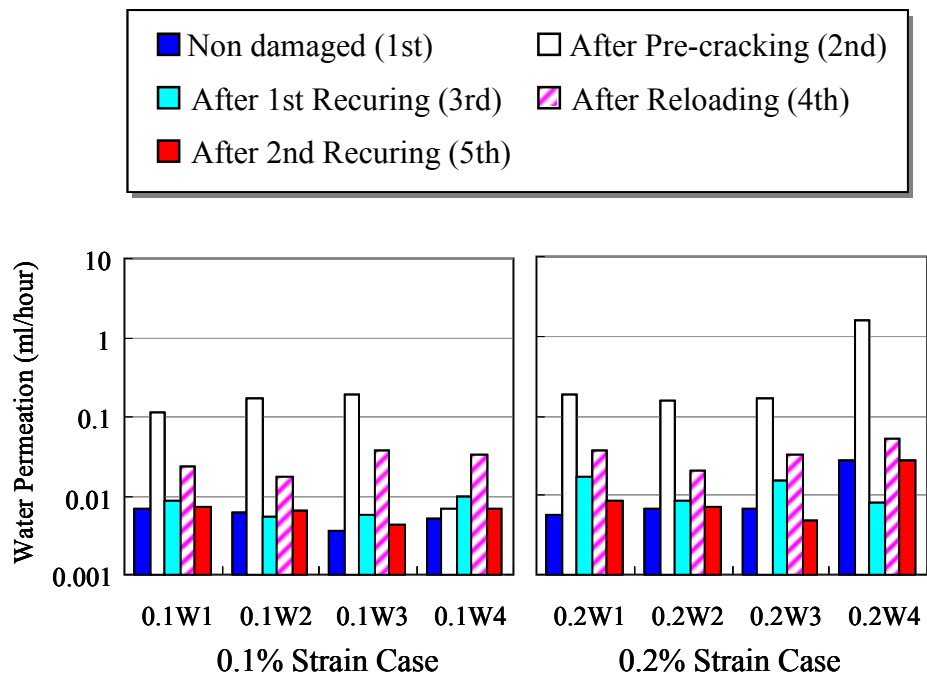
Figure 5.19 Results of Air Permeability Tests (*Some of 0.2% strain case, air permeability coef. couldn't be measured)

from the 0.1% strain case. After the 1st recuring, air permeability coefficients of 0.1% strain case in water recuring condition became to be a similar level to that of non-damaged specimen. In addition, 0.2% strain case in water recuring condition recovered to a value within the range of measuring. However, different behavior was observed in air recuring condition. In 0.1% strain case, air permeability coefficients could not reach up to the non-damaged level, although recovery trend was observed. Measuring of 0.2% strain case also was not possible. These results indicate that 28 days in water recuring was enough period to recovery up to almost same level comparable to non-damaged condition, but it is not enough to recover to the non-damaged level in the air recuring condition.

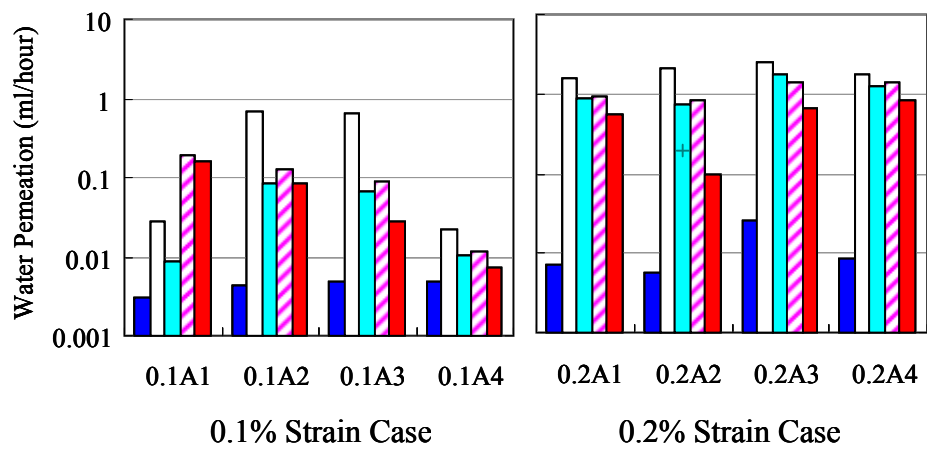
Air permeability coefficients after the reloading test (4th test) became larger than those after the 1st recuring (3rd test), but normally it was smaller than those after the pre-cracking test (2nd test). The reason seems to be insignificant increase of number of cracks and increase of the averaged crack width, and generated products within the crack provided narrow crack width. After the 2nd recuring (5th test), air permeability coefficients was decreased again to non-damaged level.

(c) Results of Water Permeability Tests

Water permeability tests also gave similar trend as the results of air permeability tests, as shown in **Figure 5.20**. Water permeations of non-damaged condition (1st test) were almost the same level each other, and those were increased by the pre-cracking test (2nd test). There was not significant difference between 0.1% strain and 0.2% strain cases, comparing to the trend in air



(a) Water Recuring



(b) Air Recuring

Figure 5.20 Results of Water Permeability Tests

permeability coefficient. Differences among each case appear after the 1st recuring (3rd test). Most significant difference was observed between air recuring and water recuring conditions. Water permeation with water recuring condition was decreased to similar level with non-damaged specimens, regardless of 0.1% and 0.2% strain cases. Water permeation with air recuring condition was slightly decreased compared to that with water recuring condition. And values in 0.2% strain case were slight higher than those of 0.1% strain case.

Water permeation increased again by the reloading test (4th test), but it was lower than that just after the pre-cracking test (2nd test). After the 2nd recuring (5th test), water permeation with water recuring condition recovered again to the non-damaged level. Little recovery was given in the air recuring condition. Generally, 0.1% strain and 0.2% strain cases with water recuring condition showed recovery performance clearly, but those with air recuring condition had no significant change during loading-recuring cycles.

5.5 Summary

The autogenous healing ability concerning protective performance of UHP-SHCC were investigated, and following conclusions can be obtained.

- (1) Autogenous healing ability of UHP-SHCC was confirmed. Air permeability coefficients and water permeation became dramatically larger by the pre-cracking test, but the performance was recovered with increasing of the recuring period. It was more efficient in water recuring condition than in air recuring condition.
- (2) Crack closure can be confirmed through the microscope image, and generated products due to autogenous healing were observed by SEM image and EDX analysis.
- (3) The repeatability of autogenous healing ability of UHP-SHCC was confirmed under twice loading-recuring cycles. Air permeability coefficients and water permeation became larger by the pre-cracking test, but it became smaller by not only the 1st recuring but also the 2nd recuring.

6. Evaluation of Autogenous Healing Ability on Bond Cracks along Rebar

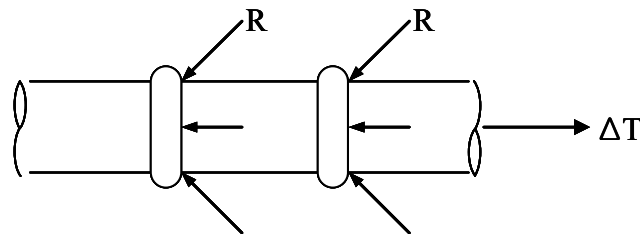
6.1 Introduction

Micro cracks occurred in concrete around tensional rebar were well known phenomenon. It causes serious problem over time. Because, the crack accelerates the penetration of substance such as water and gas, and it also makes rebar corrosion area wider. However, these micro cracks are difficult to detect until cracks develop to the surface of concrete, and it is not easy to repair the micro crack. In this study, air permeability test on concrete surface was applied to evaluate the bond cracks along rebar, and also to detect the recovery of resistance against substance by autogenous healing ability. Air permeability test is an applicable method for this case, because it is non-destructive method using surface measurement. And autogenous healing is a proper method for recovery, because the cracks are widely distributed around reinforcement but small enough to recover by the autogenous healing. In this chapter, autogenous healing ability of cracks along rebar was investigated.

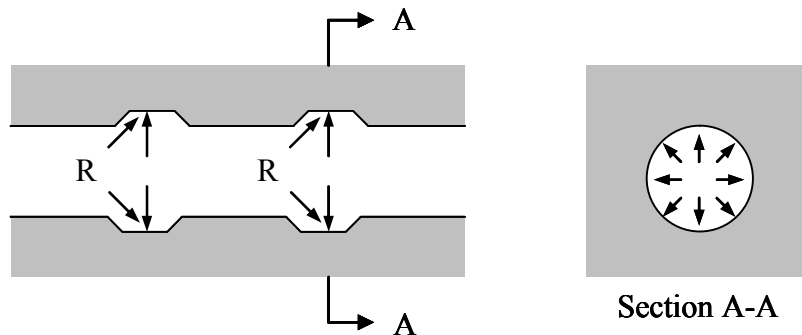
6.2 Bond Cracks along Rebar

Bond behavior between rebar and concrete is influenced by some factors, such as, chemical bond strength, friction, shape of rib, etc. Some researchers reported that the direction of bearing is influenced by a rib angle, and a force perpendicular to rebar becomes equal (Kenneth 1997). And other researchers reported that decreasing of bond in bending rebar with 50mm or 75mm concrete cover occurred by radiational force of bearing (Goto 1971). Side-split crack and pullout failure occurred as results of these bond deterioration. **Figure 6.1** shows the simple reaction of bond strength.

Goto reported that micro cracks along rebar could be possible to observe before significant bond deterioration as shown in **Figure 6.2**. It indicates that the



(a) Radiation Force of Rib by Bearing



(b) Reaction Transmission from Rib of Rebar

Figure 6.1 Simple Reaction of Bond Strength

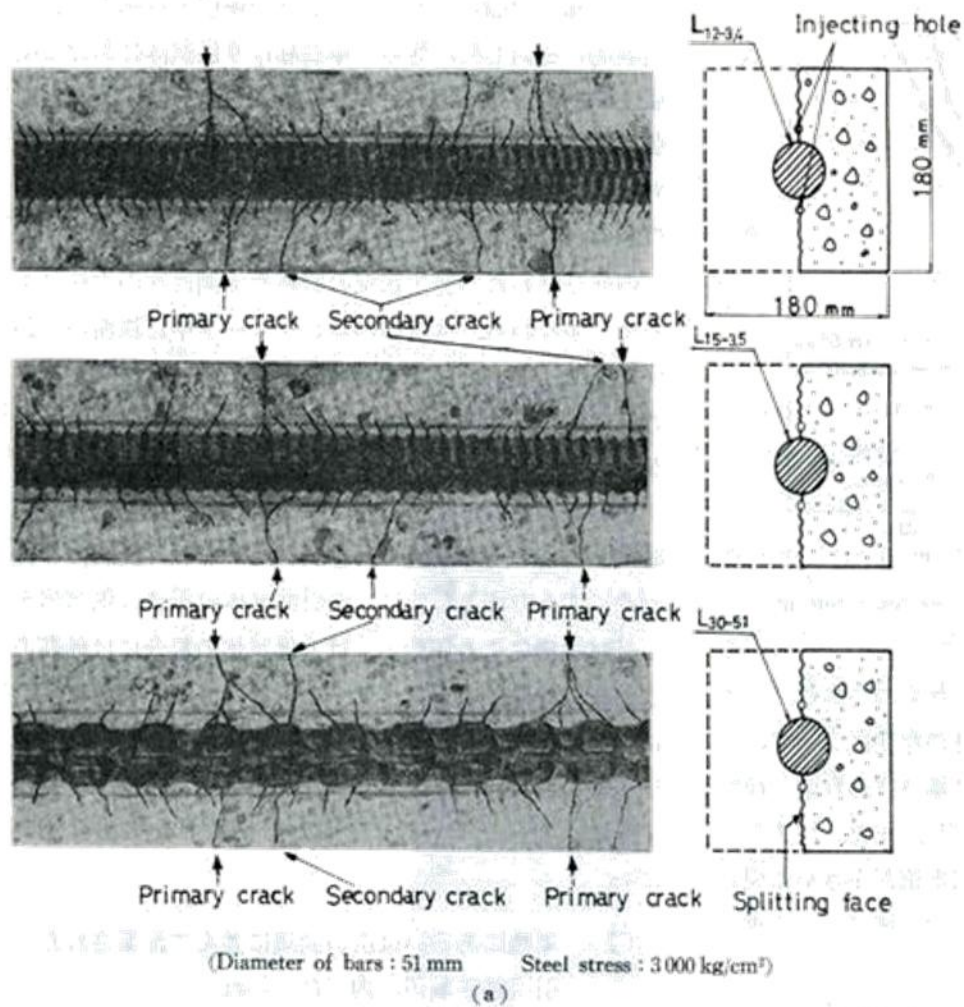


Figure 6.2 Bond Cracks along rebar (Goto Cracks, 1971)

deterioration induced by bond crack also can be recovered before significant development. In this study, the micro cracks are the target for autogenous healing because it is expected to recovery by autogenous healing.

6.3 Autogenous Healing Ability on Bond Cracks

6.3.1 Experimental Program

Tensile test was conducted to induce a bond crack in this chapter. A normal concrete and fly ash concrete were used for comparison each other, and the mix proportions were tabulated in **Table 6.1**. The water to cement ratio (W/C) was 45% in all mix, and properties of each material were as follows. An ordinary Portland cement with a density of 3.15g/cm^3 , sand with surface-dry density of 2.51g/cm^3 , a coarse aggregate with surface-dry density of 2.58g/cm^3 and with the maximum size of 20mm were used. A fly ash (Type II of JIS A 6210), which has a density of 2.38g/cm^3 , was used.

Two tests were performed using the same specimen size in this chapter; air permeability test and investigation of crack pattern through visual observation. Rectangle specimens with size of the $150 \times 150 \times 500\text{mm}$ with rebar were prepared, as shown in **Figure 6.3**, and size of cross section was considered for measuring of air permeability tests. The D22 rebar was located in the center of specimen for inducing tensile force. All specimens were demoulded at 24 hours after casting, and cured in 20°C water condition. Three specimens were prepared in each material, and two of them were for water recuring condition and other was

Table 6.1 Mix Proportions for Tensile Test

Case	W/C (%)	s/a (%)	Unit Content (kg/m^3)					Admixture (cc/m^3)
			Water	Cement	Sand	Gravel	Fly Ash	AEA†
NC	45	47	170	377	780	903	-	0.97
FC	45	47	170	377	716	903	58	0.97

AEA† : Air Entraining Agent

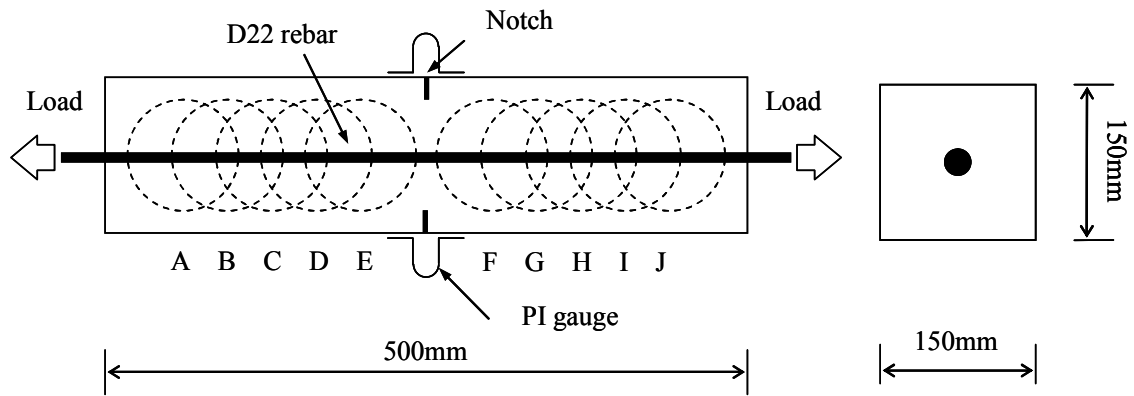


Figure 6.3 Shape of Specimen for Bond Cracks

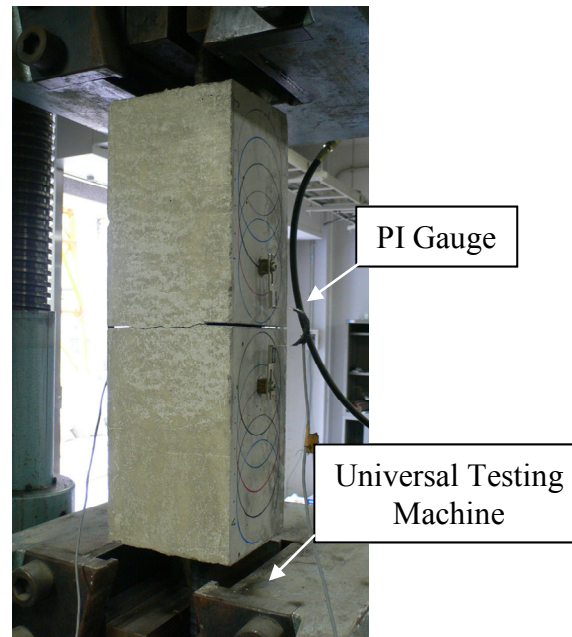


Figure 6.4 Experimental Setup

for air recuring condition. At the age of 28 days, air permeability test was performed to measure the air permeability of non-damaged condition. Ten measurement points along rebar were selected, as shown in **Figure 6.3** (broken line). The pre-cracking test was performed by Universal Testing Machine just after air permeability test, as shown in **Figure 6.4**. Unloading point was 1.0mm in crack opening, which was measured by PI gauges attached on both side of

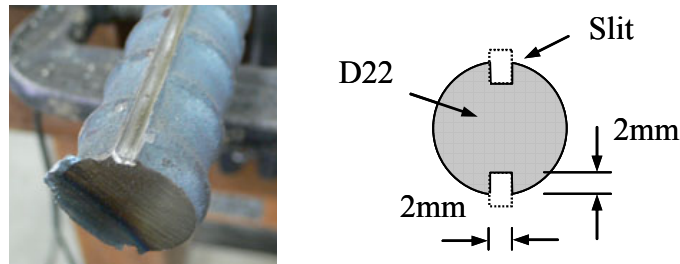


Figure 6.5 Slits for Ink Injection

the specimen. Air permeability coefficient was measured again after the pre-cracking test to measure the damaged level. After that, two of them were recured in 20°C water condition, and other was recuring in recuring room (20°C, RH 70~80%). The recuring period was 28 days, and lastly air permeability tests were performed after the recuring to evaluate autogenous healing ability.

Investigation on crack pattern was performed using the same specimen size, but rebar was different. Slits for ink injection were induced both sides of rebar, as shown in **Figure 6.5**, which was referred to previous experimental report (Maruyama 2007). Slits were cut by hand grinder, and were filled with styrofoam with thickness of 2mm to be injected by cement paste. These styrofoam were removed just before ink injection. Three specimens were prepared in each material. The pre-cracking tests were performed to be the same damage level with the specimen for air permeability tests (crack opening 1.0mm). After that, ink injection was performed for the specimen of each material to verify the induced damage. Other two specimens were recured in water condition and air condition, respectively. 28 days later, crack pattern were observed.

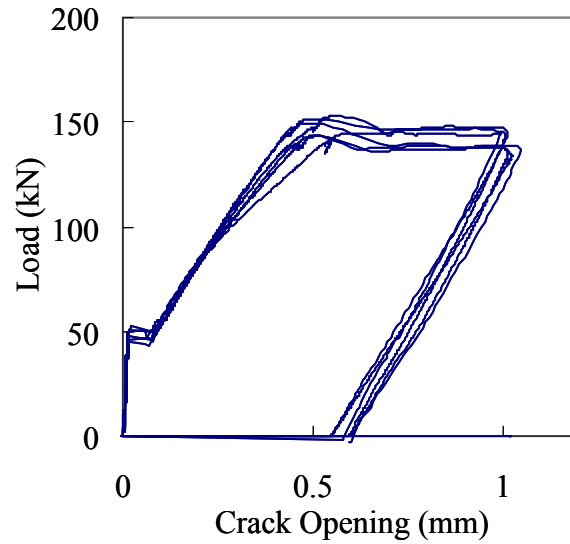


Figure 6.6 Load-Crack Opening Curves of Tensile Test

6.3.2 Experimental Results

Figure 6.6 shows the Load-Crack opening curve of each case. Main crack was occurred from the notch tip at the center of specimen, when load was almost 50kN. Crack width increased with increasing of load. **Figure 6.7** shows the result of ink injecting process during loading. Normally, a main crack induced by the notch was just also observed, but sometimes cracks in the vertical direction of main crack were observed. These vertical cracks seemed to be caused by bond crack development. A crack opening was decreased with unloading, and residual cracks were observed. After the recuring, some generated products were observed between both crack surfaces, but it was not enough to close cracks.

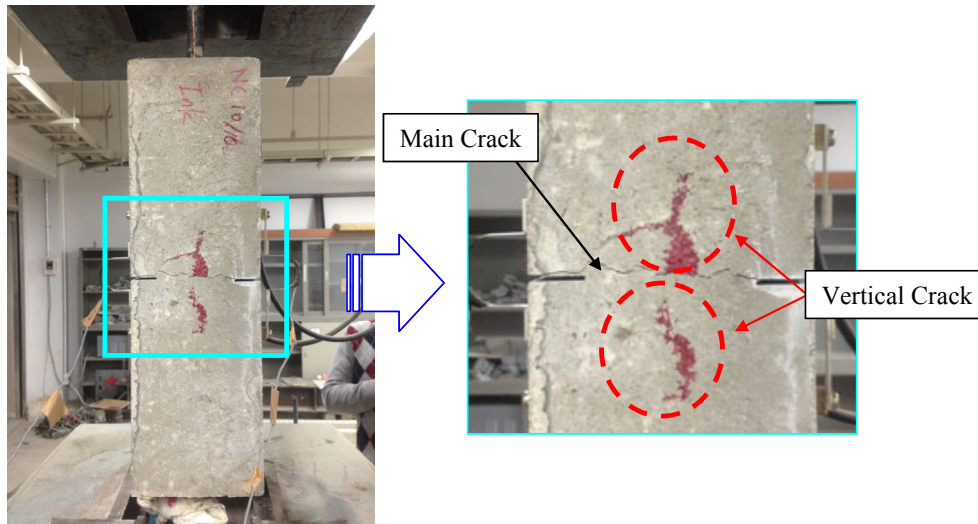
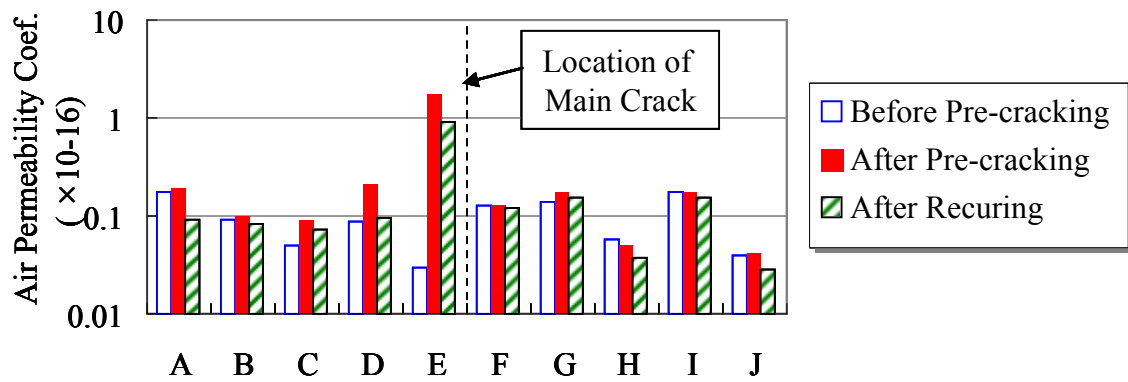


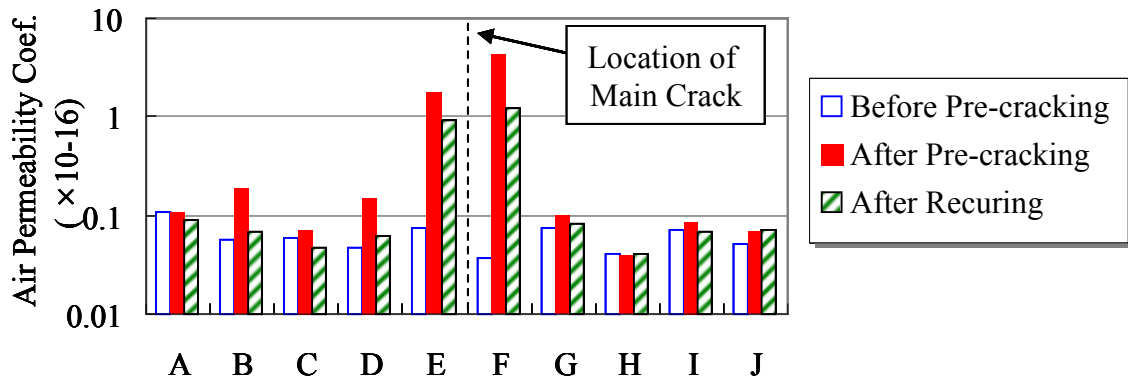
Figure 6.7 Surface Crack Deformation by Ink Injection

(a) Results of Air Permeability Tests

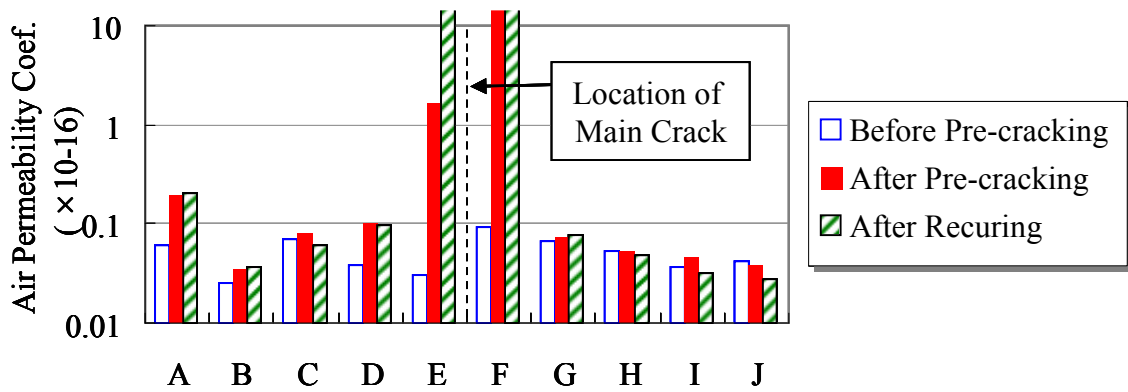
Figures 6.8 and 6.9 show the air permeability coefficients of each specimen before the pre-cracking test, after the pre-cracking test, and after the recuring, respectively. Air permeability coefficients of all specimens became larger after the pre-cracking test than those before the pre-cracking test, and it indicates that damage by the pre-cracking test until 1mm of crack opening mainly concentrated to the vicinity of main crack. Regarding the fly ash concrete in water condition, especially, a significant change was observed at D, E, and F locations, which were near the main crack induced by notch. For normal concrete, slight change was observed in the case of water recuring condition. There was no tendency of recovery in the specimens with air recuring condition.



(a) Recuring in Water Condition - 1

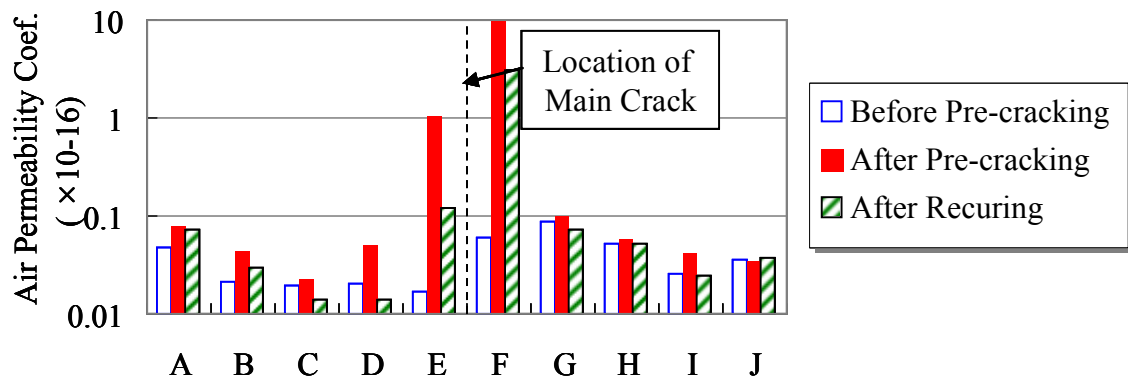


(b) Recuring in Water Condition - 2

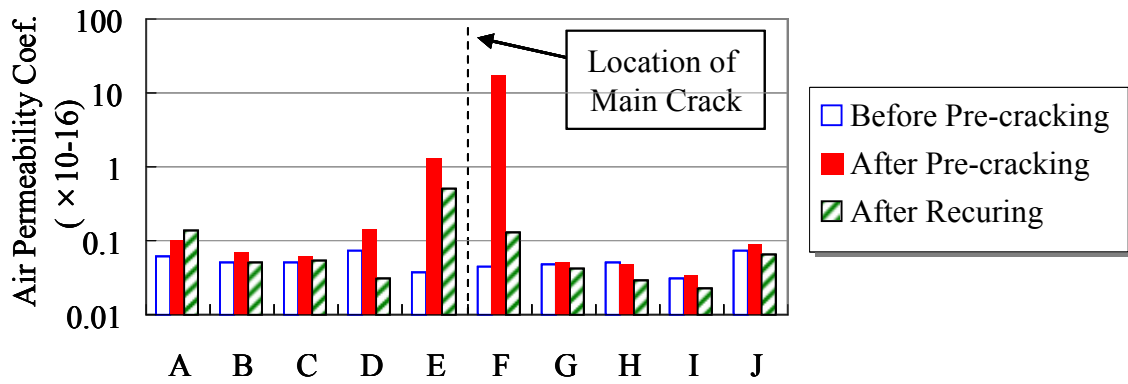


(c) Recuring in Air Condition

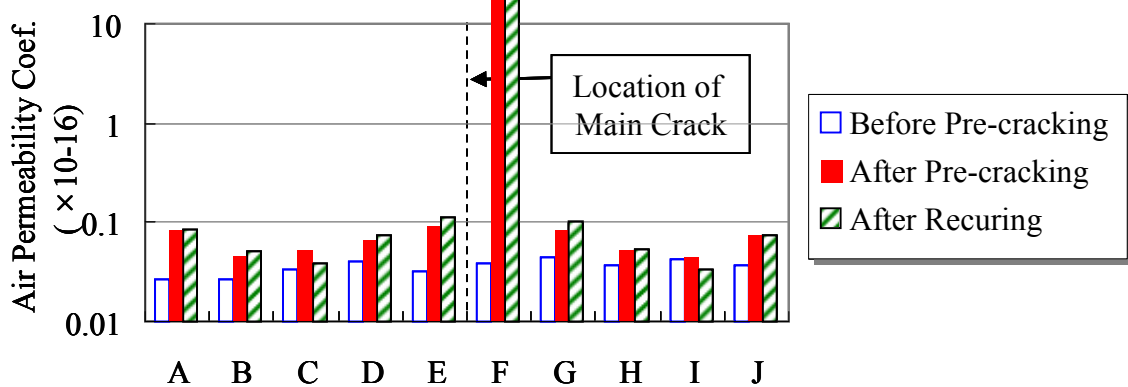
Figure 6.8 Results of Air Permeability Test of Normal Concrete



(a) Recuring in Water Condition - 1



(b) Recuring in Water Condition - 2





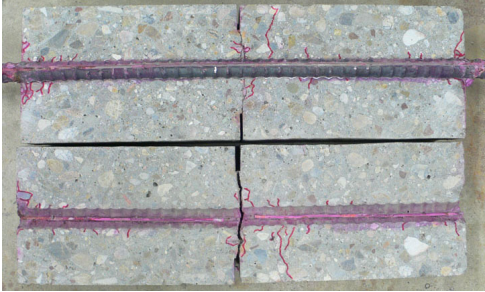
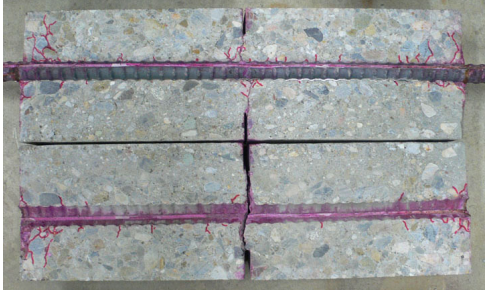
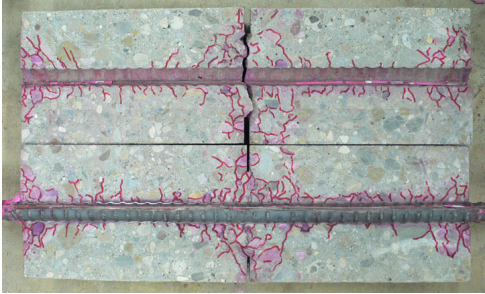

(c) Recuring in Air Condition

Figure 6.9 Results of Air Permeability Test of Fly Ash Concrete

(b) Results of Ink Injection

Investigation of crack patterns provides the recuring effect more visually. **Table 6.2** shows the dyed crack pattern by ink injection of each specimen. After the pre-cracking test, small cracks less than 2mm length were observed perpendicular to rebar. Regarding the fly ash concrete in water recuring condition, a few cracks were observed by injection, but small cracks perpendicular to rebar was not found. It seems that generated products due to autogenous healing filled the crack. However, in the air recuring condition, the observed crack pattern was similar to that after the pre-cracking test, and it means that autogenous healing was not significant. In normal concrete, similar trend was observed that water recuring was effective to close the micro cracks along rebar.

Table 6.2 Cracks Deformation by Ink Injection

	Normal Concrete	Fly Ash Concrete
After Pre-cracking		
Recurring in Water condition		
Recurring in Air condition		

6.4 Summary

In this chapter, autogenous healing ability of bond crack along rebar were experimentally investigated based on air permeability coefficient and crack patterns revealed by ink injection, and following conclusions can be obtained.

- (1) Bond cracks along rebar influence on air permeability coefficients measured from surface of concrete. Air permeability coefficients became larger by bond cracks along rebar due to tensile loading, and became smaller by recuring in water condition.
- (2) Crack patterns were investigated visually to understand the change of air permeability coefficients. After the pre-cracking test, many bond cracks occurred along rebar, and relatively severe damage was observed at the vicinity of the main crack. After the recuring in water condition, most cracks along rebar were not found. On the other hand, the specimen in air recuring did not provided the change of crack pattern. These results indicate that bond cracks along rebar closed by generated product of autogenous healing, and it causes the decreasing of air permeability coefficients.

7. Conclusions

7.1 Conclusions

The dissertation presented the experimental study on autogenous healing ability of concrete in terms of evaluation indices. The following summaries and conclusions are derived from the dissertation.

In Chapter 2, recovery index for autogenous healing ability was proposed in order to obtain sensitive evaluation. The first proposed index used the initial gradient of the Load-CMOD curve of the 2nd loading, and the recuring series and the control series (non-recured) were compared. Although typically reasonable results were deduced by this index, but several problems were noted, as the recured series and the control series should be prepared, and the gradient ratio should be calculated by the averaged value of each series. So the modified index was proposed again, which compare before and after the recuring of the same specimen. Both indices showed reliable result to investigate autogenous healing

ability of concrete, but the modified index was more efficient and convenient.

In addition, several effects on autogenous healing ability were investigated by using the proposed indices. Fly ash increased autogenous healing ability, but including short fiber showed insignificant effect in this study. Autogenous healing ability also depends on the pre-cracking age, and the recuring period. It increased with increasing in the recuring period, and decrease with delay of the pre-cracking test. Regardless of other factors, water recuring condition was more suitable than air recuring condition for autogenous healing.

The damage level of the pre-cracking test with CMOD of 0.05mm was confirmed by observation of dyed crack area using ink injection. Crack depth was about 20mm after the pre-cracking test (the age of 28 days), and autogenous healing decreased the crack depth less than 12mm in water recuring condition. However, the air recuring condition did not change the crack depth significantly

In Chapter 3, the effect of specimen size, effect of short fiber types and recuring temperature on autogenous healing ability were evaluated by using the proposed index. Autogenous healing ability decreased with increasing of specimen size, although the ratio of crack propagation length to specimen depth was the same. Polyvinylalcohol fiber (PVA) showed higher healing ability than Polyethylene fiber (PE), and it seems that the presence of hydroxide (OH⁻) of PVA fiber helps to nucleate for deposition of CaCO₃ efficiently. It was also confirmed that the recuring period was essential to autogenous healing ability than accelerated condition with high temperature.

In Chapter 4, Acoustic Emission (AE) technique was used for the evaluation of autogenous healing ability in flexural test using plain concrete and RC beam. In both test, a few AE source were detected during the 3rd loading test comparing to the pre-cracking test and the 2nd loading test. The averaged frequency of the 3rd loading test was also lower than others. It indicates the released fracture energy of generated products due to autogenous healing was lower than that of bulk concrete. However, in RC beam test, some part showed relative many detected AE source with high gradient ratio. It seems that some crack was more recovered during recuring process.

In Chapter 5, autogenous healing ability of UHP-SHCC was confirmed in protective performance point of view. Multiple fine cracks was induced by uniaxial tensile test, and air permeability test and water permeability test was conducted. Air permeability coefficients and water permeation became remarkably larger by the pre-cracking test, but recovered with increasing of the recuring period. And repeated loading and recuring cycle (two cycles) showed that UHP-SHCC has the repeatability of autogenous healing ability. Air permeability test and water permeability test showed similar sensitivity to evaluate autogenous healing ability. In addition, generated products due to autogenous healing were observed by microscope image, SEM image, and EDX analysis.

In Chapter 6, autogenous healing ability of bond cracks along rebar was investigated. Air permeability coefficients on concrete cover before and after the pre-cracking test, and after the recuring were measured in ten measurement

points along rebar. Air permeability coefficients became larger after the pre-cracking test. After 28 days recuring, air permeability coefficients became smaller and recovered to the non-damaged level in water condition, but only a slight recovery was observed in air recuring condition. Significant change was observed near the main crack. It was also confirmed by dyed crack observation. A few cracks was observed after water recuring, although cracks with air recuring condition showed a similar crack patterns to that after the pre-cracking test.

7.2 For Future Research

Based on the experimental outcome of the current study, some suggestions for future researches concerning the autogenous healing ability are summarized as follows.

In this study, autogenous healing ability was evaluated by the proposed index in the three-point bending test, and effects of several factors were investigated. However, it is not still enough accumulation, and more diverse factors must be considered. In particular, autogenous healing ability mainly depended on time length. Only the recuring period of from 21 days to 63 days was surveyed in this study. A longer recuring period must be applied to obtain the limitation of autogenous healing ability. The pre-cracking age should be also taken into account comparing to the occurrence time of micro cracks in real structure.

A constant damage level, which was CMOD of 0.05mm, was induced to all kinds of specimen in order to make easy to comparison between them in this study. But, crack depth and width varies in real condition, as the results of the RC beam test. It must be confirmed that the proposed index used in this study can be applied to different damage levels.

Two different short fibers and fly ash were used as additives in this study. There are many other kinds of additive to improve concrete performance recently.

Acoustic Emission (AE) technique was, which is one of the sophisticated techniques to observe the inside fracture of concrete, was used for evaluation of autogenous healing ability in this study. However, only a few cracks were detected after the recuring. It seems that generated products by the 28 days of

recuring were not stiff compared to the bulk concrete. A longer recuring period may increase the stiffness.

Lastly, there are no many studies about development of analysis model on autogenous healing. A hydration analysis model can be applied to autogenous healing just re-hydration of un-hydrated cement point of view in some studies, but it was under local and special condition, an analysis model to describe micro cracking and recovery due to autogenous healing are still developing. It will be very helpful to understand mechanism of recovery of strength and stiffness due to autogenous healing.

References

Asami, Y., Ken, W., Victor, C.L.I. and Junichiro, N. (2010) "**Effect of Wet-dry condition on Self-healing property of early-age ECC**", *Proceeding of the JCI*, Vol.32, No.1, pp.251-256.

Bang, S.S, Galinat, J.K and Ramakrishnan, (2001) "**Calcite precipitation induced by polyurethane-immobilized Bacillus pasteurii**", *Enzyme and Microbial Technology*, Vol.28, Issues 4-5, pp.404-409.

Edvardsen C. (1996) "**Wasserdurchlässigkeit und Selbstheilung von Trenrissen in Beton, Rheinisch-Westfälische Technische Hochschule Aachen**", Deutschland, PhD.

Edvardsen, C. (1999) "**Water permeability and autogenous healing of cracks in concrete**", *ACI Material Journal*, Vol.96, No.4, pp.448-454.

Goto, Y. (1971) "**Cracks formed in concrete around deformed tensioned bars**", *ACI Material Journal*, Vol.68, No.4, pp.244-251.

Granger, S., Loukili, A., Pijaudier-Cabot, G. and Chanvillard, G. (2005) **"Mechanical characterization of the self-healing effect of cracks in Ultra High Performance Concrete (UHPC)"**, In: *Proceedings Third International Conference on Construction Materials, Performance, Innovations and Structural Implications*, ConMat'05, Vancouver, Canada, August, pp.22-24

Granger, S., Loukili, A., Pijaudier-Cabot, G. and Behloul, M. (2006) **"Self healing of cracks in concrete: from a model material to usual concrete"**, *Proceeding the 2nd International Symposium On Advances in Concrete through Science and Engineering*, Quebec City, Canada, September, pp11-13.

Granger, S., Loukili, A., Pijaudier-Cabot, G. and Chanvillard, G. (2007) **"Experimental characterization of the self-healing of cracks in an ultra high performance cementitious material"**, *Mechanical test and acoustic emission analysis, Cement and Concrete Research*, No.37, pp.519-527.

Guang, Y., and K. van Breugel (2007) **"Potential Use of Hymostruc Cement Hydration Model for Self-Healing of Microcracks in Cementitious Materials"**, *Proceedings of the First International Conference on Self Healing Materials* 18-20 April 2007, Noordwijk aan Zee, The Netherlands.

Gue, Z.Q., He, H., Stroeve, P., Hu, J. and Stroeve, M. (2007) **"Computer Simulation Study of Concrete's Self-Healing Capacity due to Unhydrated Cement Nuclei in Interfacial Transition Zones"**, *Proceedings of the First International Conference on Self Healing Materials* 18-20 April 2007, Noordwijk aan Zee, The Netherlands.

Haddod, R.H. and Bsoul M.A (1999) **"Self-Healing of Polypropylene Fiber Reinforced Concrete; Pozzolan Effect"**, *Proceedings of Utilization of High Strength concrete*, pp.1412-1421.

Hama, Y., Fujiwara, Y., Yamashiro, Y. and Saito, T. (2007) **"Effect of Self-Healing of Mortar Using Fly Ash"**, *Proceeding of the JCI*, Vol.29, No.1, pp.303-308.

Hearn, N. (1998) **"Self-sealing, autogenous healing and continued hydration: What is the difference?"** *Materials and Structures*, Vol. 31, pp.563-567.

Heide, N., Schlangen and Van Breugel, K (2005) **"Experimental Study of Crack Healing of Early Age Crack"**, In *Proceedings Knud Hojgaard conference on Advanced Cement-Based Material*, Technical University of Denmark, June.

Homma, D., Mihashi, H. and Nishiwaki, T. (2009) **"Self-healing Capability of Fiber Reinforced Cementitious Composites"**, *Journal of Advance Concrete Technology*, Vol.7, No.2, pp.217-228.

Hosoda, A., Kishi, T., Arita, H. and Takakuwa, Y (2007) **"Self Healing of Crack and Water Permeability of Expansive Concrete"**, *Proceedings of the First International Conference on Self Healing Materials* 18-20 April 2007, Noordwijk aan Zee, The Netherlands.

Igarashi, S., Kunieda, M. and Hishiwaki, T. (2009) **"Research activity of JCI technical committee TC-075B: Autogenous healing in cementitious materials"** In: *Procededing of 4th International Conference on Construction Materials: Performance, Innovations and Structural Implications*, Nagoya August 2009, pp.89-96.

Japan Society of Civil Engineers (2005) **"Test methods of surface penetrant (draft)"** *Recommendations for design and construction about construction method of surface protection (Concrete Library of JSCE 119)*, pp.58-59.

Jacobsen, S. and Sellevold, E.J. (1996) **"Self healing of high strength concrete after deterioration by freeze/thaw"**, *Cement and Concrete Research*, Vol.26, No.1, pp.56-62.

Jacobsen, S., Marchand, J. and Boisvert, L. (1996) **"Effect of cracking and healing on chloride transport in OPC concrete"**, *Cement and Concrete Research*, Vol.26, No.6, pp.869-881.

Kamal, A., Kunieda, M., Ueda, N. and Nakamura, H. (2008) **"Evaluation of crack opening performance of a repair material with strain hardening behavior"** *Cement and Concrete Composites*, Vol.30, Issue 10, pp.863-871.

Kang, C.H., Kunieda, M., Ueda, N. and Nakamura, H (2010) **"Autogenous Healing Properties of Concrete under Flexural Loading"**, *Proceeding of Concrete Structure Scenarios Japan*, JSMS, pp.269-272.

Kang, C.H., Kunieda, M., Ueda, N. and Nakamura, H (2011) **"Autogenous Healing Properties of Concrete under Flexural Loading"**, *The Proceeding of JCI*, Vol.33, No.1, pp.1421-1426.

Kang, C.H., Kunieda, M., Ueda, N. and Nakamura, H (2012) **"Autogenous Healing Properties of Ultra High Performance Strain Hardening Cementitious Composites under Loading-Recuring Cycles"**, *The Proceeding of JCI*, Vol.34, No.1, pp.1432-1437.

Kishi, T., Ahn, T.H., Hosoda, A., Suzuki, S. and Takaoka, H (2007) **"Self-Healing Behaviour by Cementitious Recrystallization of Cracked Concrete Incorporating Expansive Agent"**, *Proceedings of the First International Conference on Self Healing Materials* 18-20 April 2007, Noordwijk aan Zee, The Netherlands.

Kunieda, M., Denarie, E., Bruehwiler, E. and Nakamura, H. (2007) **"Challenges for strain hardening cementitious composites- deformability versus matrix density"** *In: H.W. Reinhardt and A. Naaman Eds. Fifth International RILEM Workshop on High Performance Fiber Reinforced Cement Composites*, Mainz 2007, pp.31-38.

Kunieda, M., Ogura, H., Ueda, N. and Nakamura, H. (2011) **"Tensile fracture process of Strain Hardening Cementitious Composites by means of three-dimensional meso-scale analysis"**, *Cement and Concrete Composites*, Vol.33, Issue 9, pp.956-965.

Kunieda, M., Kang, C.H., Ueda, N. and Nakamura, H. **"Recovery of Protective Performance of Cracked Ultra High Performance Strain Hardening Cementitious Composites (UHP-SHCC) Subjected to Autogenous Healing"**, *Advanced Cement Technology*, (under review)

Lauer, K.R. **"Autogenous Healing of Cement Paste"**, *ACI Journal*, Vol. 52, Issue 6, pp.1065-1081.

Matsushita, H., Sue, Y. and Kiyosaki, R. (2003) **"A study of the strength recovery of mortar with an initiated crack"**, *The Proceeding of JCI*, Vol.25, No.1, pp.605-610.

Neville, A. (1995) **"Properties of Concrete"**, Fourth Edition, *Longman*.

Neville, A., (2002) **"Autogenous Healing - A concrete Miracle?"**, *Concrete International*, Vol.24, No.11, pp.76-82.

Nijland, T.G., Labi, J.A, Van Hees, P.J., Lubelli, B. and Rooij, M.d (2007) **"Self Healing Phenomena in Concretes and Masonry Mortars: A Microscopic Study"**, *Proceedings of the First International Conference on Self Healing Materials* 18-20 April 2007, Noordwijk aan Zee, The Netherlands.

Nishiwaki, T., Leite J.P. de B. and Mihashi, H. (2004) **"Enhancement in Durability of Concrete Structures with Use of High-Performance Fiber Reinforced Cementitious Composite"**, (Pre-print)

Nishiwaki, T., Mihashi, H., Jang, B. and Miura, K. (2006) **"Development of Self-Healing System for Concrete with Selective Heating around Crack"**, *Journal of Advanced Concrete Technology*, Vol.4, No.2, pp.267-275

Rodriguez-Navarro, C., Rodriguez-Gallego, M., Chekroun, K.B. and Gonzalez-Munoz, M.T. (2003) **"Conservation of Ornamental Stone by Myxococcus xanthus-Induces Carbonate Biomineralization"**, *Applied and Environmental Microbiology*, Vol.69, No.4, pp.2182-2193.

Reinhardt, H. W. and Jooss, M. (2003) "**Permeability and autogenous healing of cracked concrete as a function of temperature and crack width**" *Cement and Concrete Research*, Vol.33, Issue 7, pp.981-985.

Şahmaran, M., B.Keskin, S, Ozerkan and G., O.Yaman, I. (2008) "**Self-healin of mechanically-loaded self consolidating concretes with high volumes of fly ash**", *Cement and Concrete Composites*, Vol30, pp.872-879

Schlagen, E., Heide, N. and Breugel, K. (2006) "**Crack healing of early age cracks in concrete**", *Proceeding ECF 16 Alexandroupolis*.

Schlagen, E., Heide, N. and van Breugel K. (2006) "**Crack healing of early age cracks in concrete**" *In: M.S. Konsta-Gdoutos Ed. Measuring, Monitoring and Modeling Concrete Properties, Springer*, pp.273-284.

Torrent, R. (1992) "**A two-chamber vacuum cell for measuring the coefficient of permeability to air of the concrete cover on site**", *Material and Structures*, Vol.25, pp.358-365.

Termkhajornkit, P., Nawa, T. and Kurumisawa, K. (2006) "**Effect of water curing conditions on the hydration degree and compressive strengths of fly ash-cement paste**", *Cement and Concrete Composites*, No.28, pp.781-789.

Termkhajornkit, P., Nawa, T., Yamashiro, Y. and Saito, T. (2009) "**Self-healing ability of fly ash-cement systems**", *Cement and Concrete Composites*, No.31, pp.195-203.

Van Breugel, K. "**Self-healing en vloeistofdichtheid**", *Cement*, No. 7, pp. 85-89.

Victor C.L, Yun M.L. and Chan. Y.W (1998) "**Feasibility study of a passive smart self-healing cementitious composite**", *Elsevier Science Ltd., Composites B*, 29B (1998), pp.819-827

Wakatsuki, K., Kamada, T., Kunieda, M. and Rokugo, K. (2000) "**Fracture Mechanics Study on Estimation of Crack Depth in Concrete by Ultrasonic Method**", *Cement Science and Concrete Technology*, No.54, pp568-575.

Wang, G., Guo, Z.Q., Yu, J. and Shui, Z. (2007) "**Effect of Self-Healing Materials on Steel Reinforcement Corrosion of Concrete**", *Proceedings of the First International Conference on Self Healing Materials* 18-20 April 2007, Noordwijk aan Zee, The Netherlands.

Jawad, Y.A., Jordan, I. and Dehn, F. (2005) "**Self-Healing of Self-Compacting Concrete**", *In proceeding of the International Conference on Services Computing (SCC)*, Section 9, pp.1023-1029.

Yingzi, Y., Michael, D.L., En-Hya, Y. and Victor C.L. (2009) "**Autogenous healing of engineered cementitious composites under wet-dry cycle**", *Cement and Concrete Research*, No.39, pp.382-390.

You, Y., Qian, C., Miao, C., Ye, G. and Van Breugel, K. (2007) "**Effect of Carboxylic Acids on The Self-Healing Performance of Cementitious Materials**", *Proceedings of the First International Conference on Self Healing Materials* 18-20 April 2007, Noordwijk aan Zee, The Netherlands.

Zamorowski, W. (1985) "**The phenomenon of Self-regeneration of concrete**", *The international Journal of Cement Composites and Lightweight Concrete*, Vol.7, Number 2, pp.199-201

